


8-2017

Membranes for Food and Bioproduct Processing

Alexandru Marius Avram
University of Arkansas, Fayetteville

Follow this and additional works at: <http://scholarworks.uark.edu/etd>

 Part of the [Biochemistry Commons](#), [Food Processing Commons](#), [Membrane Science Commons](#), and the [Polymer and Organic Materials Commons](#)

Recommended Citation

Avram, Alexandru Marius, "Membranes for Food and Bioproduct Processing" (2017). *Theses and Dissertations*. 2375.
<http://scholarworks.uark.edu/etd/2375>

This Dissertation is brought to you for free and open access by ScholarWorks@UARK. It has been accepted for inclusion in Theses and Dissertations by an authorized administrator of ScholarWorks@UARK. For more information, please contact scholar@uark.edu, ccmiddle@uark.edu.

Membranes for Food and Bioproduct Processing

A dissertation submitted in partial fulfillment
of the requirements for the degree of
Doctor of Philosophy in Engineering with a Concentration in Chemical Engineering

by

Alexandru M. Avram
Technische Hochschule Mittelhessen
Diplom Ingenieur (FH), 2012

August 2017
University of Arkansas

This dissertation is approved for recommendation to the Graduate Council.

Dr. Ranil Wickramasinghe
Dissertation Director

Dr. Michael D. Ackerson
Committee Member

Dr. Ed Clausen
Committee Member

Dr. Peter Czermak
Committee Member

Dr. Xianghong Qian
Committee Member

Abstract

Modified membranes for process intensification in biomass hydrolysis

Production of biofuels and chemicals from lignocellulosic biomass is one of the leading candidates for replacement of petroleum based fuels and chemicals. However, conversion of lignocellulosic biomass into fuels and chemicals is not cost effective compared to the production of fuels and chemicals from crude oil reserves. Some novel and economically feasible approaches involve the use of ionic liquids as solvents or co-solvents, since these show improved solvation capability of cellulose over simple aqueous systems. Membranes offer unique opportunities for process intensification which involves fractionation of the resulting biomass hydrolysate leading to a more efficient and cheaper operation.

This research attempts to develop membranes that would usher the economics of the biochemical conversion of lignocellulosic biomass into fuels and chemicals by recycling the expensive ionic liquid. The overall aim of this work is the development of novel membranes with unique surface properties that enable the selective separation of non-reacted cellulose and hydrolysis sugars from ionic liquids.

Nanofiltration separation for application in food product engineering

With the advent of the modern, well-informed consumer who has high expectations from the nutritional value of consumed food products, novel approaches are being developed to produce nutrient-enhanced foods and drinks. As a response to the consumer needs, different techniques to recover, concentrate and retain as much as possible of bioactive compounds are being investigated. Membrane technology has the advantage of selective fractionation of food products (e.g. salt removal, removal of bitter-tasting compounds or removal of sugar for sweet taste adjustment), volume reduction, and product recovery at mild conditions. In this work, we use nanofiltration in dead-end and crossflow mode to concentrate polyphenols from blueberry pomace. Blueberry

pomace is an overlooked waste product from the juice pressing of blueberries that contains high amounts of health-beneficial antioxidants. We aim at developing a simple, yet efficient membrane process that reduces the amount of water and thus concentrates the amount of polyphenols in the retentate.

©2017 by Alexandru M. Avram
All Rights Reserved

Acknowledgements

Hereby I would like to include my sincere gratitude towards Dr. Ranil Wickramasinghe, my main PhD thesis adviser. In German we would call him Doktorvater (= doctorate dad) and I am very grateful that he took me under his protective wing and advised me in times of great despair. I specifically appreciated him for allowing me to address him by his first name and also for the speed at which he responded to emails 365/365 and 366/366 (2016 was a leap year). Some students estimate his response speed at $0.99 \times c$.

A warm “Thank you!” to all of my committee members. Dr. Clausen, with such a full plate, thank you for spontaneously accepting to join the gang.

A large number of “Thank you!”s are forwarded to the University of Arkansas and to the Chemical Engineering Department who opened their doors to me and provided me with the tools and environment to grow into a better scientist. My work and extracurricular activities have often been featured in the local Newswire. That gave me pride and excellent motivation to continue the pursuit of my education. Hereby, I would also like to mention and acknowledge Amanda Cantu, Amber Hutchinson, Tammy Lutz-Rechtin, Dr. Bob Beitle and Dr. Jerry Havens.

It is not possible to convey in words my gratitude to thank my mother and step father for supporting me through the PhD. Mama, mulțumesc din toată inima ca ai avut răbdare cu mine, ca m-ai crescut excelent și nu ai pierdut încrederea în mine! Burkhard, vielen Dank dass du mich stets unterstützt hast und dass du ein sehr guter und ehrlicher Elternteil und Freund warst!

Dedication

I dedicate these words of encouragement to all struggling graduate students.

“Knowledge, when appropriated genuinely and passionately, is both empowering and humbling. It will allow you to roughly grasp the pulse of the entire human kind, as it currently stands.”

- Alex Avram, November 13 2016

(This is an article that I wrote and published as U of A online blogger for ISS.)

Between now and then, I don't want you to be afraid of change. Change is exciting, you get to close a life chapter and begin another. On your own terms. If the latter did not end with *And they lived happily ever after*, this is your chance to re-write the ending.

Between now and then, I want you to know that you were crafted perfectly flawless. You were given everything necessary to become brave and capable. Your mind is inquisitive and locked inside are countless skills. It is up to you to unlock your potential and be the best that you can possibly be.

Between now and then, I want you to believe in your power of judgement. Always judge and analyze your next move before attempting it. Make intellectually informed decisions and stick with them. Saying what you mean and meaning what you say goes a long way.

Between now and then, I want you to be daring. If something sounds too risky and if the thought of it gives you shivers and a fuzzy feeling in your stomach, it's probably worth pursuing.

Between now and then, I don't want you to have blind faith and follow the herd. I want you to be inquisitive and train a scientific sense of discovering and explaining the unknown. Answering the *Why?* and *How?* is both challenging and endlessly rewarding. Henley would tell you that "*you are the captain of your soul and the master your fate*". There is truth in that poetic verse, because fate is not given, but self-made. Purposely put yourself in front of opportunity, recognize it and seize it when you want it. Don't wait for the odds to fall in your favor, instead re-arrange the odds so that they fall, neatly, in your favor.

Between now and then, I want you to trust in your capacity to conquer your fears and defeat your weaknesses. You are self-made and you deserve to become the best that you can be. You are your biggest hero.

Between now and then, I want you to know that things will always get better. You will be thrown in the midst of heavy storms and your strength will be trialed in unsurmountable situations. You will be knocked down and you will fall on your knees. But remember, that in spite of all, things will simply. Always. Get better. Because even the heaviest of storms eventually comes to a still-stand. And when the gloomy clouds start wondering away, that instant is your moment to take a deep breath in – *go ahead! Take a deep breath in!* – then rise up stronger and build a better storm shelter.

Table of contents

1. INTRODUCTION.....	1
1.1. THE CASE OF DWINDLING FOSSIL FUELS AND THE CONCEPT OF BIOREFINERY.....	1
1.2. LIGNOCELLULOSIC BIOMASS HYDROLYSIS	10
1.2.1. <i>Enzymatic decomposition of cellulose</i>	15
1.2.2. <i>Chemical decomposition of cellulose</i>	16
1.3. IONIC LIQUIDS	18
1.3.1. <i>Mode of cellulose dissolution by ionic liquids</i>	20
1.3.2. <i>Cellulose hydrolysis with ionic liquids</i>	21
1.3.3. <i>Separation techniques for biomass hydrolysis applications</i>	23
1.3.4. <i>Quantitative measurements</i>	27
1.4. MEMBRANE SEPARATIONS	28
1.4.1. <i>Membrane separation and classification</i>	28
1.4.2. <i>Market relevance of membrane technology</i>	30
1.4.3. <i>Nanofiltration</i>	32
1.4.4. <i>Fouling of nanofiltration membranes</i>	34
1.4.5. <i>Membrane reactors</i>	36
REFERENCES	43
2. NANOFILTRATION MEMBRANES FOR IONIC LIQUID RECOVERY	53
2.1. INTRODUCTION.....	53
2.2. EXPERIMENTAL	57
<i>Materials</i>	57
<i>Membrane modification via interfacial polymerization (IP)</i>	57

<i>Surface Characterization</i>	58
<i>Rejection experiments</i>	59
2.3. RESULTS AND DISCUSSION	62
<i>IP membranes</i>	62
<i>Surface analysis</i>	65
2.4. CONCLUSION.....	72
ACKNOWLEDGEMENTS.....	73
REFERENCES	73
3. POLYELECTROLYTE MULTILAYER MODIFIED NANOFILTRATION MEMBRANES FOR THE RECOVERY OF IONIC LIQUID FROM DILUTE AQUEOUS SOLUTIONS	76
3.1. INTRODUCTION.....	76
3.2. EXPERIMENTAL	78
<i>Materials</i>	78
<i>Static layer-by-layer deposition of PEMs</i>	79
<i>Membrane characterization</i>	80
<i>Rejection analysis</i>	82
3.3. RESULTS AND DISCUSSIONS.....	83
<i>ATR-FTIR analysis</i>	83
<i>Contact angle measurement</i>	84
<i>AFM imaging</i>	85
<i>SEM imaging</i>	87
<i>Zeta potential measurement</i>	88

<i>Rejection and permeance</i>	89
<i>Selectivity of ionic liquid over monomeric sugar</i>	93
<i>Comparative study</i>	95
3.4. CONCLUSION.....	98
ACKNOWLEDGEMENTS.....	99
REFERENCES	99
SUPPORTING INFORMATION.....	105
4. CONCENTRATION OF POLYPHENOLS FROM BLUEBERRY POMACE	
EXTRACT USING NANOFILTRATION	111
4.1. INTRODUCTION.....	111
4.2. MATERIALS AND METHODS	114
<i>Pressurized hot water extraction</i>	114
<i>Dead-end filtration</i>	115
<i>Crossflow filtration</i>	116
<i>Total polyphenol analysis</i>	117
<i>Membrane cleaning and fouling index</i>	119
4.3. RESULTS AND DISCUSSION.....	120
<i>Total polyphenols and sugar retention</i>	120
<i>Dead-end filtration</i>	121
<i>Crossflow filtration</i>	127
<i>Membrane reconditioning</i>	129
4.4. CONCLUSION.....	132
ACKNOWLEDGEMENTS.....	133

REFERENCES	134
<i>Supplemental Information</i>	137

5. CONCLUSION AND FUTURE OUTLOOK..... 143

List of Figures

Figure 1-1: US production and consumption of natural gas (above) and petroleum products (below) that include liquid fuels from 1950 through 2015. With permission from EIA.....	2
Figure 1-2: Total energy consumption in the US from 1950 through 2015 (above). Total renewable energy consumed in the US from 1950 through 2015 (below). Total biomass energy consumption includes wood, waste and biofuels. With permission from EIA.....	4
Figure 1-3: Biorefinery and potential green products.....	7
Figure 1-4: Envisioned catalytic membrane reactor system with the modified membrane unit operations for biomass catalysis and ionic liquid recycling. The pressure line is added to control membrane permeability.	10
Figure 1-5: Drawing showing schematic structure of plant cell wall with lignocellulosic components.	12
Figure 1-6: Lignin building blocks: oumaryl alcohol (I), coniferyl alcohol (II) and sinapyl alcohol (III).....	13
Figure 1-7: Example of one type of hemicellulose (arabinoxylan) with β -(1-4)-glycosidic and α -(1-3)-glycosidic bonds emphasized.	14
Figure 1-8: Cellulose molecule structure showing intra- and intermolecular weak hydrogen bonds and the covalent C1-C4 glycosidic bond.	15
Figure 1-9: Reaction pathways for cellulose acid hydrolysis. n is typically 400-1000 monomers. Adapted from Dr. L.T. Fan ¹² . With permission from SpringerLink.....	17

Figure 1-10: Examples of cations and anions used as ILs in biomass dissolution and hydrolysis.	19
Figure 1-11: Membrane classification with typical working pressure, pore size and rejected species.	28
Figure 1-12: Representation of membrane separation by size-exclusion. The feed side contains molecules of different sizes and these can permeate the membrane through channels called pores.	29
Figure 1-13: Fouling schematic showing the formation of boundary layer at membrane surface.	34
Figure 1-14: Two approaches in membrane reactors: the extractor membrane (above) and the distributor membrane (below) ^{121,122}	38
Figure 1-15: Membrane reactor scheme. Reprinted from Liu et al. ¹²⁶ , copyright (2005), with permission from Elsevier.	40
Figure 1-16: Continuous enzymatic membrane reactor. The reactor consists of a stirred tank reactor coupled to a ceramic membrane, which prevented the sorption of the pollutant and allowed the recovery and recycling of the biocatalyst. Reprinted from Arca-Ramos et al. ¹²⁷ , copyright (2015), with permission from SpringerLink.....	41
Figure 2-1: Reaction scheme for interfacial polymerization with expected products; 3-aminophenylboronic acid (BA) and piperazine (PIP) are in aqueous solution while trimesoyl chloride (TMC) is in hexane.	58
Figure 2-2: Variation of permeance and rejection of cellobiose, glucose EmimOAc and BmimCl as a function of polymerization time for modified 50 kDa PES membranes. Modification conditions were: 1.0 and 0.1 wt % PIP and BA respectively in the aqueous phase, reaction	

temperature 25°C. Insets show AFM surface analysis of selected membranes with roughness 9.4 and 38.6 nm from left to right, respectively. All AFM imaging scale resolution at 0-5 μm. 64

Figure 2-3: FTIR spectra for 30 kDa base and modified membranes. Modification conditions were: 1.0 and 0.5 wt % PIP and BA respectively in the aqueous phase, reaction temperature -4 °C, polymerization times of 1, 15 and 25 min. 66

Figure 2-4: Variation of permeance and rejection of cellobiose, and BmimCl as a function of BA concentration for modified 30 kDa modified PES membranes. Modification conditions were: 1.0 wt % PIP in the aqueous phase, reaction temperature was -4 °C for a reaction time of 15 min. Insets show AFM surface analysis of membranes modified with 0.1 and 1.0 wt % BA with roughness 31.0 and 46.6 nm from left to right, respectively. All AFM imaging scale resolution at 0-5 μm. 68

Figure 2-5: Variation of permeance and rejection of cellobiose, and BmimCl as a function of Et3N concentration for unmodified and modified 30 kDa PES membranes. The Et3N concentration was chosen such that the ratio of BA:Et3N was 1:1.5. Modification conditions were: 1.0 wt % PIP in the aqueous phase reaction temperature was -4 °C for a reaction time of 5 min. 70

Figure 3-1: Static LBL deposition of PEM on a base membrane. First, one layer is formed after contacting with the polycation solution (or polyanion for alumina), then the membrane is rinsed before dipping into the second solution of oppositely charged polyion to form one bilayer. The alumina membranes were capped with PSS to be comparable to PES. The process is repeated for the desired bilayer number (δ). 80

Figure 3-2: FTIR analysis of PEMs modified with 10, 16 and 18 PAH/PSS bilayers on PES base membrane. 84

Figure 3-3: Contact angle measurements performed with deionized water droplet solution and recorded after 3 seconds. Values for the modified membranes represent the average of four measurements taken at three distinct locations on the membrane surface. Insets show droplet formation for the two distinct base membranes. 85

Figure 3-4: AFM images at 1 μm x 1 μm resolution in two dimensional and three dimensional (3D) display. (A; A-3D) unmodified alumina oxide, roughness 3.8 nm. (B; B-3D) unmodified PES, roughness 3.6 nm. (C; C-3D) (PSS/PAH)₈PSS on alumina oxide, roughness 11.9 nm. (D; D-3D) (PAH/PSS)₁₆ on PES, roughness 5.7 nm. These membranes were not used for rejection analysis but they were previously equilibrated with deionized water until constant permeance. 86

Figure 3-5: Cross-sectional SEM images of alumina oxide and PES. A1.: unmodified 0.2 μm alumina oxide (magnification: 2000x); A2.: (PSS/PAH)₈PSS (magnification: 2000x and 8000x inset); P1.: unmodified 50 kDa PES (magnification: 400x and 2000x inset); P2.: (PAH/PSS)₉ (magnification: 500x and 2000x inset). 88

Figure 3-6: Zeta potential measurements of unmodified base membranes (black lines) and of the modified PEM membranes (colored lines). Lines connecting data markers are for guidance only. Relative error from 3 repeated measurements was $\pm 5.5\%$ 89

Figure 3-7: Permeance (bars) and solute rejection (lines with markers) as a function of (PSS/PAH)_nPSS bilayer number using alumina oxide disc as base membrane. Lines are there to guide the eye. Relative error for the rejection data was between $\pm 3.2\%$ and $\pm 5.8\%$ from triplicates. 90

Figure 3-8: Permeance (bars) and solute rejection (lines with markers) as a function of (PAH/PSS)_n bilayer number using PES as base membrane. Lines are there to guide the eye. Relative error for the rejection data was between $\pm 1.7\%$ and $\pm 5.3\%$ from triplicates. 92

Figure 4-1: Accelerated Solvent Extraction system. The pomace is loaded in the extraction cell, water is pumped through the system, and polyphenols are recovered as aqueous solution in the collection vessels.	115
Figure 4-2: Process flow of experimental setup for nanofiltration in crossflow mode. A: Feed stirred vessel; B: Piston pump; C: Permeate collection and balance; D: Crossflow cell; E: Pressure regulator and F: gas supply.	117
Figure 4-3: Effect of stirring speed on permeance. Data reflects the feed permeance after a constant volume for both membranes was collected in permeate.	123
Figure 4-4: Permeance with non-prefiltered and filtered blueberry pomace extract, 200 rpm...	124
Figure 4-5: Filtration at extended times. Stirring speed 200 rpm.	126
Figure 4-6: Crossflow filtration with 0.22 μm prefiltered feed, 200 rpm, performed at a crossflow rate of 57 mL/min and 3 bar transmembrane pressure.	128
Figure 4-7: Recovery of permeance for membranes used in dead-end mode using 0.22 μm prefiltered feed at 200 rpm. Data is shown in duplicates for each membrane and water was used as testing feed. 100% relative permeance was 14.1 and 5.4 $\text{L m}^{-2} \text{h}^{-1} \text{bar}^{-1}$ for NF270 and NF245, respectively.	131
Figure 4-8: Recovery of permeance for membranes used in crossflow mode using 0.22 μm prefiltered feed at 200 rpm. Water was used as feed and all other parameters were constant. Washing steps are shown in chronological order. For NF270 100% relative permeance corresponds to 13.2 $\text{L m}^{-2} \text{h}^{-1} \text{bar}^{-1}$ and for NF245 100% relative permeance corresponds to 4.6 $\text{L m}^{-2} \text{h}^{-1} \text{bar}^{-1}$	132

List of Tables

Table 1-1: Typical composition of lignocellulosic raw materials.	11
Table 1-2: Commercial pricing list of ionic liquids commonly used with biomass hydrolysis. ..	18
Table 1-3: Molecular weights of sugar monomers released during acid biomass hydrolysis and of ionic liquids commonly used with biomass dissolution.	24
Table 1-4: Advantages of inorganic membranes with respect to organic membranes.	37
Table 2-1: Summary of membrane modification conditions and feed streams tested.	60
Table 2-2: Molecular weight of solutes.	62
Table 2-3: Variation of rejection with PIP concentration for modified 50 kDa base PES membranes for aqueous feed streams containing single component sugars and ionic liquids. Modification conditions were: 0.1 wt % BA in the aqueous phase, reaction temperature were 25°C for a reaction time of 15 min.	63
Table 2-4: Variation of rejection with BA concentration for modified 30 kDa base PES membranes for aqueous feed streams containing single component sugars and ionic liquids. Modification conditions were: 1.0 wt % PIP in the aqueous phase reaction temperature was -4 °C for a reaction time of 15 min.	67
Table 2-5: Variation of rejection in the presence of Et3N. The Et3N concentration was chosen such that the ratio of BA:Et3N was 1:1.5. Results are for modified 30 kDa base PES membranes for aqueous feed streams containing single component sugars and ionic liquids. Modification conditions were: 1.0 wt % PIP in the aqueous phase reaction temperature was -4 °C for a reaction time of 5 min.	69

Table 2-6: Selectivity for BmimCl versus glucose or cellobiose for modified base 30 kDa PES membranes. Modification conditions were: aqueous phase 1.0, 0.1, 0.115 wt% PIP, BA Et3N respectively in the aqueous phase, reaction temperature -4 °C for a reaction time of 8 min.	71
Table 3-1: Selection of base membranes, type and amount of deposited polyelectrolytes.	79
Table 3-2: Feed compound concentration in the three model feeds and their analytical properties.	83
Table 3-3: Effect of feed pH and sampling time on compounds rejection with (PSS/PAH) ₉ PSS deposited on 0.2 µm alumina discs.	91
Table 3-4: Summary of selected modified nanofiltration membranes with selectivity and permeance.	94
Table 3-5: Comparison of this work with other similar published work on ionic liquid recycling. Comments explain some advantages (+) and disadvantages (-).	97
Table 4-1: HPLC analysis results for ASE extract and for retentate and permeate fractions after rejection in dead-end mode.	121
Table 4-2: Volume reduction and concentration factor for dead-end filtration at extended times.	127
Table 4-3: Volume reduction and concentration factor for crossflow filtration.	128
Table 4-4: Dynamic fouling index at constant permeate volume over active membrane area ratio (V/A).	130
Table 4-5: Unit operations and the recommended best procedure to assist with observed issues.	133

List of published papers

Alexandru M. Avram, Pejman Ahmadiannamini, Xianghong Qian, S. Ranil Wickramasinghe – “Nanofiltration Membranes for Ionic Liquid Recovery”. Separation and Purification Technology. Accepted for publication April 03 2017 (Chapter 2). <http://dx.doi.org/10.1080/01496395.2017.1316289>

Alexandru M. Avram, Pejman Ahmadiannamini, Anh Vu, Xianghong Qian, Arijit Sengupta, S. Ranil Wickramasinghe – “Polyelectrolyte Multilayer Modified Nanofiltration Membranes for the Recovery of Ionic Liquid from Dilute Aqueous Solutions”. Journal of Applied Polymer Science. Revision 1 of manuscript was submitted on April 19 2017 (Chapter 3).

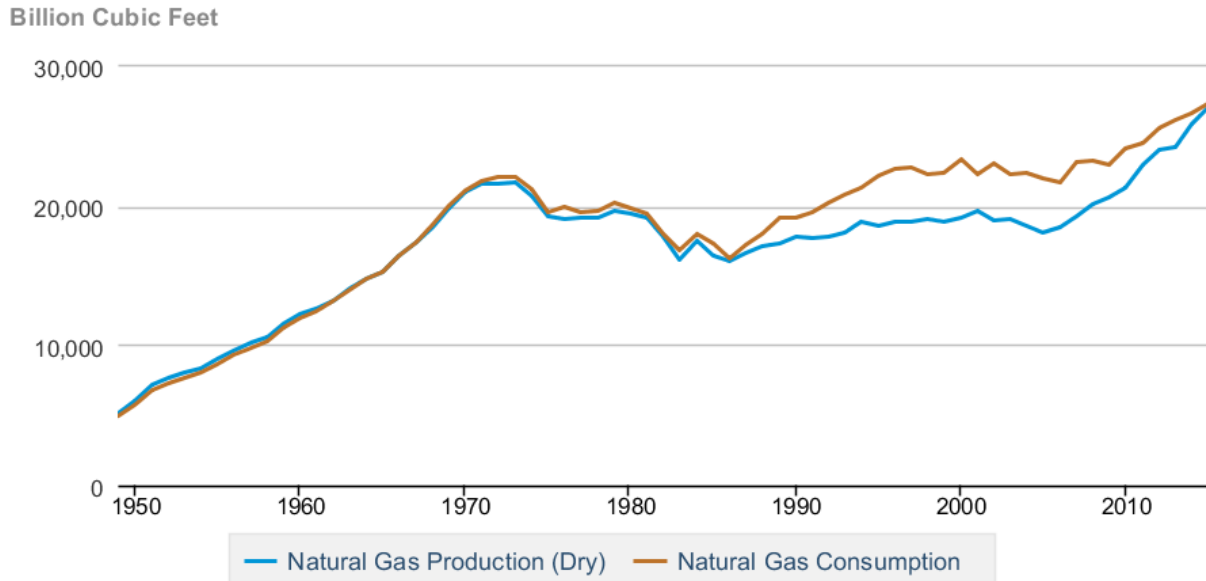
Alexandru M. Avram, Pauline Morin, Cindi Brownmiller, Arijit Sengupta, Luke R. Howard, S. Ranil Wickramasinghe – “Concentration of Polyphenols from Blueberry Pomace Extract using Nanofiltration” Food and Bioproducts Processing. Manuscript was submitted on April 30 2017 (Chapter 4).

1. Introduction

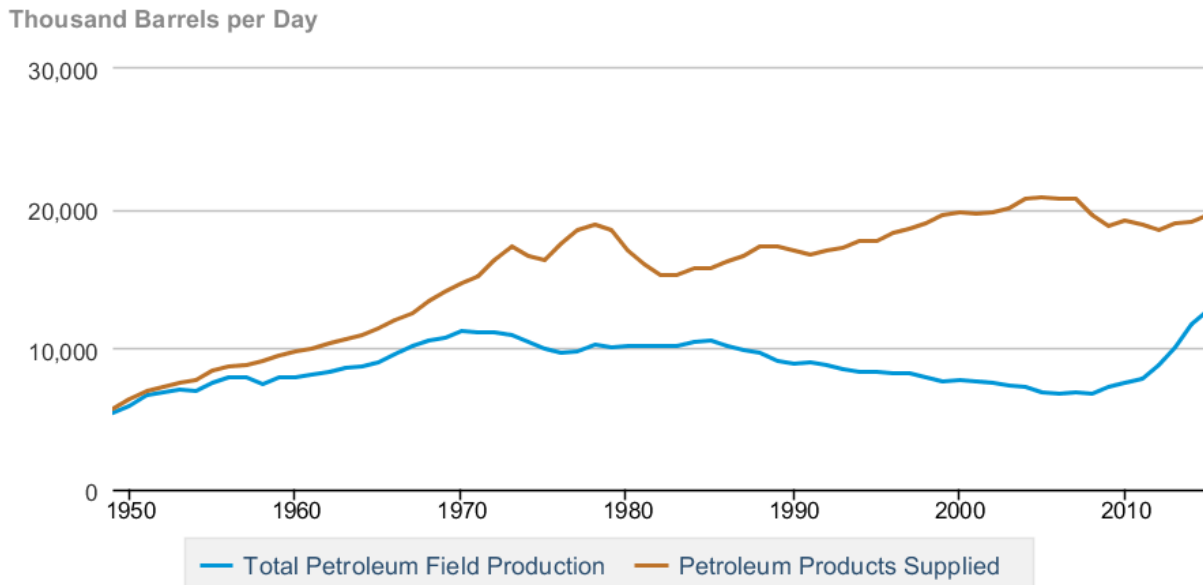
1.1. The case of dwindling fossil fuels and the concept of biorefinery

Since its incipient exploitation that started in the 19th century, crude oil or petroleum has been the most significant fossil-derived hydrocarbon source used for the production of liquid fuels on a global scale. Petroleum reservoirs were formed from the thermogenic and microbial decomposition of organic matter, known as kerogen that occurred over the last millions of years. When the surrounding temperature of kerogen is increased to about 80°C oil is produced¹ and with temperatures exceeding 140°C natural gas is produced². These two types of hydrocarbons coexist and accumulate in porous, permeable rock and move upward in order of decreasing density, owing to faults, fractures and higher permeable strata until prevented by an impermeable barrier³. Thus, the crude oil and natural gas reservoirs form. After their discovery, various extraction methods were intensively developed. Worth mentioning is the technology to crack the crude hydrocarbons into constituent smaller chain aromatics, branched and unbranched polymers, that has quickly emerged and matured into today's probably most relevant chemical engineering endeavor. The fractionated crude delivers commercial liquid fuels such as gasoline, diesel or kerosene and humanity has become irrefutably dependent on a constant high-volume delivery of these fuels to the end consumer and to all major industries.

The downside of this extraordinary process that led to the creation of high-energy packed chemical polymers is that currently (and according to the author's subjective knowledge) it cannot be re-created at a similar time and volume scale. Humanity is therefore plagued with an insatiable thirst for the "black gold" that is a dwindling resource. To put the US consumption and production of fossil fuels into perspective, **Figure 1-1** shows data from 1950 until 2015⁴.



Data source: U.S. Energy Information Administration



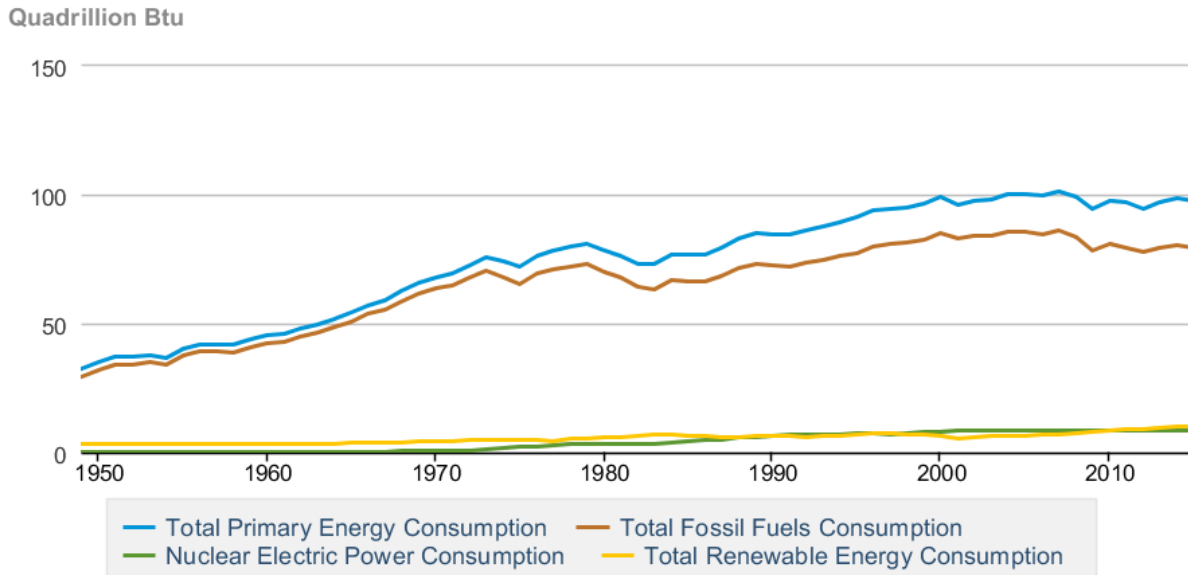
Data source: U.S. Energy Information Administration

Figure 1-1: US production and consumption of natural gas (above) and petroleum products (below) that include liquid fuels from 1950 through 2015. With permission from EIA.

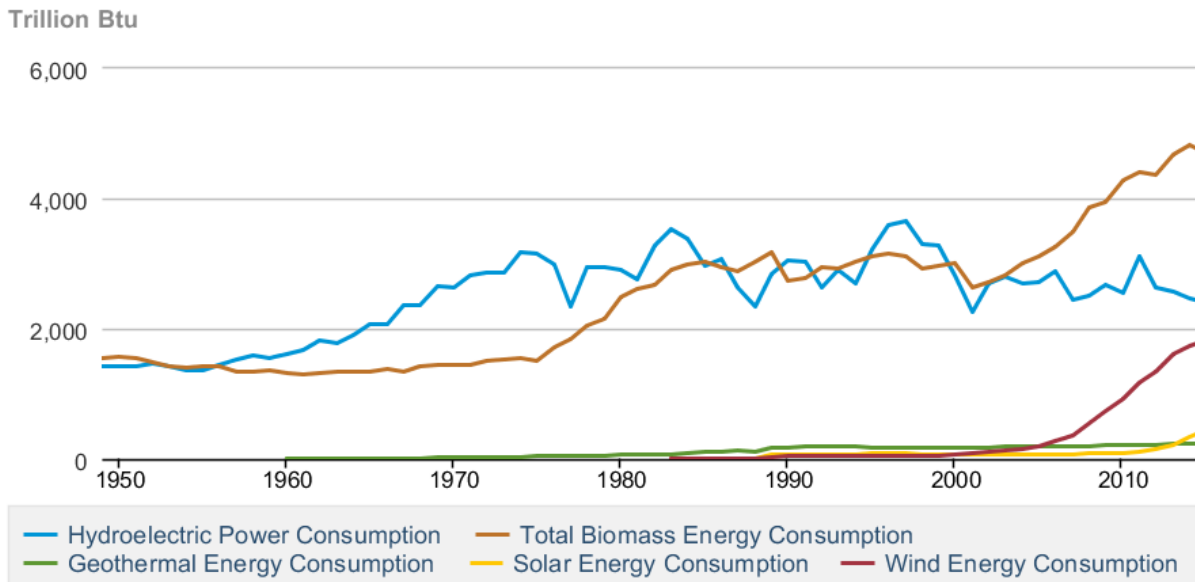
From 1950 and until 2015 the residential and industrial consumption of natural gas and petroleum products, such as liquid fuels, have seen a continuous increase that closely followed the increase

in population growth, standard of living and technological advances in the US. With the advent of the development of fracking technology that drills horizontally into oil wells and, thus reaches more into the reservoirs, the production of fossil fuels has seen a surge in the recent decade. And so, the consumption of fossil fuels is expected to continue its growth trend over the next decades. However, a few limiting factors exist. Fossil fuels are a non-renewable source of energy and their combustion is also releasing tremendous amounts of greenhouse gas (GHG) emissions into the atmosphere which have been linked to the increase in the global annual average temperatures⁵. The latter has been a source of worry for scientists worldwide as it is at the culprit of global climate change with adverse effects on humanity.

Figure 1-2 (above) shows total energy usage from 1950 to present in the US partitioned into fossil-fuel derived, nuclear and using renewable resources as raw material. **Figure 1-2** (below) shows how much of total renewables are derived from hydro, geothermal, solar, wind and biomass. It is worth noticing how biomass accounts for the most relevant portion of total. In addition to that, solar, wind and biomass have all seen a surge in their consumption in the modern decade as Americans became more interested in these types and thus the market demand increased. As a point of reference, the average American household consumed 90 million British thermal units (Btu) in 2009, based on Residential Energy Consumption Survey (RECS) data⁶.



Data source: U.S. Energy Information Administration



Data source: U.S. Energy Information Administration

Figure 1-2: Total energy consumption in the US from 1950 through 2015 (above). Total renewable energy consumed in the US from 1950 through 2015 (below). Total biomass energy consumption includes wood, waste and biofuels. With permission from EIA.

While depletion of fossil fuels has been foreseen imminent in the following decades⁷, humanity is faced with the daunting task of establishing industrial processes using renewable feedstocks which are economically feasible and have output volumes comparable with those of the mammoth-sized petroleum industry. One concept developed that could potentially supply humanity with sustainable renewable energy and that could mitigate the increasing release of GHG is the integrated *biorefinery*. According to the National Renewable Energy Laboratory a biorefinery is defined as a “facility that integrates biomass conversion processes and equipment to produce fuels, power, and chemicals from biomass”. The integrated biorefinery is any processing facility that converts biomass into value-added products that are either completely new or can replace fossil-fuel derived ones. It may involve any of the following types of integration⁸:

- process integration: follows a holistic approach for the design and operation, in that mass, energy and property are regarded as one unit
- infrastructure integration: allows for biorefinery products to access the existing infrastructure. For example, biofuels can use petroleum refinery pipelines or bio-methane can be directly injected into natural gas pipelines
- product integration: exploits the common characteristics of products from biorefinery with those from a petroleum refinery. For example, bio-ethanol can be blended into gasoline or bio-diesel into petrodiesel
- feedstock supply-chain integration: allows for timely coordination of the plant life-cycle with the production activities

- policy and environmental integration: with a tremendous potential for product pathways, adjacent bio-refineries can have connected feedstock and product streams and thus, facilitate the reduction of greenhouse gases as required by environmental regulations.

Second generation feedstocks are of specific interest with the biorefinery processes. These include forestry residues, oils, energy crops, agricultural waste and other non-edible plant material. These feedstocks are interesting to the biorefinery concept since they do not employ edible material and can thus have less of a detrimental long-term impact on food prices⁹. It follows that the biorefinery concept has the potential of becoming a promising sustainable alternative to the well-established petroleum refinery industry, since it uses renewable plant material to produce liquid fuels, gas fuels and commodity polymers that are compatible with current transport and polymer infrastructure. At the heart of bio-refinery technology is the ability to convert cellulosic feedstocks into its building blocks, which can then be further processed into useful end-user products such as bio-fuels, bio-polymers and bio-solvents (**Figure 1-3**).

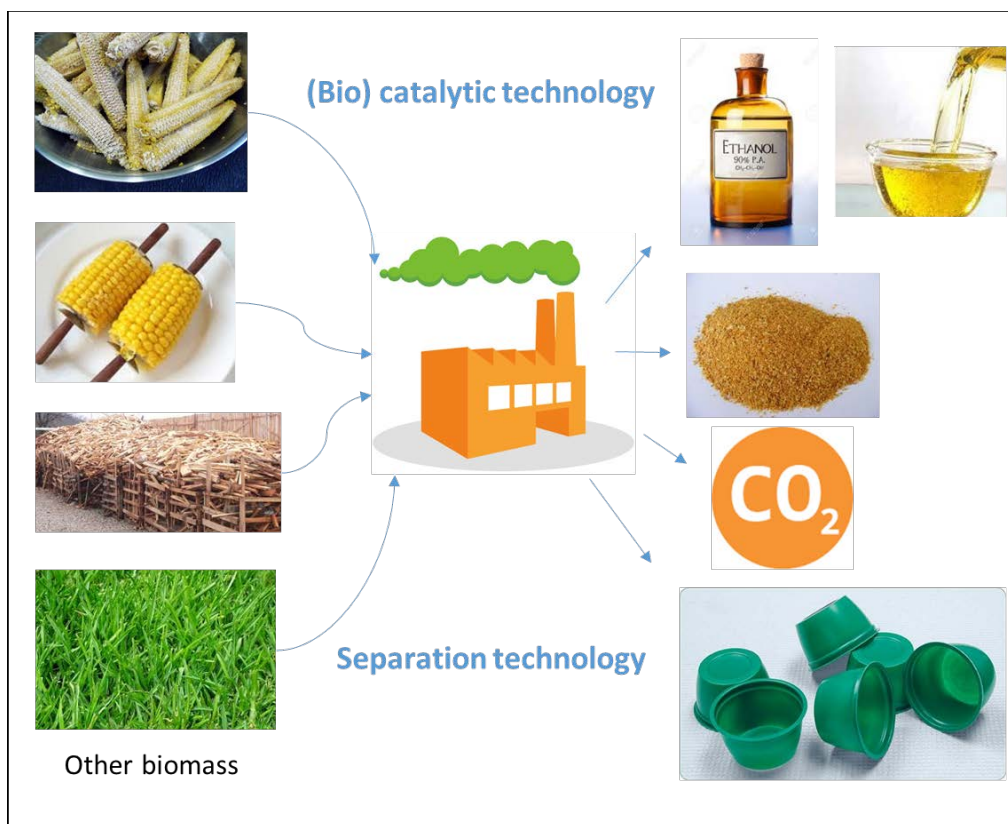


Figure 1-3: Biorefinery and potential green products.

According to Wooley *et al*¹⁰ the common process to derive bio-fuels from raw lignocellulosic biomass is comprised of five main steps: feedstock handling, pretreatment and detoxification, saccharification, fermentation, product separation and purification. Each step, in turn, is performed from a multitude of unit operations. The pretreatment is usually operated with dilute inorganic aqueous solutions, while the saccharification unit operation is mainly operated with the use of enzymes¹¹ – this is often referred to as the biochemical platform. After the pretreatment step, the hydrolysate must be treated to remove unwanted lignin and to adjust pH and temperature for the next step. The saccharification of unreacted hemicellulose and cellulose is then performed via catalyzed hydrolysis. This is because cellulosic material is extremely recalcitrant to depolymerization reactions, mainly due to its crystalline structure¹². For example, cellulose conversion requires a three-step pretreatment and hydrolysis process in order to convert the tightly

packed crystalline matrix of the cellulose biopolymer into simple sugars¹³. Once the sugars have been released into the reaction broth, the products must be separated. This unit operation is usually comprised of centrifugation, filtration and membrane separation process that detoxify and prepare the reaction product for the fermentation step. Afterwards, the cleaned product stream can be converted by diverse microorganisms into a multitude of bio-products, as discussed previously.

Dilute-acid pretreatment, including hydrolysis of hemicellulose, and cellulase enzymes comprise a significant percentage of the cost of cellulosic ethanol production, and build the rationale for the development of cheaper, more efficient strategies¹⁴. Currently, along with the use of enzymes pretreatment with dilute sulfuric acid is one of the dominant technologies to hydrolyze hemicellulosic biomass, relocate lignin and expose cellulose¹⁵ for conversion of biomass to monomer sugars. A mixture of cellulase enzymes is thereafter used to break down cellulose synergistically. The major downside associated with this technology are slow reaction rates, incomplete hydrolysis of cellulose and the degradation of monomer sugars during pretreatment¹⁶. Furthermore, the cost of the enzymes has been an inhibitory factor for the commercialization of biomass conversion technology¹⁶.

Membrane technology has seen tremendous growth in many important applications pertaining to the research and development in the energy and bio-energy industrial sectors. Membrane separations are usually classified based on their pore size and molecular weight cut-off in microfiltration, ultrafiltration, nanofiltration and reverse osmosis. Main advantages of membrane separations is that they offer tremendous variation of separation of species based on their nominal molecular size, 3-dimensional conformation and physical properties, such as charge and polarity. With careful choice of a base membrane and consequent chemical modification additional optimization can be accessed for increased selectivity of species that are otherwise complicated or

impossible to separate by alternative separation techniques (liquid-liquid extraction, precipitation, centrifugation, etc.). More on the membrane separations topic will be discussed in more detail in chapter 1.4.

Here, we propose the development of modified membranes that are to be designed and optimized for the integration as separate unit operations into a complete catalytic membrane reactor system capable of continuous biomass hydrolysis with by-product formation control and solvent recycling. In **Figure 1-4** an envisioned membrane reactor system is shown. This is a holistic approach to cellulosic biomass hydrolysis, reaction stream detoxifying and solvent recycling. At the core of this approach are the two membrane separations.

The first (catalysis) is a modified membrane by another colleague with dual separation and catalysis properties¹⁷. By attaching two polymers with poli(ionic liquid) and poli(styrene sulfonate) functional groups on the surface, these catalytic membranes can be used instead of enzymes to perform catalyzed biomass hydrolysis. In addition to that and with careful experimental design, the thermal degradation of monomeric sugars into furfurals and 5-hydroxymethylfurfural can be overcome. The latter has the potential to mitigate the need of detoxifying the product stream prior to the fermentation step. The author's main involvement with this membrane is to design the experimental setup to test its performance.

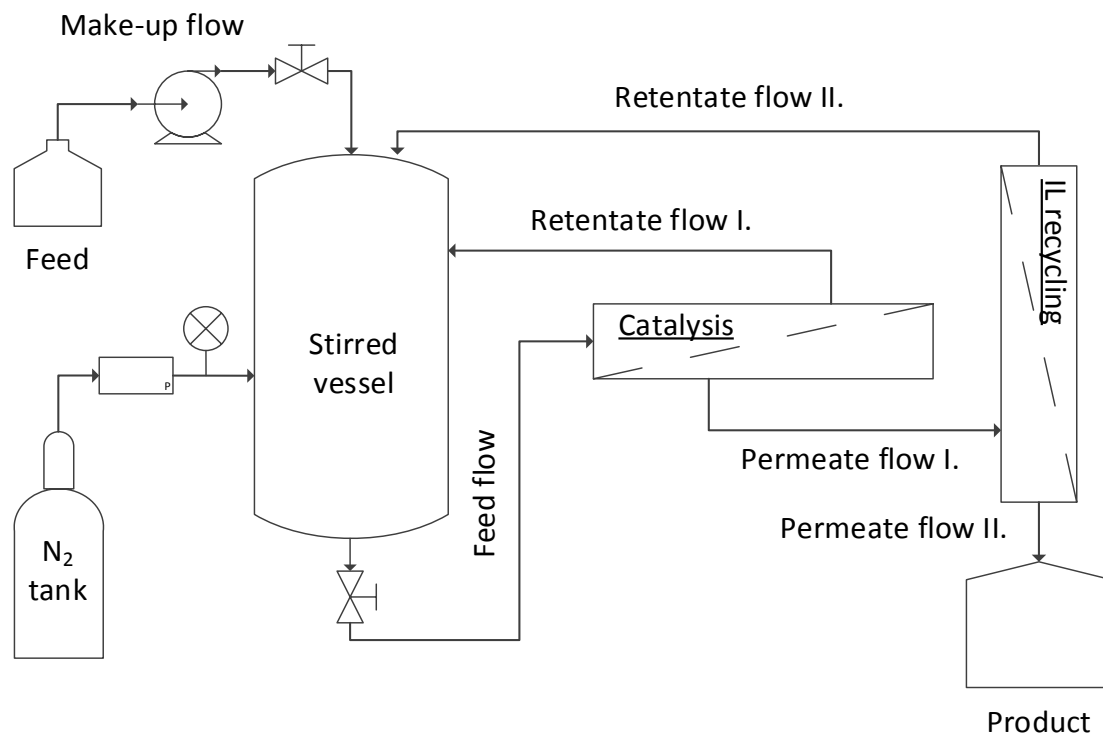


Figure 1-4: Envisioned catalytic membrane reactor system with the modified membrane unit operations for biomass catalysis and ionic liquid recycling. The pressure line is added to control membrane permeability.

The second (IL recycling) is a modified membrane via polyelectrolyte multilayer deposition or via interfacial polymerization with the purpose of recycling non-conventional biomass hydrolysis solvents, such as ionic liquids (ILs). These membranes constitute the main focus of this work. More on the topic of membrane modification, ILs as biomass hydrolysis solvents, their physical properties and their use instead of aqueous systems will be expanded in the subsequent chapter.

1.2. Lignocellulosic biomass hydrolysis

Biomass is the most abundant renewable raw material, with an estimated global regrowth of 1.1×10^{11} tons per annum¹⁸. Lignocellulosic biomass materials are formed from three main biopolymers: lignin, hemicelluloses and cellulose¹⁹. Depending on plant species and part of the plant (stems, leaves, fruit shells, etc) the average major constituents are lignin (25 wt %), hemicellulose

(25 wt %) and cellulose (40-50 wt %)^{20,21}. **Table 1-1** shows the approximate mass distribution by three categories grasses, hardwoods and softwoods.

Table 1-1: Typical composition of lignocellulosic raw materials.

Plant material	Lignin, wt. %	Hemicellulose, wt. %	Cellulose, wt. %
Grasses	10-30	25-40	25-50
Hardwoods	18-25	45-55	24-40
Softwoods	25-35	45-50	25-35

As shown schematically in **Figure 1-5**, cellulose forms crystalline fibrils with amorphous regions that are wrapped by the second most prevalent class of polysaccharide polymers, the hemicelluloses. Lignin fills out the cell walls, around the polysaccharides providing structural rigidity. Cellulosic and hemicellulosic plant material represent a very promising source of fermentable sugars with potential for significant industrial use. They are the raw ingredient for the integrated biorefinery of second generation biofuels.

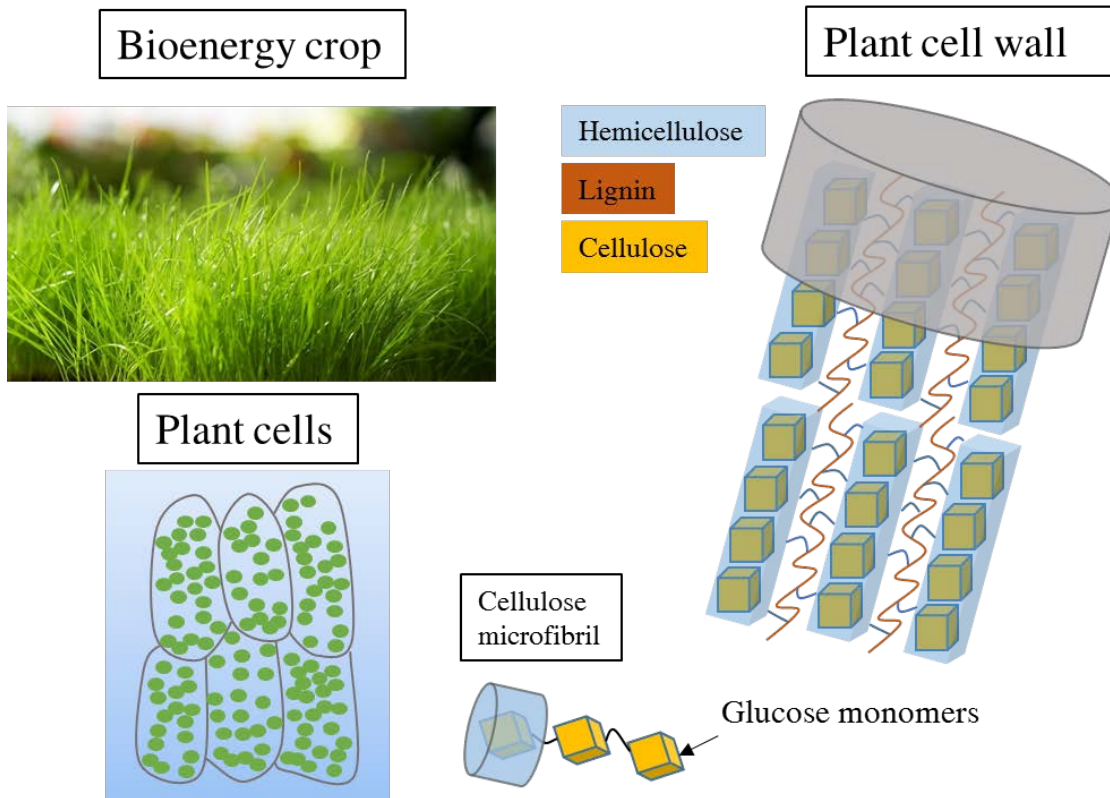


Figure 1-5: Drawing showing schematic structure of plant cell wall with lignocellulosic components. Lignin is a three-dimensional, asymmetrical biopolymer consisting of phenyl units. In plant cells, it fills out the cell walls which contain primarily linear polysaccharidic membranes providing structural rigidity to the cell. Lignin can be found in the cells of vascular plants, ferns and club mosses, but less so in algae and microorganisms²². Just like hemicellulose, it is found in the middle lamella, the secondary wall and the primary wall of the voids of cellulose microfibrils. It functions as a connection between the cells and stabilizes the cell walls of the xylem tissue. Lignin is linked to cellulose or hemicellulose via hydrogen bonds and covalently by ligno-cellulose and lignin-polysaccharide complexes, respectively^{23,24}. The primary building monomers of lignin are the coumaryl alcohols, coniferyl alcohols and sinapyl alcohols (**Figure 1-6**). These are linked asymmetrically through C-C and ether bonds giving rise to the three-dimensional structure of lignin. Interestingly, most of the linkages in the lignin molecule cannot be hydrolyzed²². In nature,

only a limited group of white-rot fungi is able to completely mineralize lignin to CO₂, while some soft-rot and brow-rot fungi can induce structural decomposition²⁵. According to Haider²⁵, this is an oxidative decomposition process performed by a wide number of microorganisms working synergistically.

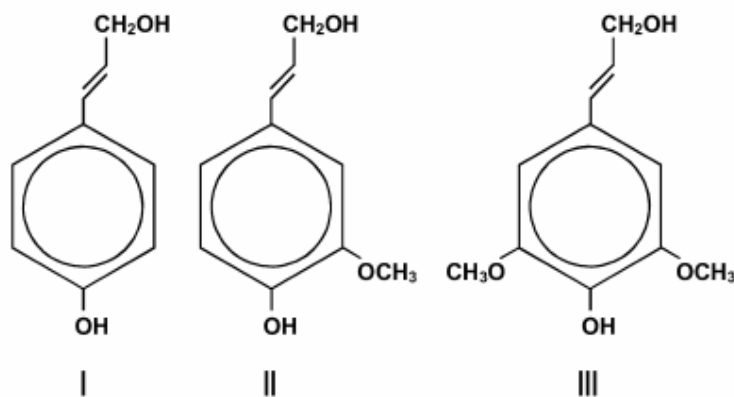


Figure 1-6: Lignin building blocks: oumaryl alcohol (I), coniferyl alcohol (II) and sinapyl alcohol (III).

Hemicellulose is the other large carbohydrate polymer of lignocellulosic biomass which, dependent on the cell type, can be a branched polymer of glucose, xylose, arabinose, galactose, fucose, mannose and glucuronic acid²⁶. Hemicelluloses consist of cellulose-like sugar units linked together with glycosidic bonds (**Figure 1-7**) and have a lower degree of polymerization than cellulose. Depending on the bond and sugar monomer, hemicellulose are often categorized in xylans, mannans, glucomannans or galactans. As opposed to crystalline cellulose, most hemicelluloses are soluble in alkaline aqueous solutions²⁴. Hemicellulose are easily decomposed by many aerobic and anaerobic fungi and bacteria²⁷.

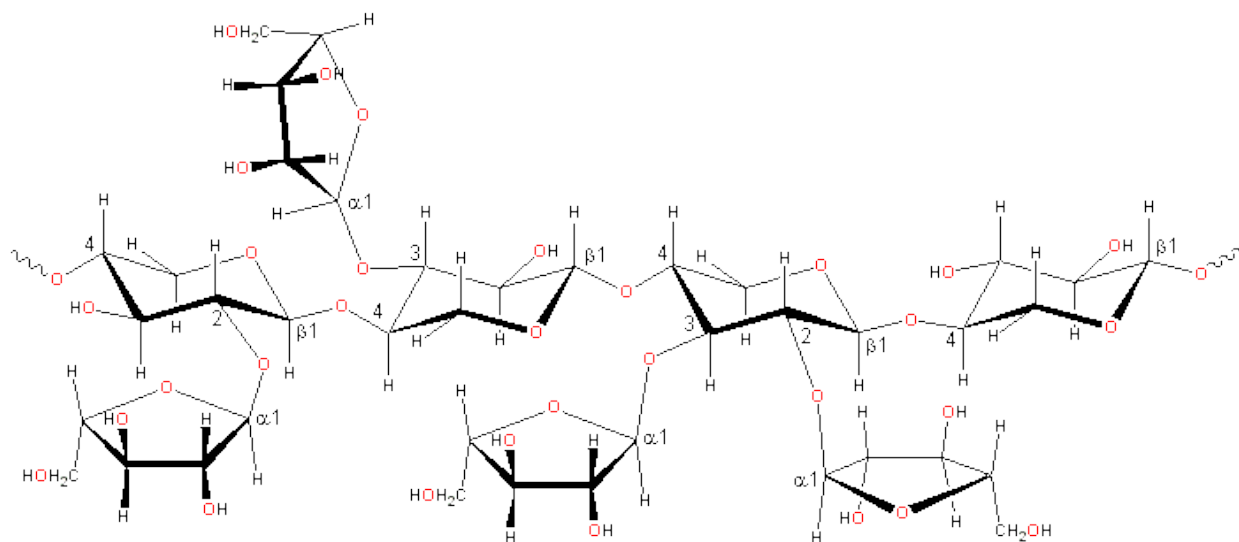


Figure 1-7: Example of one type of hemicellulose (arabinoxylan) with β -(1-4)-glycosidic and α -(1-3)-glycosidic bonds emphasized.

Cellulose is the most abundant lignocellulosic polymer, as it comprises the main structural compartments of the cell walls of lower and higher genus of plants. Cellulose is also the main component of the cell walls of algae and fungi, but it is rarely found in bacteria²⁸. It is a long linear polymer with glucose units $>10,000$ that are covalently linked by β -(1-4)-glycosidic bonds²⁹. The homogenous alignment of the hydroxyl groups on the cellulose polymer leads to the formation of thick network of H-bridges (**Figure 1-8**) and thus to a fibrillary structure with crystalline properties. Some sections of the cellulose molecule are estimated ($\sim 15\%$) to be amorphous¹². In nature, under aerobic conditions, cellulose decomposes slowly under the action of microorganisms such as fungi and eubacteria²⁵. Some families of bacteria can also decompose cellulose slowly to low molecular acids under anaerobic conditions²².

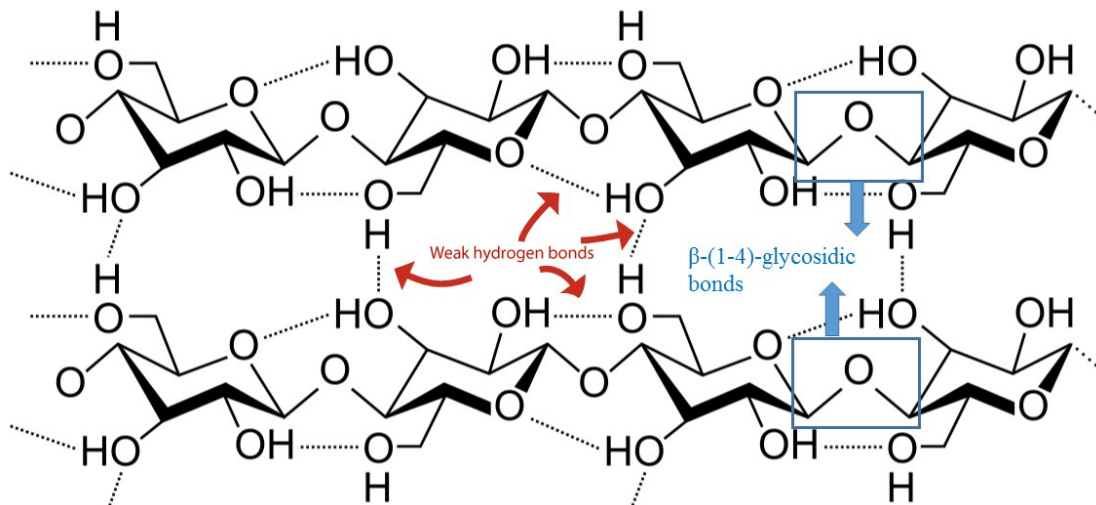


Figure 1-8: Cellulose molecule structure showing intra- and intermolecular weak hydrogen bonds and the covalent C1-C4 glycosidic bond.

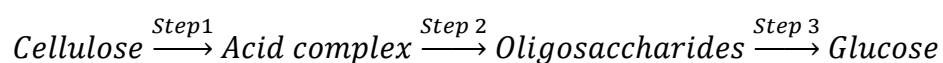
1.2.1. Enzymatic decomposition of cellulose

Lignocellulosic material is comprised of two recalcitrant polymers linked by strong covalent bonds, shielded by intricate heterogeneous structures and organized in three-dimensional structures by dense H-bond networks. This makes their natural degradation complicated, with high-molecular enzymes being heavily inhibited by depolymerization products and their catalytic action often obstructed by structural intricacy. Typically the depolymerization of cellulose occurs by the actions of a consortium of cellulases enzymes, such as endo-1,4- β -glucanases, exo-1,4- β -glucanases and β -glucosidases^{30,31}. These work together synergistically, to break the three-dimensional structure of cellulose, expose the glycosidic bonds and break them into smaller oligosaccharides and eventually to the monomer glucose. Cellulases can be organized in the cellulosome³² of cells or they can be secreted extracellularly. In anaerobic cellulase systems they are found in cellulosomes and surface-attached multienzyme complexes, while in aerobic cellulase systems they are secreted outside the cell^{33,34}. In nature, most cellulose is decomposed aerobically but 5-10% is decomposed by anaerobic organisms in animal rumens, aquatic environments and

soils. As with other enzymes the reaction mechanism is comprised of a substrate-binding site and a catalytic center performing the bond cleavage³⁵.

1.2.2. Chemical decomposition of cellulose

The cellulose polymer can be broken into polysaccharides, oligosaccharide and further into di- and monomers in the presence of a strong acid by addition of a water molecule per broken bond (acid hydrolysis). The latter breaks the covalent glycosidic bond leaving a potential aldehyde group possessing reducing power³⁶. Hydrolysis of the cellulose molecule can occur only after the crystalline structure (H-bonds) of cellulose is destroyed from swelling in concentrated acid^{37,38}. Fan¹² proposed the following simplified mechanism:



The choice of acid and its concentration significantly affects the kinetics and course of cellulose hydrolysis. In 40% hydrochloric acid, cellulose degrades only to smaller oligosaccharides at around 30°C¹². The same smaller glucose polymers are hydrolyzed to glucose via a first-order mechanism only at higher temperatures³⁹. The reaction pathway of acid hydrolysis of cellulose to glucose is widely accepted⁴⁰⁻⁴⁴ to proceed from the protonation of glycoside oxygen. This is shown schematically in **Figure 1-9**. In the first step, an intermediate complex between glycosidic oxygen and a donated proton is rapidly formed followed by the slow (reaction determining step) splitting of glycosidic bonds induced by the addition of a water molecule. The carbonium cation that was formed in the previous step has two cleavage possibilities, depending on the protonation site, as seen in **Figure 1-9**. If the glycosidic oxygen is protonated, the reaction follows path P-I, if the carboxylic oxygen is protonated then it follows path P-II. Other reaction paths have been discussed⁴⁵ but are less widely accepted¹².

The severity of the reaction plays a very important role, as glucose can be easily further hydrolyzed to 5-hydroxymethylfurfural, humins and simple organic acids⁴⁶ (e.g. levulinic acid, formic acid). For fermentation purposes, most of the latter glucose decomposition products are inhibitors and, as such in this work they are deemed undesired hydrolysis products. The catalytic membrane presented in **Figure 1-4** can combat the dehydration of glucose by membrane removal immediately after its formation.

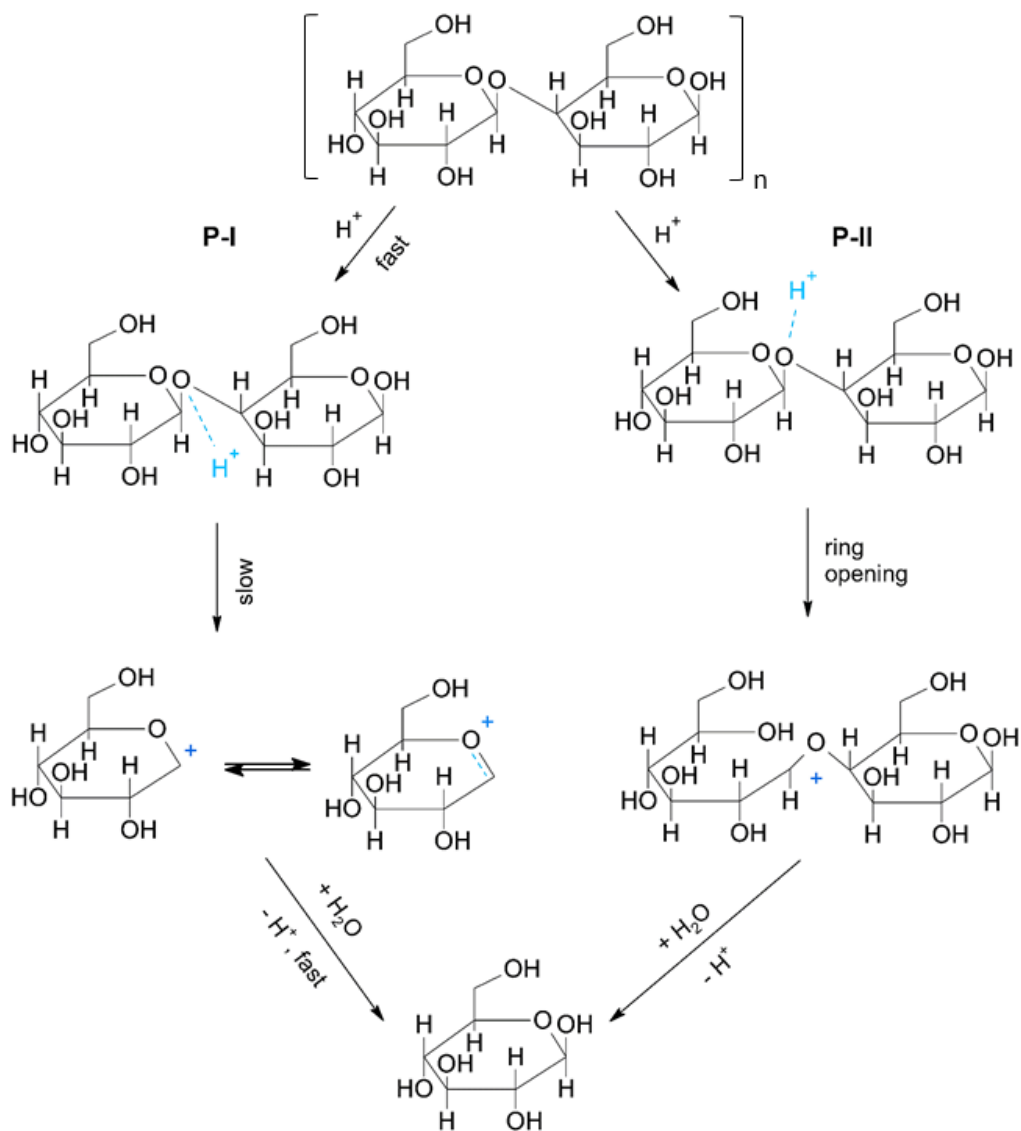


Figure 1-9: Reaction pathways for cellulose acid hydrolysis. n is typically 400-1000 monomers. Adapted from Dr. L.T. Fan¹². With permission from SpringerLink.

1.3. Ionic liquids

In this work we are using ionic liquids (ILs) as reaction solvents for biomass hydrolysis⁴⁷⁻⁴⁹. The colleague modifying the catalytic membranes has been conducting promising experimental work¹⁷ with the ILs shown in **Table 1-2** and we have used their reaction hydrolysates as well as model feeds to test the separation performance of our IL recycling membranes, as described previously in **Figure 1-4**.

Table 1-2: Commercial pricing list of ionic liquids commonly used with biomass hydrolysis.

Ionic liquid	MW, Da	Solubility of cellulose⁵⁰, wt.%	Market price, \$/kg
C2mimOAc	170.21	~ 20	1,015
C4mimOAc	198.26	~ 19	881
C2mimBr	191.07	~ 2	3,420
C4mimBr	219.12	~ 25	1,982
C2mimCl	146.62	~ 14	419
C4mimCl	174.67	~ 10	340

As eloquently rationalized by Seddon⁵¹, to describe all types of ionic liquids, that are estimated at an astounding number of 10^{12} theoretical possible combinations⁵², as merely “molten salts” is “as archaic as describing a car as a horseless carriage”. What he was trying to emphasize is the very wide palette of physico-chemical properties different ionic liquids can possess and their immense potential as novel solvents. However, in the context of lignocellulosic biomass treatment, ionic liquids are commonly defined simply as salts that are found in liquid form at around or below 100°C. The low melting point range of the ILs is important, mostly because it can mitigate solvolysis of the biomass components. In 1934, Gaenacher⁵³ first recognized the dissolution

property of N-ethylpyridinium chloride with cellulose, but it did not caught the attention of the scientific public since it only worked in the presence of nitrogen-containing bases and at relatively high temperature of 118°C. Later, in 2002, the extensive works of Rogers *et al* and Swatloski *et al*^{54,55} tested the feasibility of imidazolium ionic liquids for the dissolution of cellulose. Their successful experimental work drove the interest in these novel solvents further as many other combinations of cations and anions emerged (see **Figure 1-10** for some examples). Then, a new trend was born. Some examples of ILs application are as biomass solvents⁵⁶⁻⁵⁸, for the preparation of cellulose fibers and films⁵⁹⁻⁶¹ or to make cellulose composite materials^{62,63} as well as many other lignocellulosic biomass handling and reaction processes.

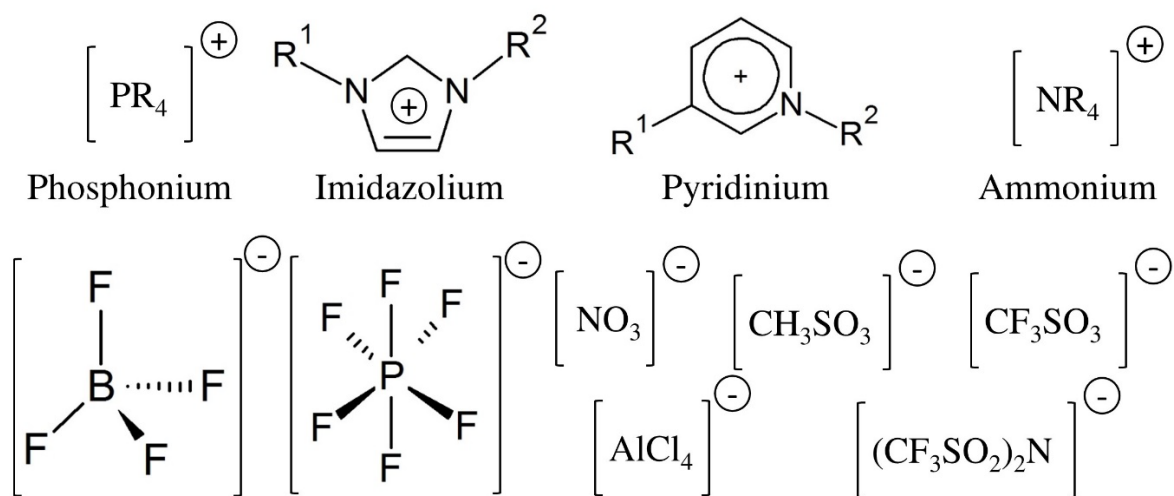


Figure 1-10: Examples of cations and anions used as ILs in biomass dissolution and hydrolysis.

ILs are excellent cellulose solvents with low vapor pressure, low toxicity, low melting points and high mass loadings (up to 39 wt %) ^{57,64}. The chemistry of dissolution is a subject of much debate in the literature, especially aggravated by the misleading data and understanding of dissolution versus decomposition. According to Wang *et al*⁵⁰ whose group wrote an excellent review on the subject, there seems to be much consensus on the properties of the anions, while the effects of cations still remain mostly controversial.

1.3.1. Mode of cellulose dissolution by ionic liquids

Anions that are powerful hydrogen bond acceptor are more efficient in solubilizing cellulose. Low-basicity anions such as dicyanamides are better at dissolving simple monomeric sugars⁶⁵ and not very efficient at dissolving cellulose⁶⁶. ILs containing non-coordinating anions such as BF_4^- or PF_6^- are unable to dissolve cellulose⁶⁷. The degree of cellulose polymerization, the process of purification and inherent structural modifications make it complicated to estimate exactly which anions will perform better but according to Wang *et al*⁵⁰ the capabilities of the following anions decrease in the following order: $\text{OAc}^- > \text{Cl}^- > \text{HCOO}^- > \text{DCA}^- = \text{NTf}_2^-$ and have to be in an excess of at least 1.5-2.5 anion:free hydroxyl groups⁶⁷. Overall, it seems that the anion's most important role is its size and the ability to penetrate the cellulose three-dimensional structure and disrupt the dense H-bond network keeping the crystalline structure strong.

Cations have a more controversial role in cellulose dissolving but they seem to be largely accountable for the structural resilience of ILs, as some are susceptible to decomposition when used in reactions systems with high severity⁶⁸. Ionic liquids containing imidazolium, pyridinium, ammonium and phosphonium cations have been more widely adopted for biomass work and most of the understanding underlying the dissolving of cellulose stems from experimental work with these. Wang *et al*⁵⁰ and Tadesse *et al*¹⁸ suggest that a lot more work needs to be done with other molecular species for more conclusive remarks to be formed. However, the effect of cations can be summarized with the fact that aromatic cations seem to work best. This is believed to be the case due to their ability to shield anion/cellulose polymer complexes, due the fact that aromatics are more easily polarized because of their delocalized charge that forms weaker cation/anions electrostatic bonds^{53,69}. As with the anions, the carbon chain length of cations seems to have an effect on the cellulose dissolving with decreasing power as the chain length increases⁷⁰.

Furthermore, the presence of oxygen atoms in the side chains of cations is believed to interfere with efficient hydrogen bonding of the anion to the cellulose molecule⁶⁵.

1.3.2. Cellulose hydrolysis with ionic liquids

Ideally, the dissolution and depolymerization of lignocellulosic biomass can be combined into one unit operation. That is, biomass containing all three macropolymers that has been only mildly pretreated, for example by comminution or other physically disruptive method, can be fed into a process that releases monomeric sugars and somehow separates the lignin as well. There are many hurdles still needed to be addressed before this ideal can be realized. For example, while there are ionic liquids out there that can be used to selectively cleave the covalent bonds holding the lignin and then precipitate it, there is still a need to harvest the monomeric sugars before they degrade. Biocatalyst are usually susceptible to inhibition even from minute amounts of ionic liquids, so an additional step of cleaning the reactants is necessary. Water is needed for the hydrolysis reaction, but adding it in concentrations higher than 20% w/w tends to reduce biomass solubility and even precipitates the reactants. Recycling of the expensive ionic liquids is still very complicated and thus a major cost drawback. Therefore much more complicated, online controlled reaction systems and intricate strategies need to be developed before economically feasible large scale dissolution and depolymerization systems can breach the bench scale. There are several studies that have investigated the feasibility of the aforementioned strategies and we present a few here.

Under mild reaction conditions (~140°C, 1 atm, ~24h) and without an added acid catalyst, cellulosic raw material dissolved in certain ionic liquids can be almost fully depolymerized (97% total reducing sugar yield) into its water-soluble building blocks⁴⁶. Zhang *et al*⁴⁶ performed experimental and computational work with ionic liquid-water mixtures as solvents for cellulose dissolution and hydrolysis. Interestingly, they observed a catalytic effect of the solvent mixture

with surprisingly high total reducing sugars yields (>90%) at diverse amounts of added water, temperature (90-140°C) and reaction times (1-24h). From computational data they attribute the catalytic effect of the solvent mixture due to a markedly increase in the water dissociation constant (K_w). The enhance in the dissociation constant and thus the increase in H^+ ions is due to the autoionization of water molecules in proximity to the IL. This property mimics that of subcritical water (340°C, 27.5 MPa⁷¹) but under much milder conditions and, if honed intensively, is considered to be of significant value when used for biomass hydrolysis.

By combining a solid catalyst with ionic liquid/water reaction media, Rinaldi *et al*⁷² researched the hydrolysis of commercial α -Cellulose in 1-butyl-3-methylimidazolium chloride. They added macroreticulated acid resins (commercial name Amberlyst 15DRY) and minute amounts of water and were able to reach a 30% glucose yield after 3h. Qian *et al*⁷³ developed a novel solid polymeric acid catalyst for use with 1-butyl-3-methylimidazolium chloride/water and 1-ethyl-3-methylimidazolium chloride/water solvents for fast (~6h) α -Cellulose depolymerization at 130°C. Poly(vinyl imidazolium chloride) and poly(styrene sulfonate) chains have been grown from the surface of commercial inorganic membranes and so dual-functioning membranes were produced. Using atom transfer radical polymerization (ATRP) and UV-initiated polymerization they grew the chains in different lengths and crosslinking degrees. The poly(vinyl imidazolium chloride) or poly(ionic liquid) chains act to solubilize the biomass reaction feed in the proximity of the acid poly(styrene sulfonate) chains.

The research group conducted hydrolysis reactions with the two ILs and measured total reducing sugars yields after 2-24h reaction times at 130-140°C. They found an optimized total reducing sugar yield of 97.4% for 6 hours reaction time using a ceramic membrane modified at UV initiator immobilization time of 15 min and 24h ATRP grafting time.

Deliberate *in situ* hydrolysis of dissolved lignocellulose with ionic liquids and added strong acids catalyst is still a subject of interesting academic small scale studies⁷⁴. A successful commercialization attempt is under way by the start-up Hyrax Energy⁷⁵. One of their concepts involves the hydrolysis of hemicellulose and cellulose in monomers and oligomers using strong water soluble acids, such as sulfuric acid. Since the biomass is completely solubilized in the ionic liquid, there is no regeneration step required and the enzymatic saccharification step is not required. This method when compared to the biocatalysis of biomass has the advantage of being faster. There are other similar studies of *in situ* hydrolysis of pure cellulose⁷⁶⁻⁷⁸ typically done with imidazolium ionic liquids and catalytic amounts of strong acids. The consensus is that only the use of acids with pK_a 's < 1.0 results in hydrolysis with appreciable glucose yields⁷⁶. Binder and Raines⁷⁷ added water in increments and observed 70-80% and 10% yields of glucose and 5-hydroxymethyl furfural, respectively. Zhang *et al*⁷⁹ added N-methylpyrrolidinone (NMP) to the reaction mixture and obtained 69% total reducing sugars and 39% glucose yield at only 70°C. The addition of the co-solvent NMP is a modification of the previous strategies presented and its role is to accelerate dissolution substantially.

Even though the combination of dissolution and hydrolysis in “one-pot” reactions has tremendous potential for the biorefinery concept, it still suffers of many road-blocking drawbacks. From a processing perspective, the separation of sugars from IL and the recycling of the IL is still an issue⁷⁴ that needs to be further improved before large scale economically feasible setups can be advanced.

1.3.3. Separation techniques for biomass hydrolysis applications

For the realization of a fully integrated and economically feasible biorefinery - the *integrated biorefinery* concept was defined in a previous chapter - there are several important unit operations

that require continuous improvement and optimization. Depending on the reaction system used, the main classes of compounds that are present in the reaction broth after the hydrolysis reaction can be categorized into: unreacted biomass, short chain soluble hydrolysis products (e.g. cellobiose), monomeric hydrolysis products (glucose, fructose, xylose, etc), degradation products (HMF, furfurals, humins, organic acids), catalyst (enzyme, solid acid catalyst or soluble acid catalyst) and solvents (ionic liquid, water, other organic solvents). In the previous chapter, methods and strategies that aim at combining both dissolution and depolymerization have been presented. One of the major drawbacks with those is the problematic separation of ionic liquid and monomeric sugars that are released during acid hydrolysis. Many of the ionic liquids that have excellent properties for biomass dissolution and hydrolysis have molecular weights similar to the sugar monomers (**Table 1-3**).

Table 1-3: Molecular weights of sugar monomers released during acid biomass hydrolysis and of ionic liquids commonly used with biomass dissolution.

Chemical species	MW, Da
<i>Ionic liquids</i>	
C2mimOAc	170.21
C4mimOAc	198.26
C2mimBr	191.07
C4mimBr	219.12
C2mimCl	146.62
C4mimCl	174.67
<i>Hydrolysis sugars</i>	
Glucose	180.16
Fructose	180.16
Xylose	150.13
Cellobiose	342.30

For this reason, separation techniques that make use of molecular size differences, such as membrane separation by size-exclusion, are unusable if high selectivity is desired. There are many articles on the use of anti-solvents to precipitate lignin or cellulose in dissolution systems or unreacted cellulose in hydrolysis systems⁸⁰⁻⁸³ but it should be clear that that principle does not work when wanting to selectively recover the ionic liquid from monomeric sugars. While lignin or cellulose can be precipitated with the simple addition of water or other organic solvents such as ethanol or acetone that competes for H-bonding, this cannot be accomplished with glucose or xylose, or any simple sugar for that manner. Here, we review some examples that deal with ionic liquid recovery from biomass hydrolysates. Rinaldi *et al*⁷² precipitated the unreacted cellulose oligomers by water addition and then ran the hydrolysate through a neutral alumina column to remove the acid content. Water content was reduced by vacuum distillation, taking advantage of the low vapor pressure properties of the 1-butyl-3-methylimidazolium chloride. No attempt was made to recover the glucose and other small molecules, which the authors expect to accumulate over the course of repeated cycles recycling. They propose the stopping of reaction at the celooligomer stage to counteract the latter and report an estimated 91% recycling efficiency of IL. Wei *et al*⁸⁴ reused [C₄C₁im]Cl 7 times in the process of legume straw fractionation with ionic liquid water mixtures. The recycling procedure was simply removal of water and they observed an increase of recovered pulp after the 4th cycle. Mai *et al*⁸⁵ used ion exclusion chromatography to recycle [C₂C₁im][MeCO₂] from non-volatile sugars. Francisco *et al*⁸⁶ researched the adsorption of glucose onto zeolites from ionic liquid hydrolysates and their subsequent desorption in water. Shill *et al*⁸⁷ present an alternative procedure of recycling ILs and reconditioning them for multiple use. ILs have the property of forming a biphasic system when combined with an aqueous solution containing an kosmotropic anion, such as sulfate, phosphate or carbonate. The binodal curves for

these mixtures have been fitted to the Merchuk equations and reported previously⁸⁸. The recovery of the IL phase in these mixtures depends on the concentration of the salt and its position in the Hofmeister series. In order of decreasing recovery these are $K_3PO_4 > K_2HPO_4 > K_2CO_3$ ⁸⁷. The recovery of [Amim]Cl was reported to be 96.8%⁸⁸ and over 95% for [Emim]Ac and [Bmim]Ac⁷². Hazarika *et al*⁸⁹ used a commercial nanofiltration membrane and attempted to recover small concentrations (0.01 – 0.03 mM) of 1-n-butyl-3-methylpyridinium tetrafluoroborate from model water/IL mixtures. They reported a rejection of 98.4% without further detail on reuse of IL.

As discussed previously, ILs have been shown to accelerate the saccharification process when combined with small amounts of water⁷³. Furthermore, in combination with the solid acid membrane catalyst discussed earlier they form a re-usable reaction environment when compared to cellulose enzyme cocktails. However, the cost of the aforementioned solvents is inhibitory to the development of large scale processes (see price / kg of IL in **Table 1-2**) and this builds the rationale for the development of novel membranes that are capable of selective separation of reaction products from the expensive solvents. This is a novel and challenging endeavor as classical size separation is rendered complicated if not impossible due to the similar molecular weight of both sugar monomers and ILs, which are in the range of 150 – 200 Da. With careful tuning of the selective layer chemistry we attempt to tweak on other properties such as surface charge and hydrophobicity to attain a mediated selective separation of the charged IL molecules. Details about the chemistry of modification and the separation efficiency of the modified membranes will be discussed later in the subsequent chapters.

1.3.4. Quantitative measurements

Ionic liquids

Ionic liquids have been reported to show peculiar properties when mixed with water in high quantities. For example, Liu *et al*⁹⁰ show a plot of four different ILs (including BmimCl) where the specific conductivity in mS/cm follows a bell shaped curve increasing from below 1 M aqueous solution, reaching to a maximum at 2 M and then decreasing again towards 7 M.

We wanted to make sure that we are conducting rejection experiments in the linear region and so we prepared calibration curves with BmimCl, EmimCl and EmimOAc and observed the ensuing trend. Throughout the analyzed range we did not observe the bell shaped character. We also prepared mixtures of ILs and hydrolysis sugars (glucose, xylose, fructose and cellobiose) to test interference with the sugar analysis method and also did not observe any peculiarity in the calibration curves. The ionic liquid concentration was quantified using a handheld conductivity meter from VWR (Symphony SP70C, Houston, TX) equipped with a 2-electrode conductivity cell of epoxy/platinum and a nominal cell constant of 1.0 cm⁻¹ (Thermo Scientific, Beverly, MA).

Hydrolysis sugars

High-performance liquid chromatography (HPLC) can be successfully used in the quantitative determination of small molecular weight sugars that are representative for biomass hydrolysates. In this work we have used two different HPLC columns with customized analysis protocols to establish calibrations curves for the following sugars: Cellobiose, Glucose, Xylose and Fructose. For the determination of sugars from IL solutions, we have used the colorimetric 3,5-dinitrosalicylic acid (DNS) method. Both HPLC and DNS methods are described in the materials and method section of chapter 2.

1.4. Membrane separations

1.4.1. Membrane separation and classification

Membranes are versatile separation tools that can be found in all chemical, biochemical, pharmaceutical and environmental industrial branches. When the molecular weight-cut off between a desired molecule and the contaminating molecules (e.g. cell debris from a fermentation broth) is large enough, membranes can easily be employed to separate the previous from the latter. Depending on their pore size, membrane can be generally classified into microfiltration (<10 μm), ultrafiltration (<0.1 μm), nanofiltration (<0.01 μm) and reverse osmosis (<0.001 μm). This is schematically summarized in **Figure 1-11**. Each class of membrane has found countless applications in relevant industries.

	Typical pressure, bar	Rejected species	Pore size, μm
Reverse Osmosis	30-60	Bacteria, Fatty acids, Proteins, Dimers, Minerals	10^{-4} - 10^{-3}
Nanofiltration	20-40	Bacteria, Fatty acids, Proteins, Dimers	10^{-3} - 10^{-2}
Ultrafiltration	1-10	Bacteria, Fatty acids, Proteins	10^{-2} - 10^{-1}
Microfiltration	<1	Bacteria, Fatty acids, Small proteins	10^{-1} - 10^1

Figure 1-11: Membrane classification with typical working pressure, pore size and rejected species.

For example, microfiltration membranes are often used as a first step in polishing a desired protein. In more complicated cases, the surface of the membrane can be tuned in such a way to alter or add additional properties to the base membrane. For example, membrane surface charge can be changed (positive to negative or vice-versa) with the deposition of polyelectrolytes or, as another example, catalytic end groups can be grafted on the surface.

One can think of a membrane as an interface, which materializes as a thin barrier layer controlling the mass transfer exchange between two phases. The two phases are usually referred to as feed and permeate, with the latter containing the feed solvent with less or nearly none of the rejected compounds (**Figure 1-12**). The mass transfer is controlled not only by the external forces and the fluid properties but also by the characteristics of the film material, e.g. the membrane.

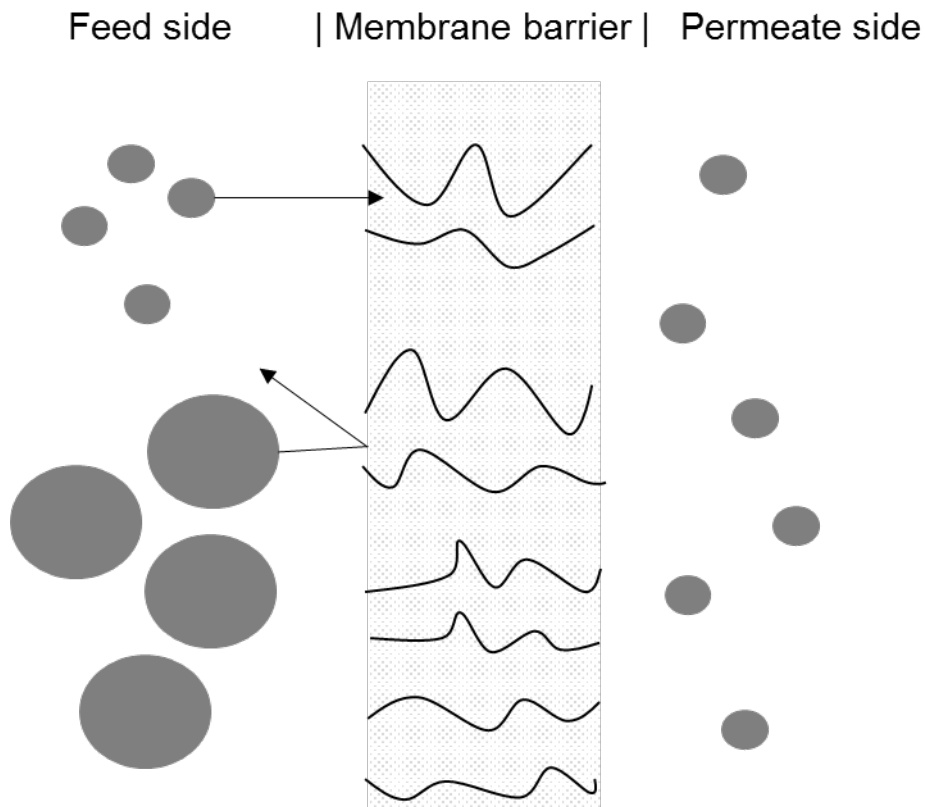


Figure 1-12: Representation of membrane separation by size-exclusion. The feed side contains molecules of different sizes and these can permeate the membrane through channels called pores.

By changing the surface chemistry and morphology of a base membrane, new or improved performance properties such as increased resistance to fouling, higher permeability and selectivity as well as higher rejections can be obtained. From conducting such modifications to base membranes, modified membranes could then serve not only as a separating tool but also as a catalyst or adsorber, thus saving time and resource in real-time reaction processes. Multi-functional modified membranes have, therefore, the potential to combine multiple unit operations. By integrating them in the design of chemical or bio-chemical reactors, new avenues are created for economically more feasible reaction processes.

1.4.2. Market relevance of membrane technology

The global market for membranes and membrane modules sales in 1998 was approximately \$4.4 billion, including gas and liquid separation processes⁹². The US share was at least 40% and 29% were shared by Europe and the Middle East⁹³. With an estimated net annual growth rate (CAGR) of 6.6%, the membrane sales surpassed \$5 billion in the US alone at the beginning of 2005. In 1998 hemodialysis had the largest consumer market followed by microfiltration, ultrafiltration and reverse-osmosis, respectively. About 50% of the reverse-osmosis market was monopolized by Dow/FilmTec and Hydranautics/Nitto products. Current other large manufacturers are DuPont, Osmonics, Pall and Millipore.

Currently, the global market for all membrane separations is expected to grow at a CAGR of 9.47% and is projected to reach a value of 32.14 billion by 2020⁹⁴. Ceramic membranes is the membrane segment projected to grow at a CAGR of 11.96% between 2015 and 2020 due to their outstanding performance under harsh parameters and their less likeliness to foul. However, their fast market expansion is limited by their high cost of manufacture. Other membrane types such as ion-exchange and carbon membranes have a cumulated CAGR of 12.05%. The latter types are

especially growing in interest for battery and energy applications. Nanofiltration technology is amongst the separation technology with the highest CAGR of 12.55%. Due to the trend in political incentives, their main applications are in water and waste water treatment. In all the membrane separation classes, novel modified membranes are expected to emerge for very specific applications and gain on the global market with their versatility.

Membranes have become essential, well-established technologies for water desalination, wastewater treatment, energy generation, bio-pharmaceutical production, food packaging as well as other industrially significant products. When compared to industrially produced membranes, modified membranes are usually tailor-made for very specific applications and, in this report, we will focus mainly on catalytic membranes for membrane reactors. For example, enzymes can be covalently attached to ceramic membranes using glutaraldehyde and a previously adsorbed polymer (e.g. gelatin) giving rise to a series of advantages. The immobilized enzyme will provide catalytic function while the membrane will remove the necessity of subsequent catalyst separation and recovery. Polymers with functional groups, such as acidic sulfonate groups, can be grown or attached on the surface of base membranes for a similar dual function. A more unique and possibly less exploited modification technique is that of pore-filled membranes with diverse chemical or bio-chemical catalysts. For this procedure, the larger porous side of a membrane is filled with catalytic material and then inserted “upside-down” in the membrane holder, that is, with the feed entering through the larger porous size.

Membranes can also be classified according to their nature, geometry and separation regime. Specifically, they can be classified into organic, inorganic and hybrids of the latter two. The choice of membrane type to be used in membrane reactors depends on parameters such as the productivity,

separation selectivity, membrane life time, mechanical and chemical integrity at the operating conditions, and process costs.

When membranes are incorporated in reactors, the resulting setup is often referred to as *membrane reactor*. This setup adds tremendous potential to membrane technology due to the possibility of online control, automatization and unit operation combination.

1.4.3. Nanofiltration

The separation limits of nanofiltration membranes is often expressed with the molecular weight cut-off (MWCO) value. This represents the molecular size in Dalton (Da) units of an idealized molecule which the membrane can reject to 90% or higher. The MWCO of commercially available nanofiltration membranes lies in the range of 200 – 1000 Da, between the ultrafiltration and reverse osmosis ranges (**Figure 1-11**). Mass transfer in nanofiltration is based on two mechanisms: sieving and charge effects^{95,96}. Diffusive transport of uncharged molecules remains pressure independent but concentration dependent, while convective transport increases with pressure^{97,98}. Typical pressures for nanofiltration applications are above 5 bar⁹⁹, but these can vary a lot with different systems. Major applications of nanofiltration include the fractionation of salts¹⁰⁰, oligosaccharides¹⁰¹, small sugars¹⁰² and other molecules, in water treatment¹⁰³⁻¹⁰⁵ as well as for rejections in organic solutions⁹⁹. For example Mahdi *et al.*¹⁰² attempted to modify nanofiltration membranes from depositing polyelectrolytes on the surface of poly(ethersulfone) and they attained increased selectivity for disaccharide versus monosaccharides. Zhang *et al.*¹⁰⁶ used interfacial polymerization from combining the usual trimesoyl chloride with a natural material (tannic acid) to fabricate novel composite material membranes that showed good permeability and increased anti-fouling properties. Yung *et al.*¹⁰⁷ incorporated ionic liquids in the aqueous phase of interfacial polymerization and developed nanofiltration membranes with comparably better rejection and flux

than commercial NF-270 and NF-90 from Dow Filmtec. More recently, a paper published in Science¹⁰⁸ advanced the applications of modified nanofiltration membranes by developing very smooth or crumpled sub-10 nm selective interfacial polymerization layers with excellent permeability towards organic solvents.

Due to their versatility when considering the design of membrane (or membrane reactor) systems, nanofiltration technology has found many application in the food sciences as well^{109,110}. Notable applications are in the volume reduction, selective separation, desalination and fractionation of plant juices and extracts and in the dairy industry for post-processing of dairy products. For example the concentration of health-beneficial polyphenols from fruit juices has seen recent development. Versari *et al.*¹¹¹ used nanofiltration membranes to concentrate grape juice and to increase the sugar content in the concentrate for wine production. Cassano *et al.*¹¹² used nanofiltration membranes with molecular weight cut-off in the range 200-1000 Da to recover bioactive compounds from artichoke brines.

In this work we use commercially available ultrafiltration membranes and proceed by modifying their selective layer for nanofiltration applications. The surface chemistry is modified via layer by layer polyelectrolyte deposition or from growing polyamide thin layers. The chemical modifications allow for control and tweaking of mass transfer properties and thus of rejection and permeability. The two modifications procedures will be treated in more details in chapters 2 and 3. In chapter 4 we use two commercially available nanofiltration membranes to optimize the concentration of polyphenols from blueberry pomace and then build a custom crossflow membrane system to test its feasibility in the continuous volume reduction of blueberry extract.

1.4.4. Fouling of nanofiltration membranes

Membrane separation technology offers many advantages for diverse industrial applications, many of them pertaining to downstream unit operations. These advantages include no phase changes (with the exception of some membrane separations, such as pervaporation), simpler scale up than other similar methods, relatively low energy consumption, often simple experimental/mechanical setup, low maintenance costs and less space requirement¹¹³. However, most membrane process are plagued by concentration polarization and subsequent fouling and cake formation which decrease flux, can affect rejection and also shorten membrane life. As such, membrane fouling is one of the important economic challenges for industrial processes¹¹⁴. Membrane fouling can be defined as the process that leads to loss of performance of a membrane due to deposition of dissolved or suspended molecules on its active surface, at its pore openings or inside the pores¹¹⁵. Depending on how much of the initial performance in terms of permeance can be recovered from simply washing with water, the severity of membrane fouling can be classified in: (i) reversible fouling; (ii) irreversible fouling.

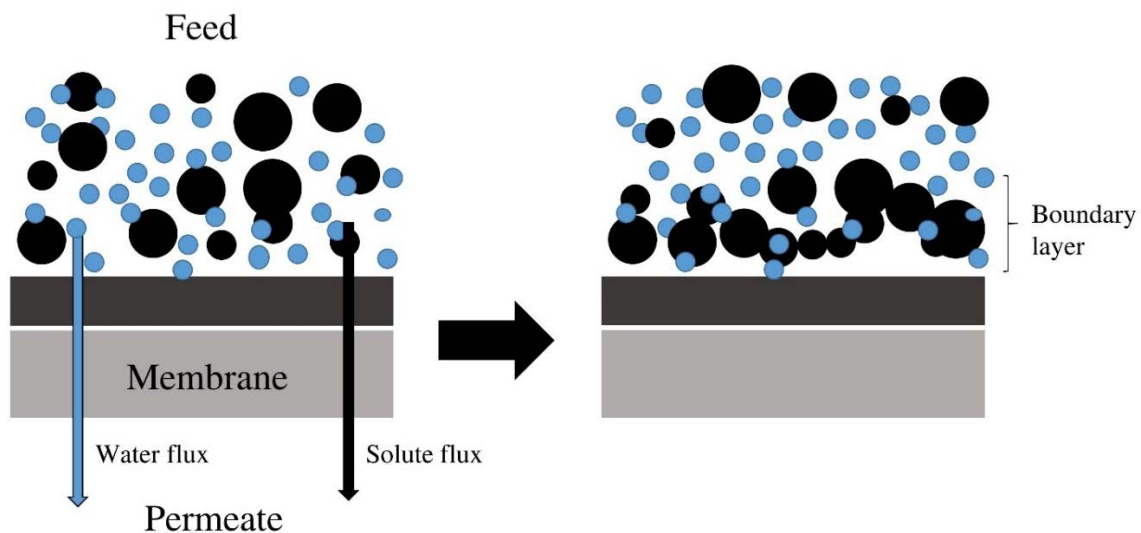


Figure 1-13: Fouling schematic showing the formation of boundary layer at membrane surface.

In **Figure 1-13** a schematic shows what happens during rejection of compounds from a feed containing compounds of different molecular sizes. During concentration polarization (CP), compounds found on the feed side start to agglomerate near the surface of the selective layer and form the CP boundary layer. The boundary layer thickness can be used to quantify the extent of concentration polarization. Schäfer et al¹¹⁶ summarized what are the most important effects that could increase membrane fouling in nanofiltration or reverse osmosis separations:

- (i) chemical reaction of solutes with membrane material
- (ii) adsorption of low molecular mass compounds at the membrane polymer
- (iii) irreversible gel formation of solutes
- (iv) bacterial growth
- (v) deposition of dispersed fine or colloidal matter
- (vi) precipitation of substances that have exceeded solubility threshold.

In nanofiltration, the separation process is driven by pressure and the mass transfer proceeds by convective and diffusive transfer. For salt separations, additional electrostatic interactions play an important role in concentration polarization and thus affect membrane performance. E.g. a Donnan effect stemming from the membrane surface charge can lead to a difference in rejection according to ion charge interactions¹¹⁷. In any case, membrane fouling can be a complex phenomenon and any or all of the aforementioned mechanism can work together to decrease membrane performance. Therefore, recovery methods have to be developed to decrease the negative effects of fouling and recover the membrane performance. Typical recovery methods include washing with water, sonicate, wash with other solvents such as ethanol, methanol, mild acids or mild bases or thermal treatments¹¹⁸.

1.4.5. Membrane reactors

The modified membranes of this work, as depicted in **Figure 1-4**, were designed and optimized as part of the intention to be implemented in a membrane reactor setup. In this subchapter we describe the membrane reactor and then provide the reader with several literature reviewed examples of such setups which inspired the writer to develop his ideas.

According to IUPAC, the definition of a membrane reactor is a system capable of concomitantly performing a chemical (or bio-chemical) reaction and a membrane-based separation, all within the same physical device. As such, the membrane not only plays the role of a separator, but can also take a role in the reaction itself (catalytic membrane). Both organic and inorganic membranes can be successfully employed in the design of membrane reactors. The table below summarizes some of the advantages and disadvantages of inorganic membranes with respect to polymeric membranes.

Table 1-4: Advantages of inorganic membranes with respect to organic membranes.

Advantages	Disadvantages
Long-term stability at high temperatures	High capital cost
Resistance to harsh environments (e.g. pH)	Embrittlement phenomenon
Resistance to high pressure drops	Low membrane surface per module volume
Inertness to microbiological degradation	Difficulty of achieving high selectivities in large microporous membranes
Easier to clean after fouling	Not many manufactures available
Easier catalytic activation	Difficult membrane to design module sealing at high temperatures

Inorganic membranes are usually more costly than polymeric membranes. However, they possess advantages such as resistance towards solvents, high mechanical stability and elevated resistance at high operating temperatures. Therefore, in some cases, although the capital costs of ceramic membranes are higher than those of polymeric membranes, their prolonged operational lifetime can balance out the initial costs^{119,120}. On the other hand, polymeric membranes are more affordable and their surface chemistry is often easier to modify and tune according to application requirements.

Membrane reactors can be designed with several main operating configurations. These can be seen below in **Figure 1-14**.

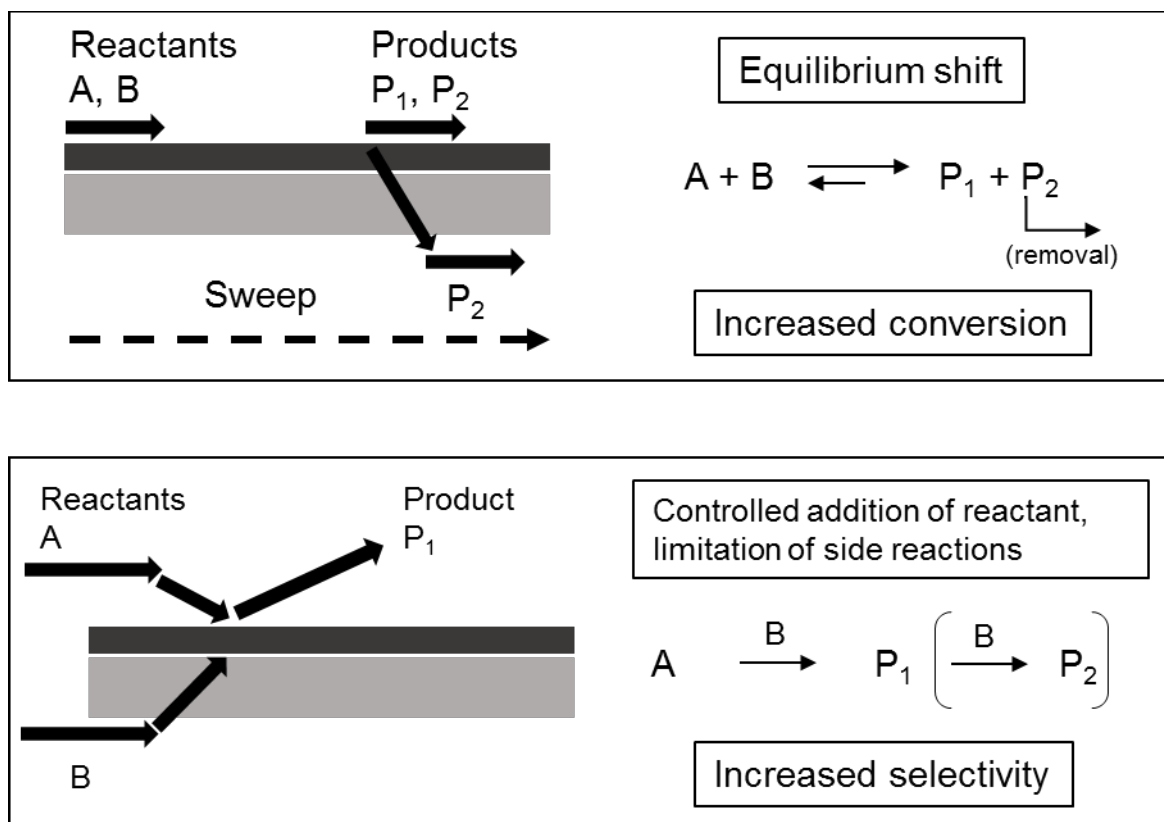


Figure 1-14: Two approaches in membrane reactors: the extractor membrane (above) and the distributor membrane (below) ^{121,122}.

The extractor (**Figure 1-14**, above), which can be used for increased reactant conversion. For example, in the generic reaction $A + B \rightarrow P_1 + P_2$, by removing the desired product P_2 not only can the downstream process be simplified but also the equilibrium of the chemical reaction can be shifted towards the product side. The second class of operating membrane reactor is the distributor (**Figure 1-14**, below), which can be used for increased selective product formation. For example, in a generic reaction with $A + B \rightarrow P_1$, where, at high B concentration also product P_2 is formed, a controlled feed rate of B can be used to selectively inhibit the production of the undesired product P_2 . Thus, with the possibility of using a large variety of organic and inorganic base membranes that each can be modified with many unique functionalities, the amount of modified membranes that can be potentially implemented in membrane reactors becomes

considerably vast. Most of the other configurations, that tend to be even more application-specific, are usually designs derived thereafter. Some examples are the:

- catalytic membrane reactor,
- packed bed membrane reactor,
- catalytic nonperm-selective membrane reactor,
- nonperm-selective membrane reactor and the
- reactant-selective packed bed reactor.

A first example for a specific application are modified membranes for fuel cell applications. A fuel cell is an electrochemical device that converts chemical energy directly into electrical energy. While the most common membranes used are Nafion® or modified versions of it, some advancements have been made using others base materials. E.g. Gohil *et al*¹²³ developed novel pore-filled polyelectrolyte membranes using etched polycarbonate as base membrane that were filled with poly(vinyl alcohol). The poly(vinyl alcohol) deposited inside the porous materials was stabilized by crosslinking the filling material matrix with glutaraldehyde. The scientists tested their novel materials in cathodic microbial fuel cells by assessing the deposited amount of filling material and its correlation to their peak power density measured in mW/cm². They found that the performance is highly dependent upon physico-chemical properties such as water uptake, proton conductivity and gel content and concluded that the water and hydronium anions inside the pores act a proton transfer medium making them ideal for microbial fuel cells applications.

Another team of scientists¹²⁴ developed an active, selective and durable water-gas shift catalytic membrane for use in membrane reactors. The authors screened the most promising combination of Rhodium/Lanthanium/Platinum/Silicon catalyst and compared this to the more common Chromium/Iron catalyst to produce ultrapure hydrogen (<10 ppm of CO). The Fe-Cr are the most often used catalysts in fuel cell membrane reactors where they are employed in the industrial

purification of hydrogen, which is to be used to produce ammonia and other petrochemical products¹²⁵. This type of catalysts were shown to be very selective under steady-state operation. However, Liu *et al*¹²⁶ have shown that the stability of Fe-Cr catalysts is adversely affected by often stop-start operation modes and chromium toxicity is also another downside. After screening different parameters and catalyst recipes, the researchers concluded that the Pt(0.6)/La₂O₃(27)SiO₂ combination resulted in the most active, non-methane forming and the most stable under the water-gas-shift reaction conditions catalytic membrane.

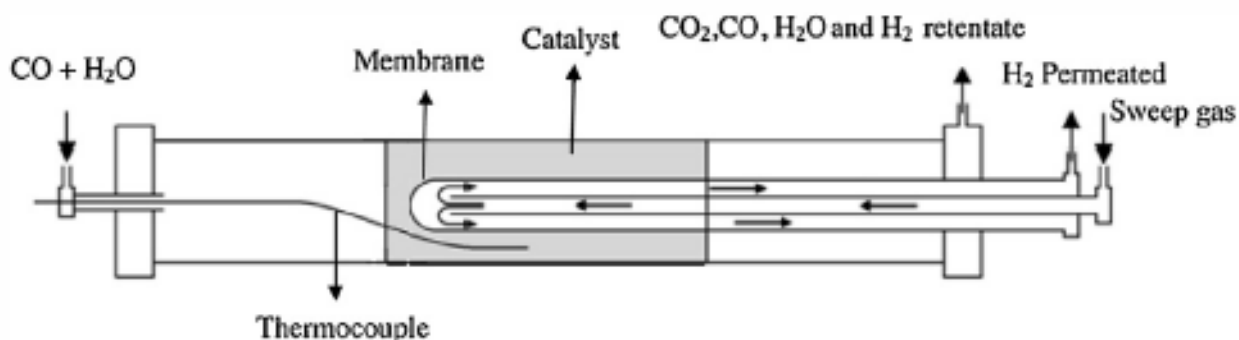


Figure 1-15: Membrane reactor scheme. Reprinted from Liu et al. ¹²⁶, copyright (2005), with permission from Elsevier.

Previously discussed examples of applications were modifications of polymer membranes. However, and more often now, inorganic membranes, such as ceramic membranes, are attracting the attention of scientific research. In a current article, Arca-Ramos *et al*¹²⁷ looked at the potential of a ceramic membrane reactor for the laccase-catalyzed removal of bisphenol-A from secondary effluents. Endocrine disrupting compounds, which are found in communal waste waters, have been suspected to alter the functions of the endocrine system and, thus, cause adverse health effects in living organisms or their offspring¹²⁸. Natural and artificial endocrine disrupters are released into the environment through sewage systems, because conventional wastewater treatment plants can only partially degrade the hormone compounds. One viable solution is through the use of bio-

chemical treatment with enzymes, such as laccase. Laccase are promising catalysts, because they only require O_2 as final electron acceptor in order to catalyze the oxidative degradation of the endocrine disruptors into products that lack the associated hormone-mimicking activity¹²⁹. The main goal of the researcher team was to develop a catalytic membrane reactor for continuous removal of a hydrophobic micropollutant, contained in a model wastewater feed. Nearly complete removal of bisphenol A (95%) was achieved under the investigated parameters.

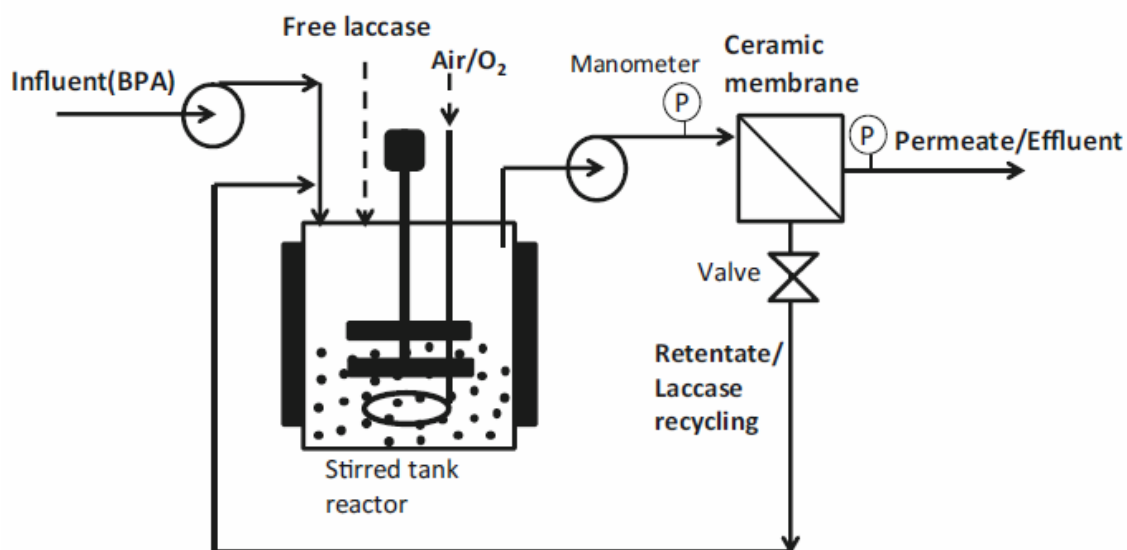


Figure 1-16: Continuous enzymatic membrane reactor. The reactor consists of a stirred tank reactor coupled to a ceramic membrane, which prevented the sorption of the pollutant and allowed the recovery and recycling of the biocatalyst. Reprinted from Arca-Ramos et al.¹²⁷, copyright (2015), with permission from SpringerLink.

Xu *et al*¹³⁰ designed a monolithic catalyst for biodiesel production in a fixed-bed membrane reactor. The research group deposited Ca-Mg-Al hydrotalcite as a second carrier on the inert honeycomb ceramic surface of a base membrane and then loaded KF on the support as an active component. Then the KF/Ca-Mg-Al hydroalcite/honeycomb ceramic monolithic catalyst was packed in a membrane reactor system for the production of biodiesel from the transesterification of soybean oil and methanol. The monolithic catalyst was evenly embedded in the ceramic

membrane, the shape of the honeycomb-like base membrane can be seen in the figure inset. For the chemical reaction, soybean oil and methanol were added into the feedstock vessel in a molar ratio of 1:24, where the reactants were well mixed. The reactant mixture was then pumped into the membrane reactor and the unreacted methanol was recycled back in the feed loop. Biodiesel yield up to 91.7% were obtained and the catalyst showed a reasonable stability, according to the authors. As stated before, when it comes to a process that includes the combination of a reaction or conversion with separation, membranes have mainly found application in a sequential mode, with the reaction part followed by the separation part. The integration of both reaction and separation in the same physical unit has then been defined as a membrane reactor. The general advantages of membrane reactors as compared to sequential reaction-separation systems are: higher reaction rates, lower energy requirement, possibility of heat integration and reduced secondary product formation. With these advantages in mind, compact process equipment that can be operated with a high degree of flexibility has been envisioned and developed¹³¹. Furthermore, because of the capacity to reduce undesired reaction product formation and because of the more efficient use of energy, the development of membrane reactors has paved the way to more sustainable processes for the future^{132,133}.

Disadvantages of catalytic membrane reactors remain the fact the industry is still not ripe in this area and as many hurdles are overcome new issues are being discovered¹³⁴. The amount of catalyst and its stability on the membrane support are key concerns that need to be addressed¹³⁵. Scaling up the modification chemistry from lab scale to industrial scale will impose great difficulties as will the design of adequate membrane casings.

References

1. Tissot BP, Welte DH. *Petroleum formation and occurrence*. 2nd ed. Berlin: Springer-Verlag; 1984.
2. Stainforth J. *New insights into reservoir filling and mixing processes in understanding petroleum reservoirs: Toward an integrated reservoir engineering and geochemical approach*. London: Special Publications Geological Society; 2004.
3. Letcher TM. Future energy - improved, sustainable and clean options for our planet. . 2008.
4. EIA. Energy information administration. <https://www.eia.gov>. Updated 2016. Accessed 11/08, 2016.
5. Global Climate Change. Exploring the environment. http://ete.cet.edu/gcc/?/globaltemp_ghgandtemp/. Updated 2017. Accessed 03/23, 2017.
6. EIA. Residential energy consumption survey. <https://www.eia.gov/consumption/residential/>. Updated 2015. Accessed 11/11, 2016.
7. Rhodes CJ. The oil question: Nature and prognosis. *Sci Prog*. 2008;91(Pt 4):317-375.
8. Stuart P, El-Halwagi M. *Integrated biorefineries. design, analysis and optimization*. Boca Raton, FL: CRC Press; 2013.
9. NYTimes. Corn ethanol increases tacos price. <http://www.nytimes.com/2007/01/19/world/americas/19tortillas.html>. Updated 2007. Accessed 12/08, 2106.
10. Wooley R, Ruth M, Sheehan J, Ibsen K, Majdeski H, Galvez A. Lignocellulosic biomass to ethanol process design and economics utilizing co-current dilute acid prehydrolysis and enzymatic hydrolysis current and futuristic scenarios. . 1999.
11. Huang HJ, Ramaswamy S, Tschirner UW, Ramarao BV. A review of separation technologies in current and future biorefineries. *Separation and Purification Technology*. 2008;62(1):1-21.
12. L.T. Fan MG, Y.H.Lee. *Cellulose hydrolysis*. Springer; 1987.
13. Demirbas MF. Biorefineries for biofuel upgrading: A critical review. *Appl Energy*. 2009;86:S151-S161.
14. Vertes AA, Qureshi N, Yukawa H, Blaschek HP, eds. *Biomass to biofuels: Strategies for global industries*. 1st ed. Wiley; 2010.

15. Pandey A, Larroche C, Ricke S, Dussap C, Gnansounou E, eds. *Biofuels: Alternative feedstocks and conversion processes*. 1st ed. Academic Press; 2011.
16. National Renewable Energy Laboratory. Evaluation of pretreatments of biomass for enzymatic hydrolysis of cellulose. . 2012;1249196981.
17. Qian X, Lei J, Vu A, Sun X, Wickramasinghe SR. Novel polymeric solid acid catalysts for cellulose hydrolysis. *Abstracts of papers of the American Chemical Society*. 2014:247.
18. Tadesse H, Luque R. Advances on biomass pretreatment using ionic liquids: An overview. *Energy & Environmental Science*. 2011;4(10):3913-3929.
19. Higuchi T. *Biochemistry and molecular biology of wood*. Springer Series in Wood Science ed. Syracuse NY: Springer; 1997.
20. Chum HL. *The electrochemistry of biomass and derived materials*. American Chemical Society; 1985.
21. Saravanan V, Waijers DA, Ziari M, Noordermeer MA. Recovery of 1-butanol from aqueous solutions using zeolite ZSM-5 with a high si/al ratio; suitability of a column process for industrial applications. *Biochem Eng J*. 2010;49(1):33-39.
22. Kogel-Knabner I. The macromolecular organic composition of plant and microbial residues as inputs to soil organic matter. *Soil Biol Biochem*. 2002;34(2):139-162.
23. Fengel D, Wegener G. *Wood: Chemistry, ultrastructure, reactions*. Kassel: Verlag Kassel; 2003.
24. Sjostrom E. *Wood chemistry: Fundamentals and applications*. Second Edition ed. San Diego: Academic Press; 1993.
25. Haider K. *Problems related to the humification processes in soils of the temperature climate*. Vol. 7 ed. New York: Soil Biochemistry.
26. CARPITA N, GIBEAUT D. Structural models of primary-cell walls in flowering plants - consistency of molecular-structure with the physical-properties of the walls during growth. *Plant J*. 1993;3(1):1-30.
27. Swift MJ. *Decomposition in terrestrial ecosystems*. Studies in ecology ed. Blackwell; 1979.
28. De Leeuw JW, Largeau C. *A review of macromolecular organic compounds that comprise living organisms and their role in kerogen, coal and petroleum formation*. Organic Geochemistry ed. New York: Plenum Press; 1993.

29. Perez J, Munoz-Dorado J, de la Rubia R, Martinez J. Biodegradation and biological treatments of cellulose, hemicellulose and lignin. *Int Microbiol.* 2002;5:53-63.
30. Hatakka A. *Biodegradation of lignin*. Lignin, humic substances and coal ed. New York: Wiley-WCH; 2001.
31. Leonowicz A, Matuszewska A, Luterek J, et al. Biodegradation of lignin by white rot fungi. *Fungal Genet Biol.* 1999;27(2-3):175-185.
32. Mathews SL, Pawlak J, Grunden AM. Bacterial biodegradation and bioconversion of industrial lignocellulosic streams. *Appl Microbiol Biotechnol.* 2015;99(7):2939-2954.
33. Fontes CMGA, Gilbert HJ. Cellulosomes: Highly efficient nanomachines designed to deconstruct plant cell wall complex carbohydrates. *Annu Rev Biochem.* 2010;79:655-681.
34. Pason P, Kyu K, Ratanakhanokchai K. Paenibacillus curdlanolyticus strain B-6 xylanolytic-cellulolytic enzyme system that degrades insoluble polysaccharides. *Appl Environ Microbiol.* 2006;72(4):2483-2490.
35. BEGUIN P, AUBERT J. The biological degradation of cellulose. *FEMS Microbiol Rev.* 1994;13(1):25-58.
36. Wenzl H. *The chemical technology of wood*. 111 5th Avenue, New York, New York: Academy Press, Inc.; 1970.
37. Goto K, Sakai Y, Kamiyama Y, Kobayashi T. The rate of cellulose hydrolysis by a small amount of concentrated sulfuric acid. *Agr Biol Chem.* 1971;35(1):111-114.
38. WHALLEY E. Pressure effect and mechanism in acid catalysis .1. *Transactions of the Faraday Society.* 1959;55(5):798-808.
39. Goldstein I. *Organic chemicals from biomass*. Florida: CRC Press; 1981.
40. BERINGER F, SANDS S. The synthesis, acidity and decarboxylation of substituted mesitoic acids. *J Am Chem Soc.* 1953;75(14):3319-3322.
41. BUNTON C, LEWIS T, LLEWELLYN D, VERNON C. Mechanisms of reactions in the sugar series .1. the acid-catalysed hydrolysis of alpha-methyl and beta-methyl and alpha-phenyl and beta-phenyl D-glucoopyranosides. *Journal of the Chemical Society.* 1955:4419-4423.
42. Freudenberg K, Blomqvist G. Die hydrolyse der cellulose und ihrer oligosaccharide. *Chem Institut d. Universitaet Heidelberg.* 1935;68:2070.

43. Hammett L, Paul M. The relation between the rates of some acid catalyzed reactions and the acidity function, H₀. *JACS*. 1934;56:830.
44. NEVELL T, UPTON W. Hydrolysis of cotton cellulose by hydrochloric-acid in benzene. *Carbohydr Res*. 1976;49(JUL):163-174.
45. Szetli J. *Saurehydrolyse glycosidischer bindungen*. Leipzig: VEB; 1975.
46. Zhang Y, Du H, Qian X, Chen EY-. Ionic liquid-water mixtures: Enhanced K_w for efficient cellulosic biomass conversion. *Energy Fuels*. 2010;24:2410-2417.
47. Amarasekara AS, Owereh OS. Hydrolysis and decomposition of cellulose in bronsted acidic ionic liquids under mild conditions. *Ind Eng Chem Res*. 2009;48(22):10152-10155.
48. Li C, Zhao ZK. Efficient acid-catalyzed hydrolysis of cellulose in ionic liquid. *Advanced Synthesis & Catalysis*. 2007;349(11-12):1847-1850.
49. Li C, Wang Q, Zhao ZK. Acid in ionic liquid: An efficient system for hydrolysis of lignocellulose. *Green Chem*. 2008;10(2):177-182.
50. Wang H, Gurau G, Rogers RD. Ionic liquid processing of cellulose. *Chem Soc Rev*. 2012;41(4):1519-1537.
51. Seddon K. Ionic liquids for clean technology. *J Chem Technol Biotechnol*. 1997;68(4):351-356.
52. Ramnial T, Ino D, Clyburne J. Phosphonium ionic liquids as reaction media for strong bases. *Chem Commun*. 2005(3):325-327.
53. Graenacher C, inventor1934.
54. Rogers R, Seddon K. Ionic liquids - solvents of the future? *Science*. 2003;302(5646):792-793.
55. Holbrey J, Swatloski R, Reichert W, et al. Getting started with ionic liquids: An experience-based tutorial. *Abstr Pap Am Chem Soc*. 2003;226:U620-U620.
56. Liu Q, Zhang Z, Zhang F. Progress in biocatalytic reactions in ionic liquids. *Prog Chem*. 2005;17(6):1060-1066.
57. Heinze T, Schwikal K, Barthel S. Ionic liquids as reaction medium in cellulose functionalization. *Macromol Biosci*. 2005;5(6):520-525.
58. Mazza M, Catana D, Vaca-Garcia C, Cecutti C. Influence of water on the dissolution of cellulose in selected ionic liquids. *Cellulose*. 2009;16(2):207-215.

59. Bagheri M, Rodriguez H, Swatloski RP, Spear SK, Daly DT, Rogers RD. Ionic liquid-based preparation of cellulose-dendrimer films as solid supports for enzyme immobilization. *Biomacromolecules*. 2008;9(1):381-387.
60. Quan S, Kang S, Chin I. Characterization of cellulose fibers electrospun using ionic liquid. *Cellulose*. 2010;17(2):223-230.
61. Turner M, Spear S, Holbrey J, Rogers R. Production of bioactive cellulose films reconstituted from ionic liquids. *Biomacromolecules*. 2004;5(4):1379-1384.
62. Sun N, Swatloski RP, Maxim ML, et al. CELL 285-cellulose composite fibers prepared from ionic liquid-based solution. *Abstr Pap Am Chem Soc*. 2008;235.
63. Rahatekar SS, Rasheed A, Jain R, et al. Solution spinning of cellulose carbon nanotube composites using room temperature ionic liquids. *Polymer*. 2009;50(19):4577-4583.
64. El Seoud OA, Koschella A, Fidale LC, Dorn S, Heinze T. Applications of ionic liquids in carbohydrate chemistry: A window of opportunities. *Biomacromolecules*. 2007;8(9):2629-2647.
65. Zhao H, Baker GA, Song Z, Olubajo O, Crittle T, Peters D. Designing enzyme-compatible ionic liquids that can dissolve carbohydrates. *Green Chem*. 2008;10(6):696-705.
66. Xu A, Wang J, Wang H. Effects of anionic structure and lithium salts addition on the dissolution of cellulose in 1-butyl-3-methylimidazolium-based ionic liquid solvent systems. *Green Chem*. 2010;12(2):268-275.
67. Swatloski R, Spear S, Holbrey J, Rogers R. Ionic liquids: New solvents for non-derivitized cellulose dissolution. *Abstr Pap Am Chem Soc*. 2002;224:U622-U622.
68. Nieto de Castro CA. Thermophysical properties of ionic liquids: Do we know how to measure them accurately? *J Mol Liq*. 2010;156(1):10-17.
69. Fernandes AM, Rocha MAA, Freire MG, Marrucho IM, Coutinho JAP, Santos LMNBF. Evaluation of cation-anion interaction strength in ionic liquids. *J Phys Chem B*. 2011;115(14):4033-4041.
70. Erdmenger T, Haensch C, Hoogenboom R, Schubert US. Ionic liquids and their application in cellulose chemistry. *Abstr Pap Am Chem Soc*. 2007;233.
71. Srokol Z, Bouche A, van Estrik A, Strik R, Maschmeyer T, Peters J. Hydrothermal upgrading of biomass to biofuel; studies on some monosaccharide model compounds. *Carbohydr Res*. 2004;339(10):1717-1726.
72. Rinaldi R, Meine N, vom Stein J, Palkovits R, Schueth F. Which controls the depolymerization of cellulose in ionic liquids: The solid acid catalyst or cellulose? *ChemSusChem*. 2010;3(2):266-276.

73. Qian XH, Lei J, Wickramasinghe SR. Novel polymeric solid acid catalysts for cellulose hydrolysis. *Rsc Advances*. 2013;3(46):24280-24287.
74. Brandt A, Grasvik J, Hallett JP, Welton T. Deconstruction of lignocellulosic biomass with ionic liquids. *Green Chem*. 2013;15(3):550-583.
75. Hyraxenergy. <http://hyraxenergy.com/>. Updated 2016. Accessed 12/06, 2016.
76. Vanoye L, Fanselow M, Holbrey JD, Atkins MP, Seddon KR. Kinetic model for the hydrolysis of lignocellulosic biomass in the ionic liquid, 1-ethyl-3-methyl-imidazolium chloride. *Green Chem*. 2009;11(3):390-396.
77. Binder JB, Raines RT. Fermentable sugars by chemical hydrolysis of biomass. *Proc Natl Acad Sci U S A*. 2010;107(10):4516-4521.
78. Binder JB, Blank JJ, Cefali AV, Raines RT. Synthesis of furfural from xylose and xylan. *ChemSusChem*. 2010;3(11):1268-1272.
79. Liu L, Zhang Y, Zhang L, et al. Highly specific revelation of rat serum glycopeptidome by boronic acid-functionalized mesoporous silica. *Anal Chim Acta*. 2012;753:64-72.
80. Fort DA, Remsing RC, Swatloski RP, Moyna P, Moyna G, Rogers RD. Can ionic liquids dissolve wood? processing and analysis of lignocellulosic materials with 1-n-butyl-3-methylimidazolium chloride. *Green Chem*. 2007;9(1):63-69.
81. Sun N, Rahman M, Qin Y, Maxim ML, Rodriguez H, Rogers RD. Complete dissolution and partial delignification of wood in the ionic liquid 1-ethyl-3-methylimidazolium acetate. *Green Chem*. 2009;11(5):646-655.
82. Viell J, Marquardt W. Disintegration and dissolution kinetics of wood chips in ionic liquids. *Holzforschung*. 2011;65(4):519-525.
83. Dibble DC, Li C, Sun L, et al. A facile method for the recovery of ionic liquid and lignin from biomass pretreatment. *Green Chem*. 2011;13(11):3255-3264.
84. Wei L, Li K, Ma Y, Hou X. Dissolving lignocellulosic biomass in a 1-butyl-3-methylimidazolium chloride-water mixture. *Ind Crop Prod*. 2012;37(1):227-234.
85. Ngoc Lan Mai, Nam Trung Nguyen, Kim J, Park H, Lee S, Koo Y. Recovery of ionic liquid and sugars from hydrolyzed biomass using ion exclusion simulated moving bed chromatography. *J Chromatogr A*. 2012;1227:67-72.
86. Francisco M, Mlinar AN, Yoo B, Bell AT, Prausnitz JM. Recovery of glucose from an aqueous ionic liquid by adsorption onto a zeolite-based solid. *Chem Eng J*. 2011;172(1):184-190.

87. Shill K, Padmanabhan S, Xin Q, Prausnitz JM, Clark DS, Blanch HW. Ionic liquid pretreatment of cellulosic biomass: Enzymatic hydrolysis and ionic liquid recycle. *Biotechnol Bioeng.* 2011;108(3):511-520.
88. Deng Y, Chen J, Zhang D. Phase diagram data for several salt plus salt aqueous biphasic systems at 298.15 K. *J Chem Eng Data.* 2007;52(4):1332-1335.
89. Swatloski R, Spear S, Holbrey J, Rogers R. Dissolution of cellulose with ionic liquids. *J Am Chem Soc.* 2002;124(18):4974-4975.
90. Liu W, Cheng L, Zhang Y, Wang H, Yu M. The physical properties of aqueous solution of room-temperature ionic liquids based on imidazolium: Database and evaluation. *J Mol Liq.* 2008;140(1-3):68-72.
91. Intechopen. Membrane classification. <http://www.intechopen.com/source/html/37613/media/image11.png>. Accessed 12/05, 2016.
92. Paul R, Yampolskii Y. *Polymeric gas-separation membranes*. CRC Press; 1994.
93. Katoh M, Inone M, Hashimoto T, Furono N. Hydrocarbon vapor recovery with membrane technology. . 1993.
94. MarketsandMarkets. Projection of market value for membrane separations. <https://www.marketsandmarkets.com/>. Accessed 09/15, 2016.
95. Goulas A, Grandison A, Rastall R. Fractionation of oligosaccharides by nanofiltration. *J Sci Food Agric.* 2003;83(7):675-680.
96. Goulas A, Kapasakalidis P, Sinclair H, Rastall R, Grandison A. Purification of oligosaccharides by nanofiltration. *J Membr Sci.* 2002;209(1):321-335.
97. RAUTENBACH R, GROSCHL A. Separation potential of nanofiltration membranes. *Desalination.* 1990;77(1-3):73-84.
98. ERIKSSON P. Nanofiltration extends the range of membrane filtration. *Environ Prog.* 1988;7(1):58-62.
99. Vandezande P, Gevers LEM, Vankelecom IFJ. Solvent resistant nanofiltration: Separating on a molecular level. *Chem Soc Rev.* 2008;37(2):365-405.
100. Xu Y, Lebrun RE. Comparison of nanofiltration properties of two membranes using electrolyte and non-electrolyte solutes. *Desalination.* 1999;122(1):95-105. doi: [http://dx.doi.org/10.1016/S0011-9164\(99\)00031-4](http://dx.doi.org/10.1016/S0011-9164(99)00031-4).
101. Bowen W, Mukhtar H. Characterisation and prediction of separation performance of nanofiltration membranes. *J Membr Sci.* 1996;112(2):263-274.

102. Malmali M, Wickramasinghe SR, Tang J, Cong H. Sugar fractionation using surface-modified nanofiltration membranes. *Separation and Purification Technology*. 2016;166:187-195.
103. Nyström M, Kaipia L, Luque S. Fouling and retention of nanofiltration membranes. *J Membr Sci*. 1995;98(3):249-262. doi: [http://dx.doi.org/10.1016/0376-7388\(94\)00196-6](http://dx.doi.org/10.1016/0376-7388(94)00196-6).
104. Archer A, Mendes A, Boaventura R. Separation of an anionic surfactant by nanofiltration. *Environ Sci Technol*. 1999;33(16):2758-2764.
105. Hagemeyer G, Gimbel R. Modelling the rejection of nanofiltration membranes using zeta potential measurements. *Sep Purif Technol*. 1999;15(1):19-30.
106. Zhang Y, Su Y, Peng J, et al. Composite nanofiltration membranes prepared by interfacial polymerization with natural material tannic acid and trimesoyl chloride. *J Membr Sci*. 2013;429:235-242.
107. Yung L, Ma H, Wang X, et al. Fabrication of thin-film nanofibrous composite membranes by interfacial polymerization using ionic liquids as additives. *J Membr Sci*. 2010;365(1-2):52-58.
108. Karan S, Jiang Z, Livingston AG. Sub-10 nm polyamide nanofilms with ultrafast solvent transport for molecular separation. *Science*. 2015;348(6241):1347-1351.
109. Jiao B, Cassano A, Drioli E. Recent advances on membrane processes for the concentration of fruit juices: A review. *J Food Eng*. 2004;63(3):303-324.
110. Cassano A, Drioli E, Galaverna G, Marchelli R, Di Silvestro G, Cagnasso P. Clarification and concentration of citrus and carrot juices by integrated membrane processes. *J Food Eng*. 2003;57(2):153-163.
111. Versari A, Ferrarini R, Parpinello G, Galassi S. Concentration of grape must by nanofiltration membranes. *Food Bioprod Process*. 2003;81(C3):275-278.
112. Cassano A, Cabri W, Mombelli G, Peterlongo F, Giorno L. Recovery of bioactive compounds from artichoke brines by nanofiltration. *Food Bioprod Process*. 2016;98:257-265.
113. Kang G, Cao Y. Application and modification of poly(vinylidene fluoride) (PVDF) membranes - A review. *J Membr Sci*. 2014;463:145-165.
114. Tomer N, Mondal S, Wandera D, Wickramasinghe SR, Husson SM. Modification of nanofiltration membranes by surface-initiated atom transfer radical polymerization for produced water filtration. *Sep Sci Technol*. 2009;44(14):3346-3368.
115. Koros W, Ma Y, Shimidzu T. Terminology for membranes and membrane processes (reprinted from pure & appl chem, vol 68, pg 1479-1489, 1996). *J Membr Sci*. 1996;120(2):149-159.

116. Schafer A, Andristos N, Karabelas A, Hoek E, Schneider R, Nystrom M. Fouling in nanofiltration. In: *Nanofiltration - principles and applications*. Elsevier; 2004:169-239.
117. Levenstein R, Hasson D, Semiat R. Utilization of the donnan effect for improving electrolyte separation with nanofiltration membranes. *J Membr Sci*. 1996;116(1):77-92.
118. Mondal S. Polymeric membranes for produced water treatment: An overview of fouling behavior and its control. *Reviews in Chemical Engineering*. 2016;32(6):611-628.
119. Liu P, Ciora R, Tsotsis T, Sahimi M. Development of a CO₂ affinity ceramic membrane. *Abstr Pap Am Chem Soc*. 2003;225:U855-U855.
120. Ciora R, Fayyaz B, Liu P, et al. Preparation and reactive applications of nanoporous silicon carbide membranes. *Chem Eng Sci*. 2004;59(22-23):4957-4965.
121. Meng L, Kanezashi M, Tsuru T. Catalytic membrane reactors for SO₃ decomposition in Iodine–Sulfur thermochemical cycle: A simulation study. *Int J Hydrogen Energy*. 2015;40(37):12687-12696.
122. Rios GM, Belleville M, Paolucci-Jeanjean D. Membrane engineering in biotechnology: Quo vamus? *Trends Biotechnol*. 2007;25(6):242-246.
123. Gohil JM, Karamanev DG. Novel pore-filled polyelectrolyte composite membranes for cathodic microbial fuel cell application. *J Power Sources*. 2013;243:603-610.
124. Lombardo EA, Cornaglia C, Munera J. Development of an active, selective and durable water-gas shift catalyst for use in membrane reactors. *Catal Today*. 2016;259:165-176.
125. Babita K, Sridhar S, Raghavan KV. Membrane reactors for fuel cell quality hydrogen through WGSR - review of their status, challenges and opportunities. *Int J Hydrogen Energy*. 2011;36(11):6671-6688.
126. Liu X, Ruettinger W, Xu X, Farrauto R. Deactivation of pt/CeO₂ water-gas shift catalysts due to shutdown/startup modes for fuel cell applications. *Appl Catal B-Environ*. 2005;56(1-2):69-75.
127. Arca-Ramos A, Eibes G, Feijoo G, Lema JM, Moreira MT. Potentiality of a ceramic membrane reactor for the laccase-catalyzed removal of bisphenol A from secondary effluents. *Appl Microbiol Biotechnol*. 2015;99(21):9299-9308.
128. European C. Community strategy for endocrine disrupters. . 2007.
129. Cabana H, Jones JP, Agathos SN. Elimination of endocrine disrupting chemicals using white rot fungi and their lignin modifying enzymes: A review. *Eng Life Sci*. 2007;7(5):429-456.

130. Xu W, Gao L, Xiao G. Biodiesel production optimization using monolithic catalyst in a fixed-bed membrane reactor. *Fuel*. 2015;159:484-490.
131. Dixon A. *Modeling and simulation of heterogeneous catalytic processes, volume 45*. 40th ed. Academic Press; 1999.
132. Saracco G, Neomagus H, Versteeg G, van Swaaij W. High-temperature membrane reactors: Potential and problems. *Chem Eng Sci*. 1999;54(13-14):1997-2017.
133. SARACCO G, VELDSINK J, VERSTEEG G, VANSWAAIJ W. Catalytic combustion of propane in a membrane reactor with separate feed of reactant .1. operation in absence of trans-membrane pressure-gradients. *Chem Eng Sci*. 1995;50(12):2005-2015.
134. TSOTSIS T, CHAMPAGNIE A, VASILEIADIS S, ZIACA Z, MINET R. The enhancement of reaction yield through the use of high-temperature membrane reactors. *Sep Sci Technol*. 1993;28(1-3):397-422.
135. Malmali M, Stickel J, Wickramasinghe SR. Investigation of a submerged membrane reactor for continuous biomass hydrolysis. *Food Bioprod Process*. 2015;96:189-197.

2. Nanofiltration membranes for ionic liquid recovery*

* This chapter is adapted from a published paper by: Alexandru M. Avram, Pejman Ahmadiannamini, Xianghong Qian, S. Ranil Wickramasinghe. Separation and Purification Technology. Published April.03.2017. <http://dx.doi.org/10.1080/01496395.2017.1316289>

* All experiments were conducted by Mr Alexandru Avram with some assistance from Dr Pejman Ahmadiannamini. Prof Qian guided the experimental work and Prof Wickramasinghe helped with editing the manuscript.

Abstract

Nanofiltration membranes have been developed by interfacial polymerization using base PES ultrafiltration membranes. By varying the concentration of the reactive monomers present as well as the reaction conditions, the structure of the polymerized barrier layer has been modified. Here the ability to concentrate low molecular weight sugars while allowing dissolved ionic liquids in aqueous solution to be recovered in the permeate has been investigated for application in biomass hydrolysis. The results obtained here indicate that the selectivity for 1-butyl-3-methylimidazoliumchloride (BmimCl) over glucose can be as high as 36.6. The membrane permeance was $2.31 \text{ L m}^{-2} \text{ h}^{-1} \text{ bar}^{-1}$.

2.1. Introduction

Ionic liquids are molten salts at room temperature which are non-volatile and therefore have no measurable vapor pressure.¹ Today they find applications as electrolytes in batteries, lubricants in bearings and as green solvents.^{2,3} Numerous studies indicate that ionic liquids could be an emerging solvent for pretreatment of lignocellulosic biomass.⁴⁻⁶ Due to the very high recalcitrance of lignocellulosic biomass, deconstruction of the biomass is essential prior to fermentation. The deconstruction step typically known as pretreatment, involves a number of objectives: breakdown

of the carbohydrate-lignin complex, disruption of the cellulose crystallinity and hydrolysis of hemicellulose.⁷⁻¹⁰

Most pretreatment processes have disadvantages. Dilute acid pretreatment produces furfural and acetic acid which are inhibitory to the microorganisms used during fermentation.¹¹ Alkali pretreatment leads to the formation of xylo-oligomers which are inhibitory to the enzymes used for saccharification.¹² Biological methods tend to be slow and mechanical methods involve high energy and equipment costs.

Ionic liquids provide an alternative method of biomass deconstruction. They act by dissolving the biomass which allows for much better access of the enzymes used for hydrolysis of cellulose. Further, ionic liquids have been shown to reduce the crystallinity of the cellulose leading to higher glucose yields during enzymatic saccharification.¹³

Depending on the chemical structure of the anion and cation pair, ionic liquids differ considerably in physico-chemical properties such as hydrophobicity, charge, molecular weight and viscosity.¹⁴ Tadesse *et al.* published an extensive list of ionic liquids with applications in biomass deconstruction.¹⁵ The key mechanism for biomass solubilization is the ability of the ionic liquid to break the dense hydrogen bonding network that holds together the crystalline structure of recalcitrant bio-polymers.

Unfortunately, the high cost of ionic liquids means that efficient recovery and recycle of the ionic liquid is essential for an economically viable process. Here, we investigate the feasibility of developing nanofiltration membranes for ionic liquid recovery. Though initially developed for water softening applications, today nanofiltration is finding applications in numerous areas where separation of dissolved solutes in the size range 150 to 1000 Da is required.¹⁶

Few studies have considered nanofiltration for ionic liquid recovery. Han *et al.* consider the use of nanofiltration to recover ionic liquids from ionic liquid mediated Suzuki coupling reactions.¹⁷ Krockel and Kragel investigated the recovery of nonvolatile products from solutions containing ionic liquids while Gan *et al.* investigated filtration of ionic liquid mixtures containing methanol, ethanol and water.^{18,19} Their focus however was on the rheological properties of ionic liquid mixtures rather than recovery of ionic liquids.

Ables *et al.* have considered the use of commercially available nanofiltration membranes for purification of ionic liquids in biorefining applications.²⁰ Using model feed solutions consisting of ionic liquids and water, the efficiency of concentrating the ionic liquid in the retentate was investigated. These investigators concluded that the osmotic pressure differences between the feed and permeate acted against the separation of ionic liquid from ionic liquid/water mixtures limiting the maximum concentration of ionic liquid that could be obtained. Rejection of sugars dissolved in the ionic liquid was also investigated. The rejection of sugars was strongly membrane dependent.

In a more recent study, Ables *et al.* have investigated the use of membrane processes for recovery of glucose from an enzymatic hydrolysis process using ionic liquid pretreated cellulose.¹³ Three membrane based unit operations were considered: ultrafiltration for enzyme and cellulose recovery (in the retentate), nanofiltration for cellobiose and ionic liquid recovery in the retentate and electro dialysis for removal of ionic liquid from the glucose. They indicate that the major cost of the process is the ionic liquid. Compared to the current selling price of glucose the proposed process is not economical.

These previous studies indicate the challenges involved in recovering ionic liquid from ionic liquid/water/sugar mixtures. Recovery of the ionic liquid will be necessary if the unique properties

of ionic liquids for deconstructing lignocellulosic biomass and reducing the crystallinity of cellulose are to be leveraged in future biorefineries. Here, we have created nanofiltration membranes with different barrier properties in order to investigate the feasibility of recovering ionic liquids. Our aim is to maximize the ionic liquid recovered in the permeate while obtaining as high a rejection of dissolved sugars as possible. Using base ultrafiltration membranes as a support structure, we have used interfacial polymerization (IP) to create a dense polyamide layer. Interfacial polycondensation has been widely used to grow a thin polyamide skin layer on a porous substrate.²¹ Karan *et al.* have indicated that careful control of the interfacial polymerization process can lead to high rejection and high flux nanofiltration membranes for molecular separations.²² Common reactive monomers are diamines such as piperazine (PIP), m-phenylenediamine (MDP) and p-phenylenediamine (PPD) and acid chloride monomers such as trimesoyl chloride (TMC), isophthaloyl chloride (IPC) and 5-isocyanato-isophthaloyl chloride (ICIC).²³ Here we focus on the reaction of TMC with PIP which has been shown to lead to successful commercial thin film composite polyamide nanofiltration membranes.

Recent publications highlight the ability to tune the performance of these nanofiltration membranes by inclusion of novel monomers as well as inorganic additives.^{24,25} Here we have incorporated 3-aminophenylboronic acid (BA) in the IP layer to control the sugar selectivity and permeance of the membrane. Studies with boronic acid have shown that the steric conformation of the hydroxyl group connected to the boron can act as an on/off switch for forming bonds with the hydroxyl groups on sugars.²⁶⁻²⁹ Evidence shows that the growth of the skin layer is located on the organic solvent side of the interface.^{21,23} Thus by including BA in the aqueous phase, we aim to impede the passage of sugars while enhancing the passage of ionic liquids. Membrane performance has been determined using model feed streams consisting of (1) aqueous sugar

solutions, (2) aqueous ionic liquid solutions and (3) three component sugar, water and ionic liquid mixtures.

2.2. Experimental

Materials

The following chemicals were obtained from Sigma Aldrich (St. Louis, MO): triethylamine (Et₃N, 99% purity), 1-butyl-3-methylimidazoliumchloride (BmimCl, 98% purity), 1-ethyl-3-methylimidazolium acetate (EmimOAc, 90% purity), D-(+)-glucose, D-(+)-xylose, D-(-)-fructose. 1,3,5-benzenetricarbonyl chloride (trimesoyl chloride, TMC, 98% purity) was obtained from Alfa Aesar (Heysham, England); 3-aminophenylboronic acid monohydrate (BA, 98% purity) from AK Scientific (Union City, NJ), anhydrous piperazine (PIP) from Tokyo Chemical Industry (Portland, OR), and D-(+)-cellobiose from MP Biomedicals (Solon, OH). Hexane (HPLC grade), hydrochloric acid (37% v/v) and 30 and 50 kDa ultrafiltration membranes were purchased from EMD Millipore (Billerica, MA). All aqueous solutions were prepared with deionized water at 18.0 MΩ·cm produced with Thermo Scientific, model Smart2Pure 12 UV/UF (Waltham, MA).

Membrane modification via interfacial polymerization (IP)

Ultrafiltration membranes (30 and 50 kDa) were washed overnight in DI water. The membranes were then immersed in an aqueous solution containing PIP at concentrations varying from 0.1 to 1.5 wt % under continuous stirring for 4 hours. The BA concentration in the solution varied from 0.05 to 1.0 wt %. Next, the wet membranes were hung vertically for 5 minutes to let excess solution drip off the surface. The remaining droplets were wiped off with a clean teflon O-ring. The wet membranes were then placed in a custom-made teflon holder to only expose the barrier surface (feed side) of the membrane to an organic phase consisting of hexane containing 0.15 wt % TMC for various times. The polymerization time is the time for which the hexane solution was

in contact with the membrane filled with aqueous solution. The polymerization was conducted at either 25°C or -4°C. The polymerization was stopped when the organic solution was removed and the remaining organic droplets were evaporated in the fume hood for approximately 5 minutes. For some membranes Et3N was added to the organic phase in the ratio 1:1.5wt %. BA:Et3N. Finally, the modified membranes were annealed at 50°C for 30 minutes and washed with deionized water three times before storing in DI water at room temperature. **Figure 2-1** gives the overall reaction scheme.

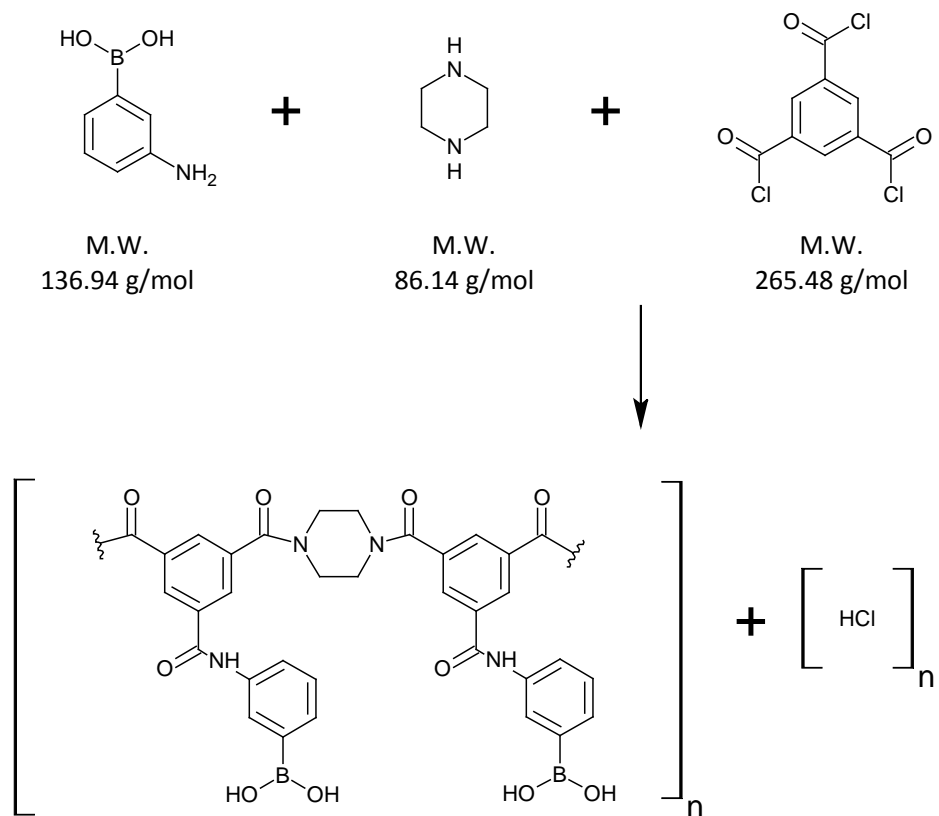


Figure 2-1: Reaction scheme for interfacial polymerization with expected products; 3-aminophenylboronic acid (BA) and piperazine (PIP) are in aqueous solution while trimesoyl chloride (TMC) is in hexane.

Surface Characterization

Attenuated total reflectance Fourier transform infrared (ATR-FTIR) spectroscopy (Shimadzu, IR Affinity-1, Kyoto, Japan) was used to analyze membrane surface chemistry after modification. The instrument was equipped with a deuterated L-alanine doped triglycine sulfate (DLATGS) detector with a resolution of 0.5-16 cm^{-1} , a germanium-coated potassium beam splitter with an incidence angle of 45° and a Pike Technologies (Madison, WI) zinc selenide ATR prism. Prior to surface analysis, the membranes were rinsed with DI water. They were then placed in a 100 mL beaker containing 70 mL DI water for 2 hours with slow stirring. The samples were dried in a vacuum oven for at least 30 minutes before analysis. Spectra were collected at room temperature over a scanning range 600–3000 cm^{-1} with a resolution of 8.0 cm^{-1} and with 50 scans per sample. Spectral analysis was performed using IR solution software (Shimadzu IR solution v1.60).

Atomic force microscopy (AFM) was performed in order to study the topography of modified and unmodified membranes. A Dimension icon with ScanAsyst sample chamber (Bruker, Camarillo, CA) was used. Membranes were air dried and analyzed in tapping mode with a silicon tip on a nitride lever. The images 5 μm x 5 μm (512 x 512 pixel) were recorded at a scanning rate of 1 Hz. A Bruker ScanAsyst air silicone tip on a nitride lever with a spring constant of 0.4 N/m (cantilever details: width = 25 μm , length = 115 μm , thickness = 650 nm) was used.

Rejection experiments

Permeance and rejection data were obtained for modified membranes in dead end filtration tests using a stirred stainless steel pressure vessel (Sterlitech HP4750, Kent, WA). Pressurized nitrogen (Airgas, Springdale, AR) was used to pump the feed through the various modified membranes, while the feed was mixed using a stirrer plate (Chemglass Optichem, Vineland, NJ). The permeate was collected in a beaker placed on a balance (Mettler Toledo PL602-S, Columbus, OH) connected

to a computer. **Table 2-1** summarizes the membrane modification conditions and model feed streams that were investigated.

Table 2-1: Summary of membrane modification conditions and feed streams tested.

Base membrane	30 and 50 kDa PES ultrafiltration membranes
Polymerization conditions	Aqueous phase DI water containing 0.1 to 1.5 wt % PIP, 0 to 1.0 wt % BA Organic phase: Hexane containing 0.15 wt % TMC, if Et3N added, BA: Et3N was 1:1.5 wt % Reaction conditions: 25°C or -4°C, polymerization times 1-25 min, annealing at 50°C for 30 min
Single component feed streams model feed streams	DI water containing cellobiose, glucose, xylose, fructose, 20 mM solution; EmimOAc, BmimCl, 115 mM solution
Multicomponent model feed streams	2% glucose and 1% BmimCl; 10% glucose and 10% BmimCl; 5% glucose and 10% BmimCl; 5% Cellobiose and 10% BmimCl

Though all experiments were conducted in dead end mode, a region of pseudo steady state operation could be established. The first 7 mL of permeate were discarded to ensure any transient effects during start up were eliminated. The next 9 mL of permeate were then used to determine rejection of dissolved solutes. This represents a reduction in volume of the original 200 mL feed solution from 3.5 to 8%. Pseudo steady state operation is observed as the change in feed conditions is very small during this period. Additional experiments suggest that pseudo steady state operation is maintained till about 25% of the original feed volume is removed in the permeate. Feed pressures were in the range 690 – 1725 kPa.

Samples from the permeate side were taken and analyzed as follows. For single component feed streams consisting of cellobiose, glucose, xylose and fructose in DI water the sugar concentration was determined using HPLC 1200 series (Agilent Technologies, Palo Alto, CA) equipped with a Hi-Plex Ca (Duo) column (Agilent, 300 x 6.5 mm length x I.D, 8 μ m pore size), injection volume: 5 μ L, mobile phase: deionized water, flow rate: 0.6 mL/minute, column temperature: 80°C, RID detector temperature: 45°C, run time: 30 minutes.

For multicomponent feed streams consisting of sugars and IL in DI water, the colorimetric 3,5-dinitrosalicylic acid (DNS) method was employed in order to determine the concentration of total reducing sugars (TRS) at 540 nm.³⁰ The ionic liquid concentration was quantified using a hand held conductivity meter Symphony SP70C (VWR, Batavia, IL) equipped with a 2-electrode conductivity cell of epoxy/platinum and a nominal cell constant of 1.0 cm⁻¹ (Thermo Scientific, Beverly, MA). Rejection of sugars and ionic liquids as well as selectivity of the membrane were calculated using the following relationships:

$$R_i = \left(1 - \frac{c_{ip}}{c_{if}}\right) \times 100\% \quad (1)$$

$$S_{i/j} = (100 - R_i)/(100 - R_j) \quad (2)$$

where c_{ip} and c_{if} are solute concentration of a given component in the permeate and feed, respectively, $S_{i/j}$ is selectivity of component i with respect to j. For each run, the first 7 mL of permeate were discarded and the next 9 mL of permeate used to determine c_{ip} and c_{if} which represented a period of pseudo steady state operation. The permeance of pure water was calculated using the following relationship:

$$P = \frac{V}{A \cdot t \cdot \Delta P} \quad (3)$$

where t is the time to collect volume V of permeate, A is membrane area, and ΔP is applied pressure.

All results were obtained in triplicate. Error bars or error ranges indicate the variation observed over the three readings.

2.3. Results and discussion

IP membranes

Unlike PIP, BA contains only one reactive amine group (**Figure 2-1**). Thus, incorporation of BA will lead to a termination event while incorporation of PIP can lead to further reaction via the second amine group. Consequently, the permeability of the IP layer will be modified by inclusion of BA. The initial focus was to determine the effect of changing the concentration of PIP and BA in order to maximize passage of ionic liquid and rejection of sugars. **Table 2-2** indicates that any separation between ionic liquid and the sugars investigated here, cannot be based on size exclusion alone as the molecular weights of the various species are very close to each other. Thus, preferential interactions between the ILs and sugars and the membrane will be critical.

Table 2-2: Molecular weight of solutes.

Compound	MW, g/mol
Cellobiose	342.3
Glucose	180.2
Xylose	150.1
Fructose	180.2
EmimOAc	170.2
BmimCl	174.7

Table 2-3 gives the effect of varying PIP concentration on rejection of individual sugars and ILs in aqueous solution. We see an increase in rejection with increasing PIP concentration until about 1.0 wt %, after which the rejection starts to decrease, probably due to a too high molar ratio PIP:BA:TMC, resulting in an increased amount of reaction by-products and/or heterogeneous cross-linking. The results indicate that by optimizing the components in the aqueous phase within the membrane pores during interfacial polymerization, one can adjust the rejection of IL versus sugars.

Table 2-3: Variation of rejection with PIP concentration for modified 50 kDa base PES membranes for aqueous feed streams containing single component sugars and ionic liquids. Modification conditions were: 0.1 wt %. BA in the aqueous phase, reaction temperature were 25°C for a reaction time of 15 min.

[PIP], wt %	Rejection, %					
	Cellobiose	Glucose	Xylose	Fructose	EmimOAc	BmimCl
0.1	2.6 ± 0.1	1.4 ± 0.0	1.1 ± 0.0	1.3 ± 0.0	2.6 ± 0.2	2.1 ± 0.1
0.3	7.3 ± 0.1	2.7 ± 0.1	1.5 ± 0.0	1.3 ± 0.0	5.0 ± 0.3	5.5 ± 0.3
0.5	68.8 ± 1.4	65.2 ± 1.1	56.0 ± 1.1	65.3 ± 0.7	61.0 ± 3.7	52.6 ± 3.2
0.6	67.1 ± 1.3	60.6 ± 0.9	45.5 ± 0.9	60.7 ± 0.6	64.1 ± 3.8	60.4 ± 3.6
0.8	71.9 ± 1.4	67.2 ± 1.1	53.5 ± 1.1	66.9 ± 0.7	77.1 ± 4.6	63.5 ± 3.8
1.0	96.4 ± 1.9	94.7 ± 1.8	89.3 ± 1.8	94.7 ± 0.9	74.3 ± 4.5	79.4 ± 4.8
1.3	82.9 ± 1.7	80.6 ± 1.5	76.1 ± 1.5	81.3 ± 0.8	79.7 ± 4.8	79.0 ± 4.7
1.5	60.2 ± 1.2	60.5 ± 1.1	56.0 ± 1.1	59.1 ± 0.6	56.4 ± 3.4	52.8 ± 3.2

Table 2-3 indicates that generally rejection of cellobiose is the highest while xylose is the lowest for all membranes. Further, rejection of glucose and fructose is similar. **Table 2-3** indicates that these trends are expected based on differences in molecular weight between the sugars. However, though the molecular weight of the ionic liquids is greater than xylose, their rejection is generally

less than xylose. The results highlight the fact that when the molecular weight of the dissolved solutes is similar (i.e. same order of magnitude), interactions between the solutes and the membrane will have a significant influence on the observed rejection.³¹ Since 1.0 wt % PIP gave the highest sugar rejection the effect of polymerization time was investigated using 1.0 wt % PIP. **Figure 2-2** gives the results for the rejection and permeance of feed streams containing cellobiose, glucose, EmimOAc and BmimCl in aqueous solution.

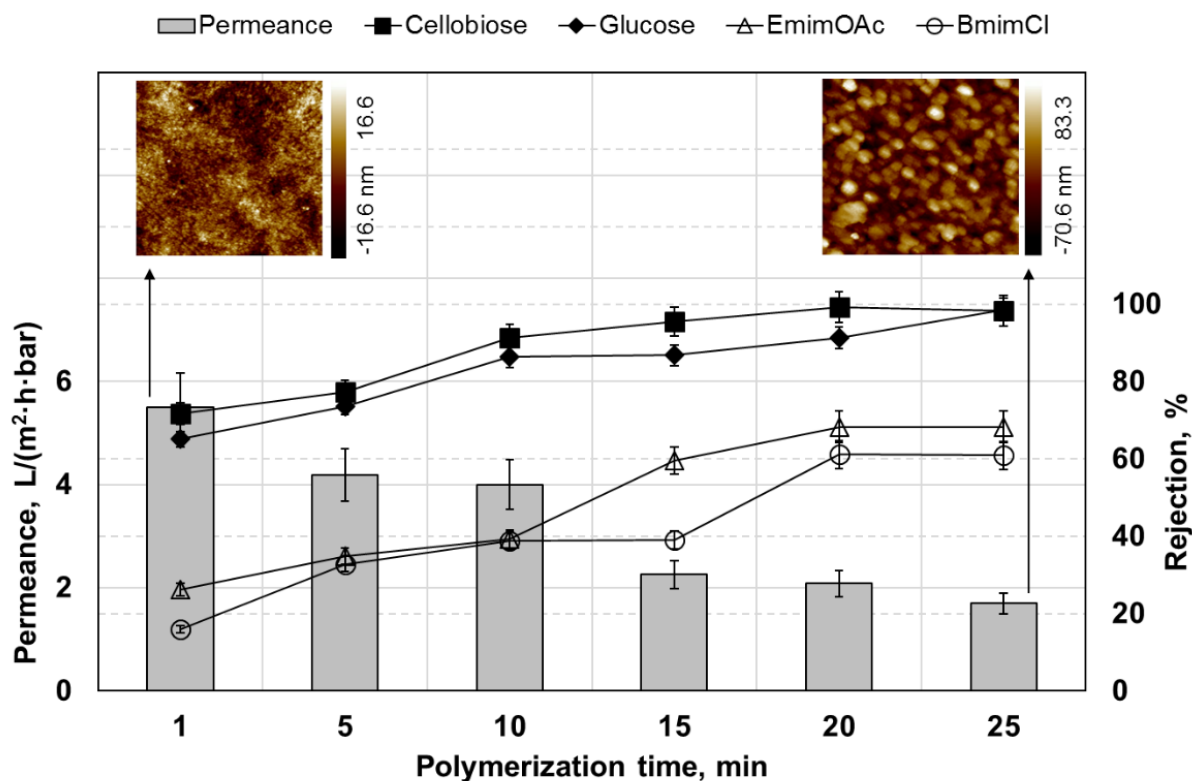


Figure 2-2: Variation of permeance and rejection of cellobiose, glucose, EmimOAc and BmimCl as a function of polymerization time for modified 50 kDa PES membranes. Modification conditions were: 1.0 and 0.1 wt % PIP and BA respectively in the aqueous phase, reaction temperature 25°C. Insets show AFM surface analysis of selected membranes with roughness 9.4 and 38.6 nm from left to right, respectively. All AFM imaging scale resolution at 0-5 μ m.

As observed in **Table 2-3**, rejection for fructose is very similar to glucose and the rejection of xylose is always the lowest of the sugars tested in this work. We focus on glucose as it is the most

abundant sugar in lignocellulosic biomass and of most commercial relevance. When the polymerization time increases, permeance decreases and rejection increases as is expected due to a thicker IP layer that is formed. The AFM images indicate that with longer polymerization times the membrane becomes rougher probably due to uneven rates of polymerization. As indicated by Mulder the polymerization is strongly affected by diffusion of the reactants through the growing polymerized barrier layer.³² In addition Karan *et al.* indicate that heat generated during the polymerization reaction can lead to local temperature variations that lead to different rates of reaction and hence increased surface roughness.²² The results suggest that the optimal polymerization time will depend on a trade-off between higher rejection and lower permeance. As can be seen for polymerization times less than 5 min the rejection of sugars is low, whereas for polymerization times greater than 15 min the permeance is low.

Additional experiments with 30 kDa PES membranes indicated that there is little difference in performance when a base 30 or 50 kDa PES membrane is used. However, due to the tighter pore structure of the barrier layer of the 30 kDa membrane, it is likely the IP layer formed on top of the barrier layer of the 30 kDa membrane will be more robust. Consequently, all further experiments were conducted using 30 kDa PES membranes. In order to minimize the effect of local temperature variation due to the heat generated during the interfacial polymerization reaction, the reaction temperature was lowered to -4 °C, and the reaction time was set at 15 min

Surface analysis

In order to verify that BA was being incorporated into the IP layer ATR-FTIR analysis of the membrane was conducted. **Figure 2-3** is an example. Spectra are shown for the base PES membrane as well as membranes modified for reaction times of 1, 15 and 25 min.

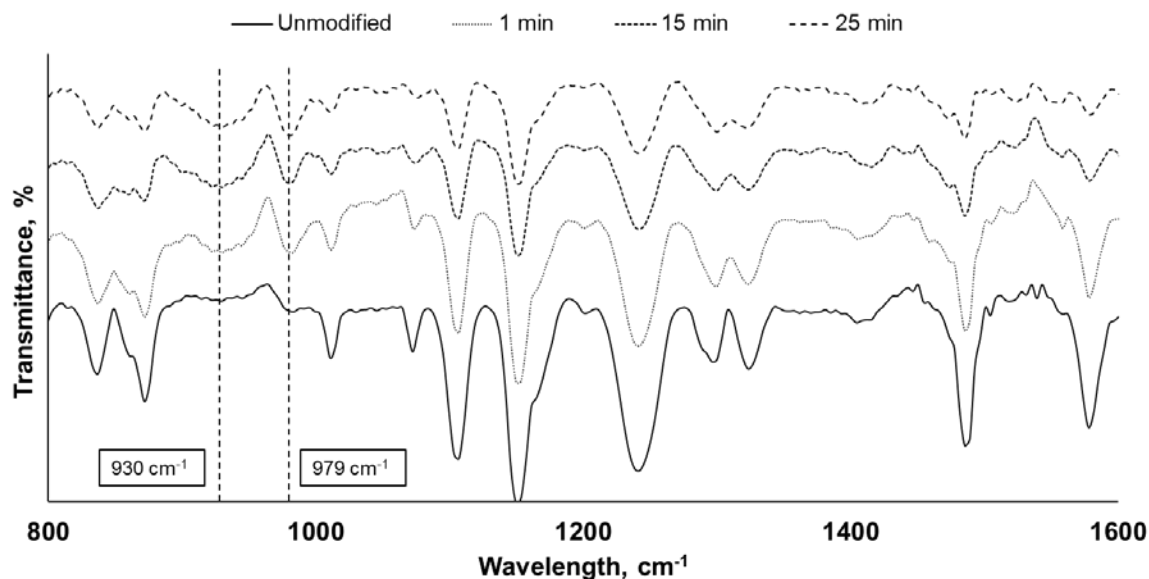


Figure 2-3: FTIR spectra for 30 kDa base and modified membranes. Modification conditions were: 1.0 and 0.5 wt % PIP and BA respectively in the aqueous phase, reaction temperature $-4\text{ }^{\circ}\text{C}$, polymerization times of 1, 15 and 25 min.

We observe two peaks that stand out from the base membrane in the regions $890\text{--}960\text{ cm}^{-1}$ and $960\text{--}995\text{ cm}^{-1}$. These correspond to the BOH deformation vibration and the BO stretching vibration, respectively and confirm the incorporation of BA in the barrier layer.^{33,34} As is expected the BA peak increases as polymerization time increases.

Table 2-4 gives the effect on rejection and permeance of varying the BA concentration for a PIP concentration of 1.0 wt % of individual sugars and ILs in aqueous solution. The general trends are the same as in Table 3; cellobiose rejection is the highest, xylose the lowest while glucose and fructose rejection is intermediate and similar. It can be seen that lower BA concentrations give better rejection, peaking at an optimum between 0.1 – 0.2 wt % BA with 97% cellobiose and 78% BmimCl rejection. Increasing the amount of boronic acid in the aqueous phase can act as a polymerization termination step due to a variety of reasons. BA has three functional groups, two diols and an amine group. However only the amine group can take part in the polycondensation

Table 2-4: Variation of rejection with BA concentration for modified 30 kDa base PES membranes for aqueous feed streams containing single component sugars and ionic liquids. Modification conditions were: 1.0 wt % PIP in the aqueous phase reaction temperature was -4 °C for a reaction time of 15 min.

[BA], wt %	Rejection, %					
	Cellobiose	Glucose	Xylose	Fructose	EmimOAc	BmimCl
0.05	92.0 ± 1.8	90.8 ± 0.9	86.7 ± 1.7	90.9 ± 1.0	75.0 ± 4.5	67.2 ± 4.0
0.1	96.4 ± 1.9	94.7 ± 0.9	89.3 ± 1.8	94.7 ± 1.0	74.3 ± 4.5	79.4 ± 4.8
0.2	96.6 ± 1.9	91.5 ± 0.9	80.5 ± 1.6	91.2 ± 0.8	74.0 ± 4.4	77.6 ± 4.7
0.5	89.2 ± 1.8	85.2 ± 0.9	77.9 ± 1.6	84.7 ± 0.7	65.5 ± 3.9	65.7 ± 3.9
1.0	27.1 ± 0.5	26.1 ± 0.3	24.7 ± 0.5	25.8 ± 0.6	28.3 ± 1.7	28.4 ± 1.7

reaction and thus act as a competitive compound with PIP. Having a larger molecular size, BA is expected to give a looser polymer network and, therefore, produce membranes with a larger nominal molecular weight cut-off and rougher surfaces. The data in **Table 2-4** suggest that BA concentrations of between 0.1 and 0.2 wt % could be used to tune sugar and ionic liquid rejection. **Figure 2-4** gives the variation of rejection and permeance of cellobiose and BmimCl as a function of BA concentration. As observed in **Table 2-3**, **Table 2-4**, and **Figure 2-2** rejection of EmimOAc and BminCl is often similar. As BmimCl is preferred for pretreatment we focus on BmimCl.

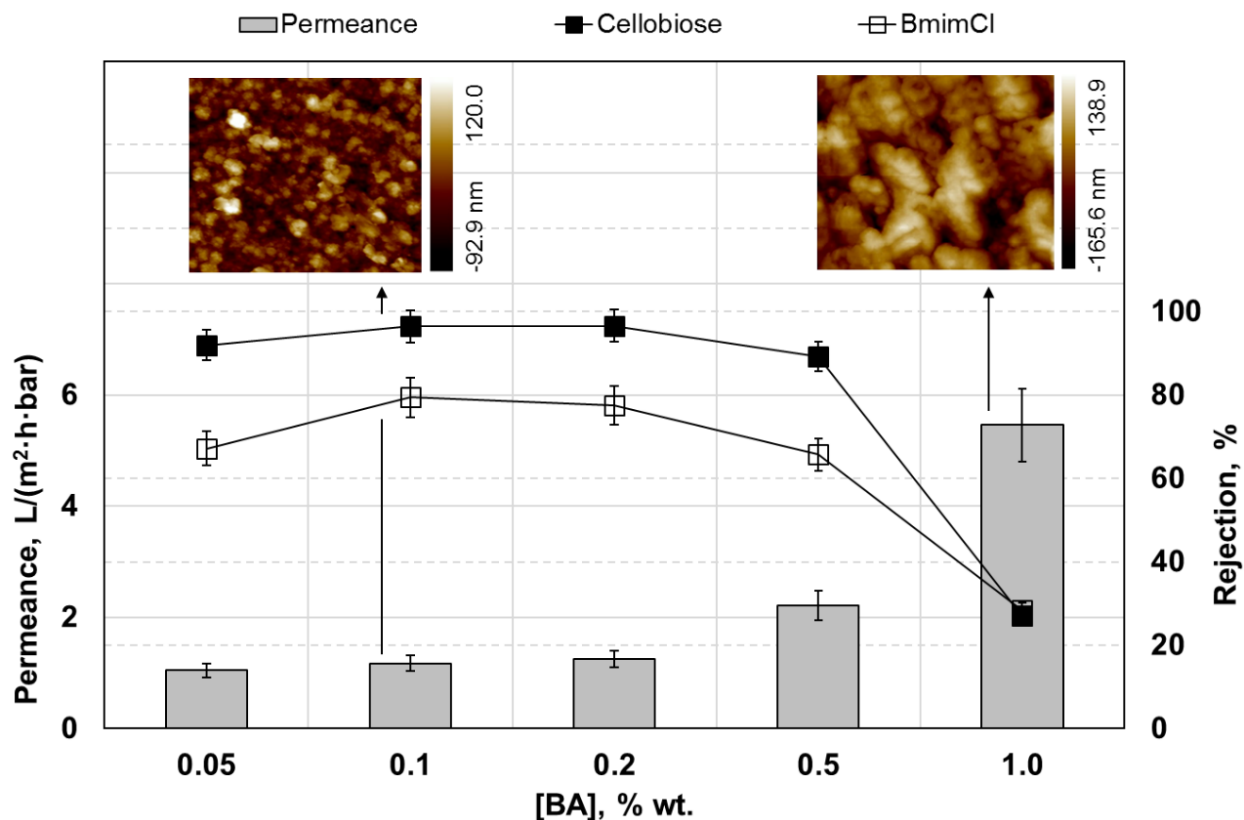


Figure 2-4: Variation of permeance and rejection of cellobiose, and BmimCl as a function of BA concentration for modified 30 kDa modified PES membranes. Modification conditions were: 1.0 wt % PIP in the aqueous phase, reaction temperature was -4 °C for a reaction time of 15 min. Insets show AFM surface analysis of membranes modified with 0.1 and 1.0 wt % BA with roughness 31.0 and 46.6 nm from left to right, respectively. All AFM imaging scale resolution at 0-5 μ m.

Though not shown, as indicated in **Table 2-4**, glucose rejection is always less than cellobiose. The AFM images indicate that increasing the BA concentration leads to increased roughness, as expected. As can be seen, addition of small amounts of BA does not affect the membrane permeance. However addition of more than 0.5 wt % BA leads to an increase in permeance and decrease in rejection. This is probably due to the increases in the amount of chain termination due to reduced crosslink density which results in a more open structure. This result suggests that addition of small amounts of reactive monomeric species like BA could be used to tune membrane performance.

As indicated in **Figure 2-1**, the reaction proceeds with the formation of hydrochloric acid as a by-product, acting as an inhibitor to skin layer formation.²¹ Thus increasing the pH of the reaction at higher BA concentration might induce a similar inhibiting effect. Consequently the effect of adding Et3N to the aqueous phase was investigated. **Table 2-5** and **Figure 2-5** show the effect of adding Et3N as a proton acceptor. Indeed, we are able to see similar rejection performance at threefold shorter polymerization times, while obtaining better permeance. The Et3N concentration was chosen such that the ratio of BA: Et3N was 1: 1.5. However the polymerization time was only 5 min.

Table 2-5: Variation of rejection in the presence of Et3N. The Et3N concentration was chosen such that the ratio of BA:Et3N was 1:1.5. Results are for modified 30 kDa base PES membranes for aqueous feed streams containing single component sugars and ionic liquids. Modification conditions were: 1.0 wt % PIP in the aqueous phase reaction temperature was -4 °C for a reaction time of 5 min.

[BA], wt %	Rejection, %					
	Cellobiose	Glucose	Xylose	Fructose	EmimOAc	BmimCl
0.05	98.5 ± 2.0	96.0 ± 1.0	85.0 ± 1.7	95.5 ± 1.0	81.2 ± 4.9	79.8 ± 4.8
0.1	99.1 ± 2.0	94.8 ± 0.9	83.3 ± 1.7	96.3 ± 1.0	78.3 ± 4.7	72.1 ± 4.3
0.2	82.3 ± 1.6	76.4 ± 0.8	67.2 ± 1.3	76.4 ± 0.8	53.8 ± 3.2	52.4 ± 3.1
0.5	82.0 ± 1.6	71.2 ± 0.7	59.1 ± 1.2	71.2 ± 0.7	34.0 ± 2.0	41.9 ± 2.5
1.0	66.6 ± 1.3	58.6 ± 0.6	50.9 ± 1.0	59.7 ± 0.6	27.1 ± 1.6	25.2 ± 1.5

While our results indicate that increasing polymerization time or BA concentration led to increased roughness, there is no direct link between the roughness of the polymerized layer and membrane performance. Karan *et al.* indicate that the roughness of the polymerized barrier layer can have a significant effect on permeance for sub 10 nm polyamide nanofilms.²² The films we have grown here are an order of magnitude or more thicker than 10 nm as suggested by the fact that IR

spectroscopy can detect the presence of BA (see **Figure 2-3**). However it is likely that if much thinner yet robust films could be polymerized on UF membrane supports, much higher permeabilities could be obtained with similar rejection properties.

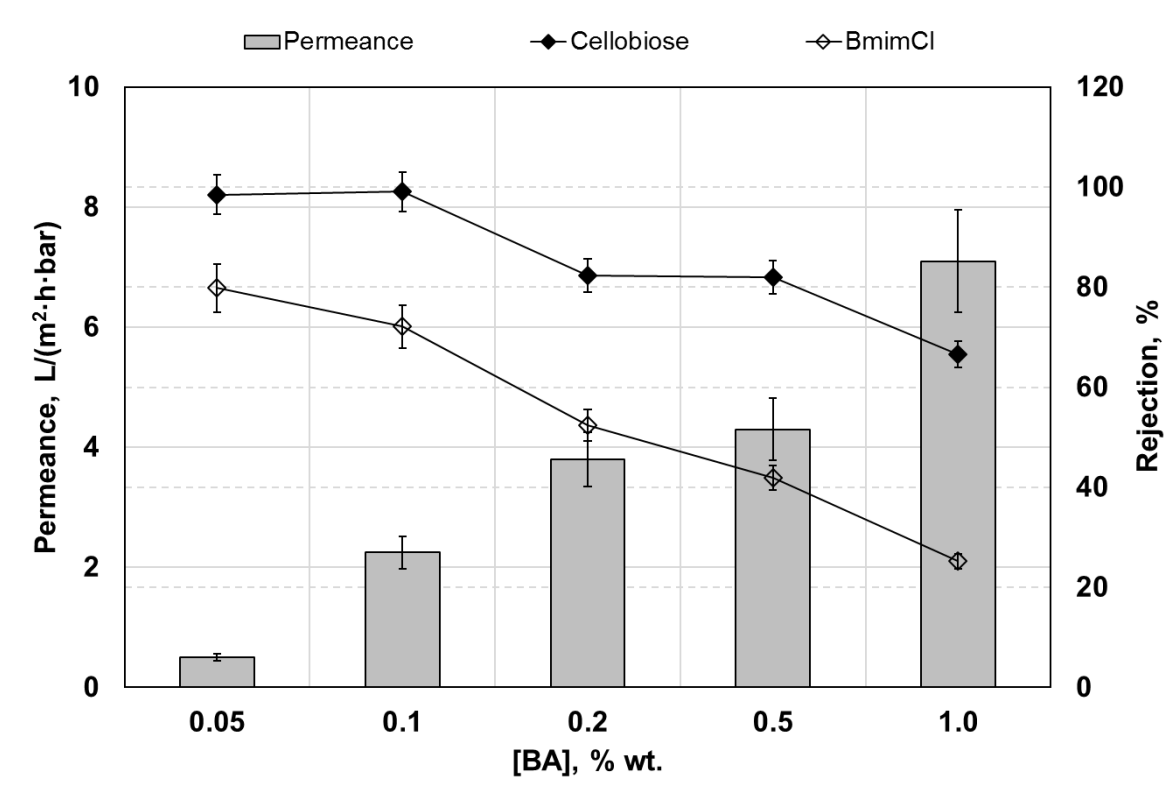


Figure 2-5: Variation of permeance and rejection of cellobiose, and BmimCl as a function of Et3N concentration for unmodified and modified 30 kDa PES membranes. The Et3N concentration was chosen such that the ratio of BA:Et3N was 1:1.5. Modification conditions were: 1.0 wt % PIP in the aqueous phase reaction temperature was -4 °C for a reaction time of 5 min.

Based on our results, the modification conditions that maximized cellobiose and glucose rejection, minimized BmimCl rejection and maximized permeate flux were as follows: aqueous phase, 1.0 wt% PIP, 0.1 wt % BA and 0.115 wt % Et3N, reaction temperature at -4 °C for 8 min. A number of membranes were modified using these conditions and tested using the mixed feed streams listed in **Table 2-6**. As can be seen selectivities varying from 6-37 for BmimCl over glucose were

obtained depending on the concentration of the two components in the feed solution. The selectivity for BmimCl over cellobiose was less than for glucose.

Table 2-6: Selectivity for BmimCl versus glucose or cellobiose for modified base 30 kDa PES membranes. Modification conditions were: aqueous phase 1.0, 0.1, 0.115 wt% PIP, BA Et3N respectively in the aqueous phase, reaction temperature -4 °C for a reaction time of 8 min.

Feed	2% glucose, 1% BmimCl	10% glucose, 10% BmimCl	5% glucose, 10% BmimCl	5% cellobiose, 10% BmimCl	Permeance L/(m ² ·h·bar)
Rejection	91.8 glucose 47.2 BmimCl	97.8 glucose 19.4 BmimCl	94.5 glucose 31.2 BmimCl	80.5 cellobiose 7.6 BmimCl	2.31 ± 0.28
Selectivity IL/sugar	6.4	36.6	12.5	4.7	

In our earlier work we investigated the feasibility of tailoring the barrier layer of nanofiltration membranes by using layer-by-layer deposition of polyelectrolytes.¹⁶ Selectivities for the various sugars were generally between 1.5 and 11.0 except for xylose over sucrose where higher selectivities were obtained. This general observation may be explained by the fact that the molecular weight of sucrose is 342, much larger than xylose (see **Table 2**). The selectivities obtained here are higher than the selectivities for fractionation of sugars. These results highlight the feasibility of tuning the properties of the IP layer to induce specific interactions that inhibit passage of sugars relative to ionic liquids.

Our results indicate that as the rejection and hence selectivity of the membrane increases the permeance decreases. From a practical perspective however it will be essential to ensure the permeance of the membrane is high enough for a viable separation process. Karan *et al.* indicated that IP layers consisting of thin sub 10 nm thickness, do exhibit high permeabilities.²² Thus

development of sophisticated polymerization methods to carefully control the thickness and three dimensional structure of the IP layer will be essential.

The results in **Table 2-6** indicate that the concentration of the solute species will affect the selectivity of specific solutes in real feed streams. Further as indicated by Ables *et al.* the maximum concentration of ionic liquid that can be obtained will be limited by the osmotic pressure differences between the feed and permeate.²⁰ While concentration of the rejected sugars will be beneficial in the subsequent fermentation step, the toxicity of the ionic liquid to the microorganisms used during fermentation will dictate the maximum allowable concentration of residual ionic liquid in the hydrolysate prior to fermentation. It is likely that the feasibility of using ionic liquids for pretreatment will depend on the development of an economically viable multistep process for ionic liquid recovery and recycle. Development of novel high performance nanofiltration membranes could be a part of such a process.

2.4. Conclusion

Nanofiltration could find applications in the conversion of lignocellulosic biomass into chemicals and fuels. Here the ability of concentrate low molecular weight sugars while recovering dissolved ionic liquids in the permeate has been explored. Given the advantages of ionic liquids for pretreatment of biomass as well as their high cost, effective separation process for recovery and recycle of the ionic liquid will be essential. Given the similarity in molecular weight between ionic liquids of relevance for pretreatment and low molecular weight sugars such as glucose, sized based separations alone will be ineffective. However, for nanofiltration membranes, both size and interactions between solute species and the IP layer determine the selectivity of these membranes. Our results indicate that careful control of the thickness and structure of the IP layer will be essential to maximize rejection of sugars, recovery of ionic liquids in the permeate and the

permeance of the membrane. In addition to development of appropriate membranes integration of a nanofiltration step in the entire process must be considered as it will determine the viability of nanofiltration for ionic liquid recovery.

Acknowledgements

Financial support from the National Science Foundation CBET 1264896 is gratefully acknowledged.

References

1. Elgharbawy AA, Alam MZ, Moniruzzaman M, Goto M. Ionic liquid pretreatment as emerging approaches for enhanced enzymatic hydrolysis of lignocellulosic biomass. *Biochem Eng J.* 2016;109:252-267.
2. Shobukawa H, Tokuda H, Susan MAH, Watanabe M. Ion transport properties of lithium ionic liquids and their ion gels. *Electrochim Acta.* 2005;50(19):3872-3877.
3. Ye CF, Liu WM, Chen YX, Yu LG. Room-temperature ionic liquids: A novel versatile lubricant. *Chemical Communications.* 2001(21):2244-2245.
4. Gross AS, Bell AT, Chu JW. Entropy of cellulose dissolution in water and in the ionic liquid 1-butyl-3-methylimidazolium chloride. *Physical Chemistry Chemical Physics.* 2012;14(23):8425-8430.
5. Li C, Zhao ZK. Efficient acid-catalyzed hydrolysis of cellulose in ionic liquid. *Advanced Synthesis & Catalysis.* 2007;349(11-12):1847-1850.
6. Li C, Wang Q, Zhao ZK. Acid in ionic liquid: An efficient system for hydrolysis of lignocellulose. *Green Chem.* 2008;10(2):177-182.
7. Raj T, Gaur R, Dixit P, et al. Ionic liquid pretreatment of biomass for sugars production: Driving factors with a plausible mechanism for higher enzymatic digestibility. *Carbohydr Polym.* 2016;149:369-381.
8. Samayam IP, Hanson BL, Langan P, Schall CA. Ionic-liquid induced changes in cellulose structure associated with enhanced biomass hydrolysis. *Biomacromolecules.* 2011;12(8):3091-3098.

9. Vandebossche V, Brault J, Vilarem G, et al. A new lignocellulosic biomass deconstruction process combining thermo-mechano chemical action and bio-catalytic enzymatic hydrolysis in a twin-screw extruder. *Industrial Crops and Products*. 2014;55:258-266.
10. Grzenia DL, Schell DJ, Wickramasinghe SR. Membrane extraction for detoxification of biomass hydrolysates. *Bioresour Technol*. 2012;111:248-254.
11. Jonsson LJ, Martin C. Pretreatment of lignocellulose: Formation of inhibitory by-products and strategies for minimizing their effects. *Bioresour Technol*. 2016;199:103-112.
12. Qing Q, Yang B, Wyman CE. Xylooligomers are strong inhibitors of cellulose hydrolysis by enzymes. *Bioresour Technol*. 2010;101(24):9624-9630.
13. Abels C, Thimm K, Wulforth H, Spiess AC, Wessling M. Membrane-based recovery of glucose from enzymatic hydrolysis of ionic liquid pretreated cellulose. *Bioresour Technol*. 2013;149:58-64.
14. Zavrel M, Bross D, Funke M, Buchs J, Spiess AC. High-throughput screening for ionic liquids dissolving (ligno-)cellulose. *Bioresour Technol*. 2009;100(9):2580-2587.
15. Tadesse H, Luque R. Advances on biomass pretreatment using ionic liquids: An overview. *Energy & Environmental Science*. 2011;4(10):3913-3929.
16. Malmali M, Stickel JJ, Wickramasinghe SR. Sugar concentration and detoxification of clarified biomass hydrolysate by nanofiltration. *Separation and Purification Technology*. 2014;132:655-665.
17. Han S, Wong HT, Livingston AG. Application of organic solvent nanofiltration to separation of ionic liquids and products from ionic liquid mediated reactions. *Chemical Engineering Research & Design*. 2005;83(A3):309-316.
18. Krockel J, Kragl U. Nanofiltration for the separation of nonvolatile products from solutions containing ionic liquids. *Chem Eng Technol*. 2003;26(11):1166-1168.
19. Gan Q, Xue ML, Rooney D. A study of fluid properties and microfiltration characteristics of room temperature ionic liquids C-10-min NTf₂ and N-8881 NTf₂ and their polar solvent mixtures. *Separation and Purification Technology*. 2006;51(2):185-192.
20. Abels C, Redepenning C, Moll A, Melin T, Wessling M. Simple purification of ionic liquid solvents by nanofiltration in biorefining of lignocellulosic substrates. *J Membr Sci*. 2012;405:1-10.
21. Morgan P. *Condensation polymers: By interfacial and solution methods, (polymer reviews)*. Interscience Publishers; 1965.

22. Karan S, Jiang Z, Livingston AG. Sub-10 nm polyamide nanofilms with ultrafast solvent transport for molecular separation. *Science*. 2015;348(6241):1347-1351.
23. Lau WJ, Ismail AF, Misdan N, Kassim MA. A recent progress in thin film composite membrane: A review. *Desalination*. 2012;287:190-199.
24. Ismail AF, Padaki M, Hilal N, Matsuura T, Lau WJ. Thin film composite membrane - recent development and future potential. *Desalination*. 2015;356:140-148.
25. Lau WJ, Gray S, Matsuura T, Emadzadeh D, Chen JP, Ismail AF. A review on polyamide thin film nanocomposite (TFN) membranes: History, applications, challenges and approaches. *Water Res*. 2015;80:306-324.
26. Zhao Y, Shantz DF. Phenylboronic acid functionalized SBA-15 for sugar capture. *Langmuir*. 2011;27(23):14554-14562.
27. Liu L, Zhang Y, Zhang L, et al. Highly specific revelation of rat serum glycopeptidome by boronic acid-functionalized mesoporous silica. *Anal Chim Acta*. 2012;753:64-72.
28. Mehling T, Zewuhn A, Ingram T, Smirnova I. Recovery of sugars from aqueous solution by micellar enhanced ultrafiltration. *Separation and Purification Technology*. 2012;96:132-138.
29. Duggan PJ. Fructose-permeable liquid membranes containing boronic acid carriers. *Aust J Chem*. 2004;57(4):291-299.
30. Miller GL. Use of dinitrosalicylic acid reagent for determination of reducing sugar. *Anal Chem*. 1959;31(3):426-428.
31. Himstedt HH, Du H, Marshall KM, Wickramasinghe SR, Qian X. pH responsive nanofiltration membranes for sugar separations. *Ind Eng Chem Res*. 2013;52(26):9259-9269.
32. Mulder J. *Basic principles of membrane technology*. 2nd ed. Springer; 1996.
33. Faniran JA, Shurvell HF. Infrared spectra of phenylboronic acid (normal and deuterated) and diphenyl phenylboronate. *Can.J.Chem*. 1968;46(12):2089-&.
34. Moraes IR, Kalbac M, Dmitriev E, Dunsch L. Charging of self-doped poly(anilineboronic acid) films studied by in situ ESR/UV/vis/NIR spectroelectrochemistry and ex situ FTIR spectroscopy. *Chemphyschem*. 2011;12(16):2920-2924.

3. Polyelectrolyte multilayer modified nanofiltration membranes for the recovery of ionic liquid from dilute aqueous solutions*

* This chapter is based on a submitted manuscript: Alexandru M. Avram, Pejman Ahmadiannamini, Anh Vu, Xianghong Qian, Arijit Sengupta, S. Ranil Wickramasinghe. Journal of Applied Polymer Science. Revision 1 was submitted on April.19.2017.

* All experiments were conducted by Mr Alexandru Avram with some assistance from Dr Pejman Ahmadiannamini. Prof Qian guided the experimental work. Prof Wickramasinghe and Dr Sengupta helped with analyzing the results and editing the manuscript.

Abstract

The feasibility of nanofiltration membranes fabricated by static polyelectrolyte layer-by-layer deposition of poly(styrene sulfonate) and poly(allylamine hydrochloride) on poly(ethersulfone) ultra- and alumina microfiltration membranes for the recovery of ionic liquid from low molecular weight sugar was investigated. The surface properties of these modified membranes were correlated with their performances. The selectivity for 1-butyl-3-methylimidazolium chloride over cellobiose and glucose was found to be as high as 50.5/2.3 for modified alumina and 32.3/3.5 for modified polyethersulfone with optimized number of bilayers. The values for membrane permeance were 4.8 and 2.5 L m⁻¹ h² bar⁻¹, respectively. For low depositions, the separation mechanism was predominantly governed by size-exclusion. For higher depositions, the enhanced negative zeta potential of modified membranes suggested preferred dominating electrostatic interactions, resulting in high selectivity of ionic liquids over low molecular weight sugars. At very high depositions, the molecular weight cut-off of the membrane becomes constricting for size-exclusion effect.

3.1. Introduction

Increasing energy consumption for economic and social development coupled with environmental challenges posed by dwindling fossil-based energy sources have led to extensive activities on the research of renewable biofuels^{1,2}. In comparison to fossil fuels, biofuels have the advantages of being renewable, nontoxic, and biodegradable and have a much lower risk of contaminating the environment^{3,4}. First generation biofuels, produced directly from food crops, are controversial due

to increased grain prices, land-use competition, and intensive agricultural practices^{5,6}. Contrary to the first generation, non-edible feed stocks are exploited to produce second generation biofuels. Non-edible lignocellulosic biomass derived from agricultural wastes, forest residues, and dedicated energy crops represents an abundant renewable resource for the production of bio-based products and biofuels⁷. The typical process for biomass conversion involves three main steps: pretreatment of naturally resistant cellulosic materials, hydrolysis of cellulose into monomer sugars, and fermentation of hydrolyzed sugars^{8,9}. Due to its highly crystalline structure, lignocellulosic biomass is hardly soluble in common solvents and its economic hydrolysis into fermentable sugars remains a major challenge¹⁰⁻¹².

Ionic liquids (ILs) have shown great promise in the pretreatment, dissolution, and hydrolysis of lignocelluloses to produce biofuels¹². However, the high price for synthesis and high energy requirement for recycling could affect the economic viability of IL implementation for large-scale biofuel production¹³. Some efforts have been made to develop effective techniques for ILs recovery, such as chromatography¹⁴, salting-out precipitation¹⁵, adsorption¹⁶, extraction¹⁷, supercritical carbon dioxide¹⁸ and membrane separation¹⁹. Membrane filtration technology has proved to be effective for a large variety of industrial applications²⁰⁻²². Different membrane separation processes such as nanofiltration (NF)^{23,24}, reverse osmosis (RO)²⁵, electrodialysis (ED)²⁶ and membrane distillation (MD)²⁷ have been successfully employed to concentrate ILs aqueous solutions. However, IL recovery becomes more complicated when sugar monomers and smaller carbohydrate oligomers are present in the same solution²⁸. That is on one hand due to the fact that hydrolysate sugars have molecular sizes close to those of commonly used ILs. On the other hand, due to non-charged nature of sugars and low charge density of ILs, most NF membranes are ineffective in sugar/IL separation. Thus, a membrane with a precise molecular weight cut-off (MWCO) and a high charge density could more efficiently separate ILs from sugars. The layer-by-layer (LBL) deposition of charged polyelectrolyte pairs²⁹⁻³¹ is an attractive technique for the fabrication of nanostructured multilayer membranes due to its simplicity and control over film thickness and pore size and charge density³². It has been widely used for formation of membranes tuned for high permeance and high rejection for many diverse membrane separations, such as reverse osmosis³³, nanofiltration³⁴⁻³⁶, pervaporation and forward osmosis³⁷⁻⁴⁰ with specific applications, such as virus purification^{41,42}, sugar fractionation^{43,44} and diverse ion selective separations⁴⁵.

In this study, we have modified commercially available organic and inorganic membranes via the LBL deposition of polyelectrolytes multilayers (PEMs). The adsorption mechanism of charged polymers on membrane surface is believed to be mainly due to electrostatic interactions. Additionally, hydrogen bonding, coordination chemistry, hydrophobic interactions and chemical crosslinking also play a role in layer formation and assembly⁴⁶. Amongst the most important parameters influencing the polyelectrolyte (PE) assembly on a specific substrate, are the choice of PE pair, the ionic strengths of PE solutions, salt type and the pH of the depositing solution⁴⁶⁻⁴⁸. The fabricated nanofiltration membranes were tested for feasibility as potential recycling unit operation that could result in better economics for biomass hydrolysis employing expensive ionic liquids.

3.2. Experimental

Materials

The polyelectrolytes poly(sodium-p-styrenesulfonate) (PSS, avg. MW 70 kDa, Acros Organics, Geel, Belgium) and poly(allylamine hydrochloride) (PAH, avg. MW 15 kDa, 95% purity, AK Scientific, Union City, CA) were purchased from VWR International (Radnor, PA). The feed compounds were obtained from Sigma Aldrich (St. Louis, MO): 1-butyl-3-methylimidazolium chloride (BmimCl) (98% purity), 1-ethyl-3-methylimidazolium acetate (EmimOAc) (90% purity), D-(+)-Glucose, D-(+)-Xylose and D-(-)-Fructose. D-(+)-Cellobiose was purchased from MP Biomedicals (Solon, OH). Sodium hydroxide (NaOH, analytical grade) was purchased from Macron Fine Chemicals (Avantor Performance Materials, Center Valley, PA). Hydrochloric acid (37% v/v) was purchased from EMD Millipore (Billerica, MA). Sodium chloride (NaCl) was purchased from BDH (Radnor, PA). Deionized water was produced with Thermo Scientific, model Smart2Pure 12 UV/UF (Waltham, MA), 18.0 M Ω ·cm.

Ultrafiltration poly(ethersulfone) (PES) base membranes with molecular weight cut-off (MWCO) 50 kDa were purchased from EMD Millipore (Billerica, MA) and inorganic 0.2 μ m alumina oxide microfiltration discs with polypropylene support ring were purchased from GE Healthcare Life Sciences (Pittsburgh, PA).

Static layer-by-layer deposition of PEMs

The PEMs were deposited on a selection of base membranes using the polyelectrolytes pair (20 mM with respect to the monomer) shown in **Table 3-1**. All PE solutions were 0.5 or 1.0 M NaCl solutions. For the PE deposition on alumina base membranes the pH was adjusted to 6.5 for PSS and 3.0 for PAH. The PES base membranes were pretreated with 0.5 M NaOH at 45°C for 30 min before PE deposition and the pH was not adjusted. The pretreatment of the PES with NaOH was part of cleaning procedure. Several literatures are available on use of NaOH as cleaning solution in different kinds of membranes including PES membrane⁴⁹⁻⁵². For both base membranes, the top layer of PSS was deposited from 1.0 M NaCl.

Table 3-1: Selection of base membranes, type and amount of deposited polyelectrolytes.

Polyelectrolyte		Membrane		
<i>Name (anion ⁻, cation ⁺)</i>	<i>MW, kDa</i>	<i>Selective layer</i>	<i>MWCO or pore size</i>	<i>Deposited bilayers</i>
poly(styrene sulfonate), ⁻	70	alumina oxide	0.2 μm	(PSS/PAH) _n PSS
poly(allylamine hydrochloride), ⁺	15	poly(ethersulfone)	50 kDa	(PAH/PSS) _n

The base membranes were soaked in deionized water for 24 hours to remove preservatives and wetting additives before PEMs were deposited successively (**Figure 3-1**).

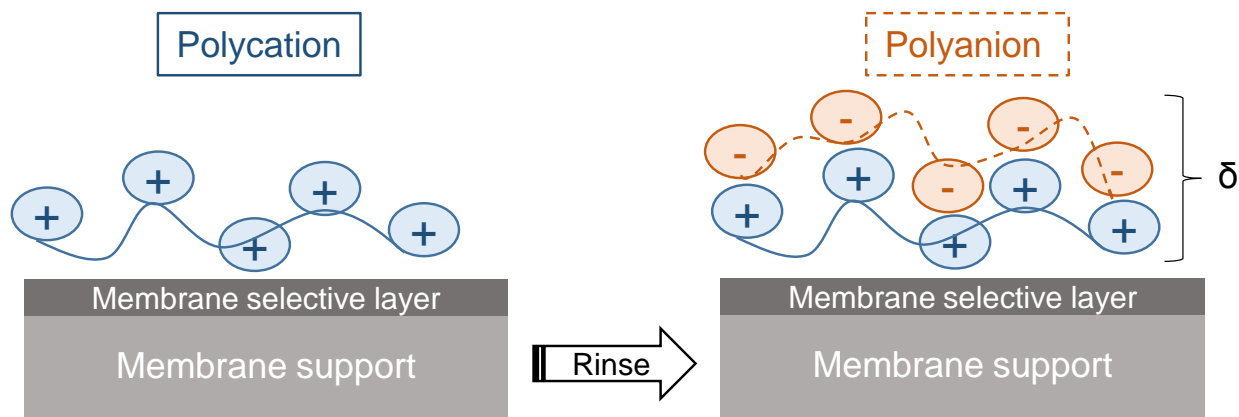


Figure 3-1: Static LBL deposition of PEM on a base membrane. First, one layer is formed after contacting with the polycation solution (or polyanion for alumina), then the membrane is rinsed before dipping into the second solution of oppositely charged polyion to form one bilayer. The alumina membranes were capped with PSS to be comparable to PES. The process is repeated for the desired bilayer number (δ).

Each polyelectrolyte layer was formed by placing the membrane in a solution of polyelectrolyte for 5 minutes, followed by rinsing with deionized water for 1 minute. Next, the membrane is placed in a solution containing the oppositely charged polyelectrolyte for 5 min followed again by rinsing for 1 min. This process was repeated as many times as to obtain the “n” desired amount of bilayers.

Membrane characterization

Attenuated total reflectance Fourier transform infrared (ATR-FTIR) spectroscopy (Shimadzu, IR Affinity-1, Kyoto, Japan) was used to analyze membrane surface chemistry before and after modification. The instrument was equipped with a deuterated L-alanine doped triglycine sulfate (DLATGS) detector with a resolution of 0.5-16 cm^{-1} , a germanium-coated potassium beam splitter with an angle of incidence of 45° and a Pike Technologies (Madison, WI) zinc selenide ATR prism. Prior to surface analysis, the membranes were rinsed with deionized water three times and then they were dried in a vacuum oven at 40°C for 6 hours. The scanning range was set as 600–2000 cm^{-1} with a resolution of 8.0 cm^{-1} and with 65 scans per sample. Spectral analysis was performed at room temperature using IR solution software (Shimadzu® IR solution).

Contact angle (Future Digital Scientific, model OCA15EC, Garden City, NY) was measured at room temperature with deionized water. The droplet volume was 2.0 μL and the dispensing speed was 0.5 $\mu\text{L}/\text{sec}$. Membrane samples were dried in vacuum oven prior to analysis and the contact

angle was captured after 3 seconds from droplet release and then measured using the circle fitting method. Each measurement was repeated 4 times.

Atomic force microscopy (AFM) was used in order to study the surface topography changes due to modification. The AFM uses a Bruker ScanAsyst (Camarillo, CA) air silicone tip on a nitride lever with a spring constant of 0.4 N/m (cantilever details: width = 25 μm , length = 115 μm , thickness = 650 nm) and is connected to a Dimension icon with ScanAsyst sample chamber (Bruker, Camarillo, CA). The images were developed at a scanning rate of 1 Hz with a resolution of 1 μm x 1 μm . Prior to analysis, the membranes were tested for permeance with deionized water and then air dried before being analyzed in tapping mode. The roughness from AFM data was calculated according to the following equation:

$$R_a = \frac{1}{N} \cdot \sum_{j=1}^N |Z_j| \quad (1)$$

where N is number of points within the box cursor and Z is peak-to-valley difference in height values. Each roughness value represents the average from 3 different surface locations.

Scanning electron microscopy (SEM) was used to characterize the cross-sectional morphology of the modified membranes. The images were analyzed using a FEI Nova Nanolab 200 Duo-Beam Workstation (Hillsboro, OR). Samples of the membranes were soaked in ethanol/water mixtures, washed with deionized water and then broken in liquid nitrogen (VWR, Batavia, IL). Prior to analysis, the samples were spotted with 10 nm layer of gold and then scanned using a 15 kV electron beam.

Zeta potential (Beckman Coulter Delsa NanoHC, Brea, CA) was equipped with a flat surface cell. Dry samples from the vacuum oven were immersed in the zeta potential analysis solution before placing them in the flat surface cell. Analysis was performed using a conductive solution of 10 mM NaCl and 1:300 diluted standard solutions for flat surface cell in triplicates.

1.1. Membrane Filtration

The performance of the PEMs was tested using three model feeds: (1) a mixture of four sugars, (2) EmimOAc and (3) BmimCl. Filtration experiments were conducted in dead-end mode (**Figure S1**). A stirred pressure vessel from Sterlitech (HP4750, Kent, WA) was filled with 200 mL feed and placed on a stirred magnetic plate (Chemglass Optichem, Vineland, NJ). The model feeds

comprised of 30 mM each cellobiose, glucose, fructose and xylose, 115 mM EmimOAc or 115 mM BmimCl. Pressurized nitrogen (Airgas, industrial grade, Fayetteville, AR) was used to pump the feed through the various modified membranes at pressures between 3-17 bar. The permeate was collected in a beaker placed on a balance (Mettler Toledo PL602-S, Columbus, OH) and the data was recorded automatically on a computer. Since ionic liquid is used as solvent for hydrolysis of biomass, the sugar concentration is expected to be low compared to the ionic liquid. Based on this argument and also from the convenience of quantification, the concentrations of sugar and ionic liquids were chosen for the present investigation.

Rejection analysis

Prior to sample analysis, the modified PEMs were first equilibrated by filtering deionized water until the permeance would remain constant. Thereafter, the feed solution was loaded into the pressure vessel and samples taken from the permeate side. The concentrations of cellobiose, glucose, xylose and fructose were determined using high performance liquid chromatography (HPLC) 1200 series (Agilent Technologies, Palo Alto, CA) equipped with a Hi-Plex Ca (Duo) column (Agilent, 300 x 6.5 mm length x internal diameter, 8 μ m pore size), injection volume: 5 μ L, mobile phase: deionized water, flow rate: 0.6 mL/minutes, column temperature: 80°C, refractive index detector detector temperature: 45°C, run time: 30 minutes. The concentrations of ionic liquid were quantified using a handheld conductivity meter Symphony SP70C (VWR, Batavia, IL) equipped with a 2-electrode conductivity cell of epoxy/platinum and a nominal cell constant of 1.0 cm^{-1} (Thermo Scientific, Beverly, MA). **Table 3-2** summarizes the analytical properties of the different feed compounds.

The rejection of sugars and ionic liquids and the selectivity of the membrane were determined using the following equations:

$$R_i = \left(1 - \frac{c_{ip}}{c_{if}}\right) \times 100\% \quad (2)$$

$$S_{i,j} = (100 - R_i)/(100 - R_j) \quad (3)$$

Where, c_{ip} and c_{if} are solute concentration of the i^{th} component in permeate and feed, respectively. $S_{i,j}$ is the selectivity of i^{th} component over j^{th} component.

Membrane water permeance was calculated from:

$$P = V/(A \cdot \Delta t \cdot p) \quad (4)$$

where V is the volume of permeated water, Δt is the time of permeation, A is membrane area, and p is applied pressure.

Table 3-2: Feed compound concentration in the three model feeds and their analytical properties.

Mixed feed sugars, 30 mM	MW, g/mol	Retention time on HPLC, min	Single feed ILs, 115 mM	MW, g/mol	Conductivity, mS/cm
Cellobiose	342.3	6.7 ± 0.01	EmimOAc	170.2	6.93 ± 0.35
Glucose	180.2	8.2 ± 0.01	BmimCl	174.7	9.51 ± 0.67
Xylose	150.1	8.9 ± 0.01			
Fructose	180.2	9.6 ± 0.03			

3.3. Results and discussions

ATR-FTIR analysis

FTIR data was collected for the base PES membrane and the modified membranes with deposited bilayers of PAH/PSS. The results are shown in **Figure 3-2**. Spectral data shows a decrease in the typical absorption peaks of the PES backbone for 1153 cm⁻¹ (asymmetric vibration of -SO₂), 1323 cm⁻¹ (symmetric vibration of -SO₂), 1489 cm⁻¹ (aromatic ring stretch of C=C) and 1578 cm⁻¹ (aromatic C-H stretch) as a function of increasing deposited bilayers. The peak at 1011 cm⁻¹ corresponds to the in plane skeleton vibration of benzene ring as suggested by Mahdi *et al.*⁵³ They have reported the growth of this peak only on deposition of bilayers of polyelectrolytes which were having benzene moieties. The conformation of the most stable structure of the base membrane might lead to the out of plane geometry of the phenyl ring showing no peak at that position for them. On the contrary, we have observed the same peak even for the base membrane itself,

revealing the preferred in plane benzene ring conformation for the base membrane. With increase in polyelectrolyte bilayer, more in plane benzene rings should be available to enhance the intensity, but there would be a sacrificial decrease from the contribution of the base membrane. Therefore, no clear trend was observed for this peak. Furthermore, the polyelectrolyte layers were deposited from solutions containing NaCl and these have been shown⁵⁴ to result in thicker polyelectrolyte layers on the surface of the virgin membrane, which coupled with the micrometer range penetration depth of FTIR, can provide a plausible explanation of the peak overlap. On the other hand, the consecutive decrease in the PES backbone peak intensity is an indicator of the thin layer growing in thickness. Also, the peak detected at 1034 cm^{-1} corresponds to the symmetric vibrational absorption of SO_3^- from PSS⁵⁵. Therefore, the latter two findings confirm the successful adsorption of polyelectrolytes.

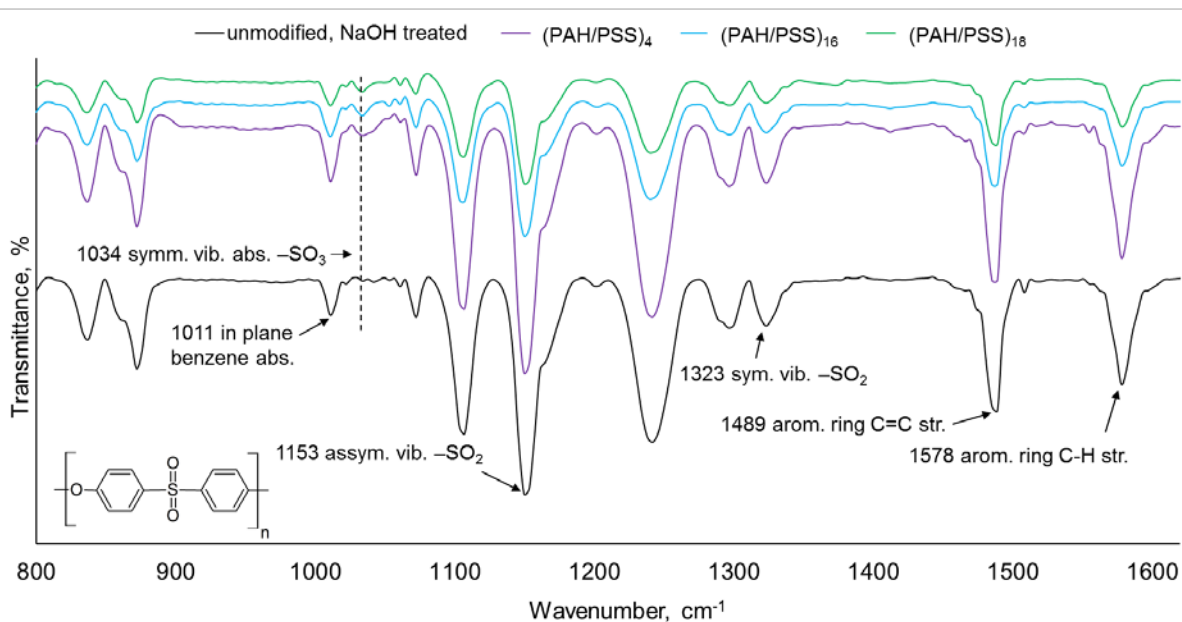


Figure 3-2: FTIR analysis of PEMs modified with 10, 16 and 18 PAH/PSS bilayers on PES base membrane.

Contact angle measurement

For understanding the hydrophilicity/hydrophobicity of the membrane, the contact angle is the most commonly used parameter. For the spontaneous flow of water through the membrane without any external pressure, the contact angle should be less than 90° . In view of the importance of contact angle on the performance of membrane, contact angle measurements were carried out (using deionized water as feed droplet) as a function of deposited bilayers (**Figure**

3-3). Our results resemble other findings from literature where it has been established that the surface contact angle is controlled primarily by the top deposited layer as well as its interpenetration with previously attached layers^{56,57}. Two insets show the considerable difference of the hydrophilic character of the base membranes. PES is rather hydrophobic while the alumina oxide membrane is very hydrophilic. After modification, both membranes show similar hydrophilic character. At higher depositions the contact angles remain constant with values between 60°-80°. This constitutes a desired effect, since more hydrophilic surfaces will improve the permeance of polar compounds and the membrane surface could be less prone to fouling. Here, the surface electrolyte PSS is a strong aromatic acid and it is believed that the contact angle results are a combined effect due to the -SO₃ groups that are present in PSS as well as the interpenetration of the previously attached PAH layer^{58,59}.

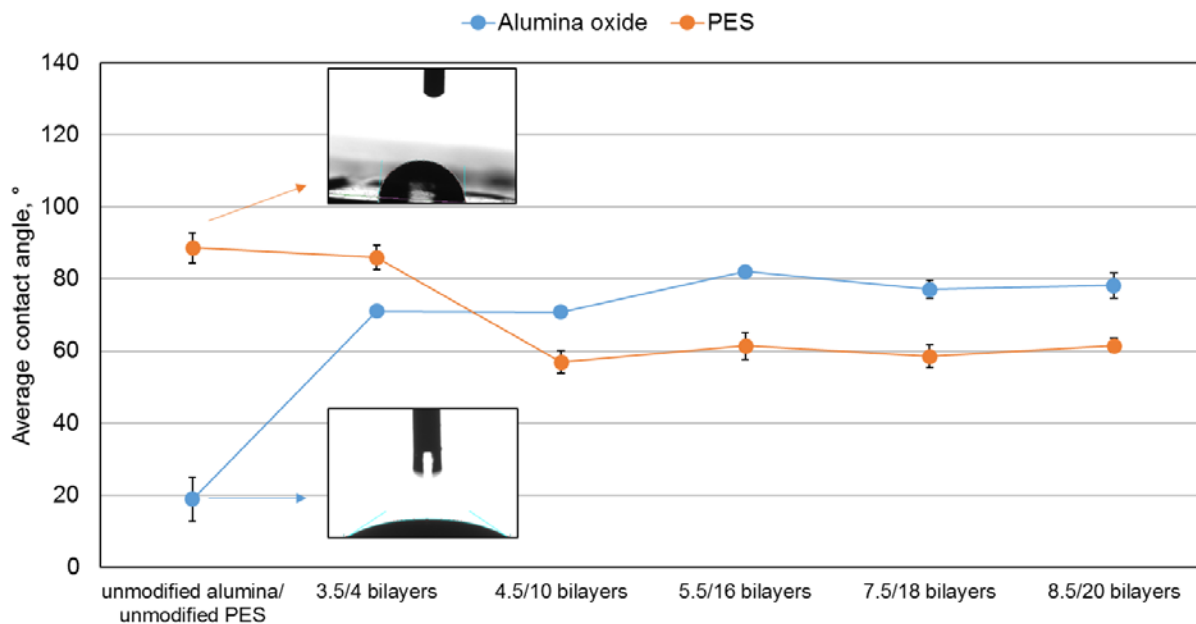


Figure 3-3: Contact angle measurements performed with deionized water droplet solution and recorded after 3 seconds. Values for the modified membranes represent the average of four measurements taken at three distinct locations on the membrane surface. Insets show droplet formation for the two distinct base membranes.

AFM imaging

Figure 3-4 shows the AFM images of the base membranes and of relevant PEMs. It was observed that the polyelectrolyte layer changes the original topography of the alumina oxide considerably

with large smooth regions, but with rougher sections around the pores. These membranes showed a rather heterogeneous surface after the modification. The modified PES membranes had a more homogenous surface, very similar to the original unmodified surface, where the polyelectrolytes seem to have covered the surface as a mold would coat a template. **Figure S2** shows the complete set of AFM images for PES membranes as a function of number of bilayers. Both of these membranes showed an overall enhancement in surface roughness on deposition of polyelectrolyte layers which was also reported by Malmali *et al.*⁵³ and Vandezande *et al.*⁶¹. **Figure S3** showed the variation of surface roughness as a function of number of polyelectrolyte bilayer on PES and alumina membrane.

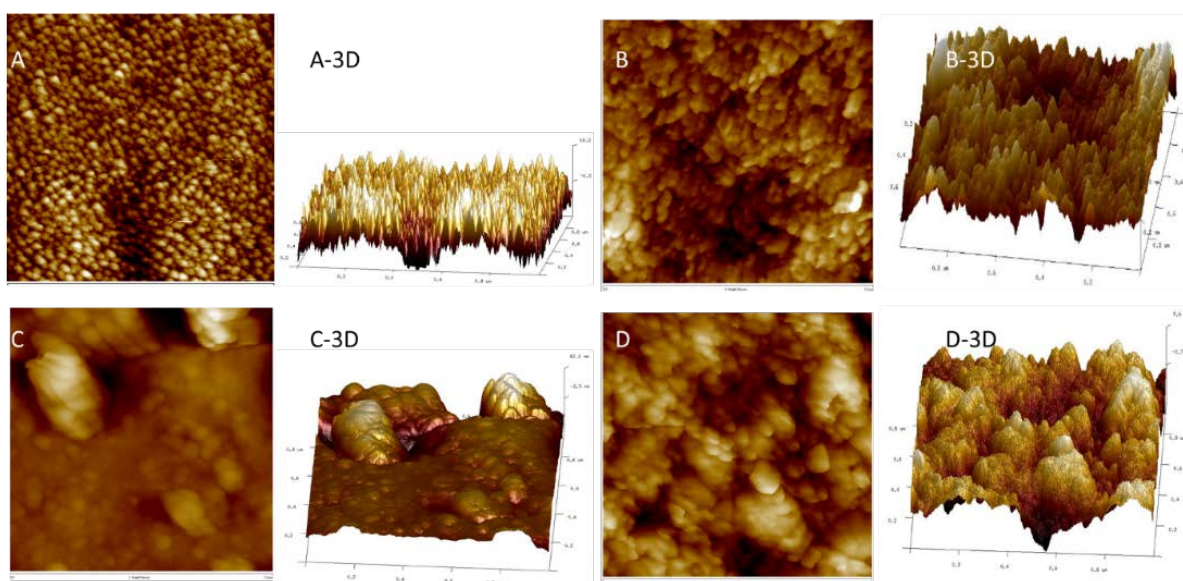


Figure 3-4: AFM images at 1 μm x 1 μm resolution in two dimensional and three dimensional (3D) display. (A; A-3D) unmodified alumina oxide, roughness 3.8 nm. (B; B-3D) unmodified PES, roughness 3.6 nm. (C; C-3D) (PSS/PAH)₈PSS on alumina oxide, roughness 11.9 nm. (D; D-3D) (PAH/PSS)₁₆ on PES, roughness 5.7 nm. These membranes were not used for rejection analysis but they were previously equilibrated with deionized water until constant permeance.

For the PES membranes, the results show that the NaOH treatment (3.6 nm) had no significant effect on the roughness of the native PES structure (3.5 nm) but that adding 4 and 10 bilayers increases the roughness to 17 nm and 16 nm, respectively. Similar trend of initial enhancement of

surface roughness was also reported in the literature on deposition of PSS and poly(diallyldimethylammonium) chloride (PDADMAC) on 5 and 50 kDa PES membrane followed by a slight decrease⁵³. This was attributed to the deposition of first layer at the entrance or inside the membrane pores which led to partial coverage of the membrane surface and then fulfilled on subsequent deposition of bilayers. When more than 10 bilayers were adsorbed on the surface, the roughness decreased considerably. This could be an effect of PE chain rearrangement and collapsing to a more rigid and condensed topography at higher bilayer numbers. A similar rearrangement has been observed by Yin *et al.*⁶⁰ when vibrational forces were applied. This research group reported a denser and more uniform membrane with smooth surface that led to better overall performance. Here, it is believed that the pressure applied during permeance tests prior to AFM analysis induced a similar reassembly and compaction of the PE bilayers.

SEM imaging

SEM images were taken of cross-sections of unmodified and modified alumina oxide and PES membranes (**Figure 3-5**). For unmodified alumina oxide, a very symmetric pore distribution can be seen. The base surface of the modified membrane has been covered in a similar manner as observed with AFM analysis and it can be seen that large, irregular PEMs have attached by protruding through the large pores. For unmodified PES, a very asymmetric membrane support can be observed along with a smooth selective layer. The base surface of the modified membrane was covered with PEMs as seen from the increase in overall thickness. A clear distinguishing between morphology of selective layer and of deposited PEMs was complicated, hence also corroborating the findings with AFM that the polyelectrolytes covered the PES membrane like a mold.

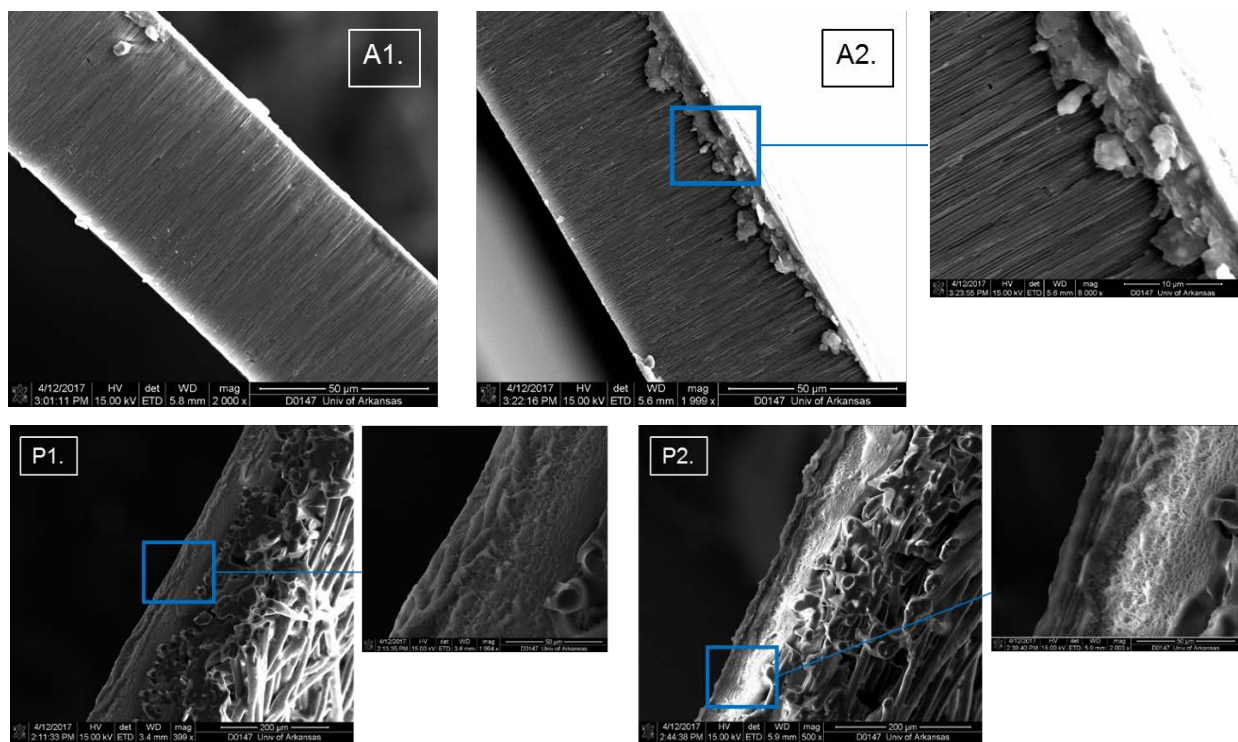


Figure 3-5: Cross-sectional SEM images of alumina oxide and PES. A1.: unmodified 0.2 μm alumina oxide (magnification: 2000x); A2.: (PSS/PAH)₈PSS (magnification: 2000x and 8000x inset); P1.: unmodified 50 kDa PES (magnification: 400x and 2000x inset); P2.: (PAH/PSS)₉ (magnification: 500x and 2000x inset).

Zeta potential measurement

The pH for zeta potential analysis for the PES membranes was adjusted manually within ± 0.2 units of the set pH. The results depicted in **Figure 3-6** show the variation of zeta potential as a function of pH. The zeta potential of modified PES membrane was found to be less sensitive than unmodified membrane. The pKa values for PAH and PSS are 8.7 and 1.0, respectively. After each bilayer deposition, the outer layer is of PSS, which is a strong electrolyte. Consequently, it leads to more stable charge dispersion resulting in less variation of zeta potential as a function of pH. It can be seen that NaOH treatment has rendered the treated unmodified membrane more negative, which was found to be in agreement with that reported by Teella *et al.*⁶¹. Their sanitized membranes were reported to be hyper sensitive to the pH due to the protonation/deprotonation of the organic acid generated during hydrolysis pretreatment.

Zeta potential analysis for the modified inorganic alumina oxide membranes (**Figure 3-6**) revealed a base membrane with positive charge at above pH 8.0 and an isoelectric point of 7.9. Due to the very brittle character of the inorganic membranes only the PEM with 8.5 bilayers was analyzed

and the zeta potential was found to be positive above pH 5.0 and negative beyond that. The isoelectric point was registered at pH 5.8 with a zeta potential between +5 and -5 mV.

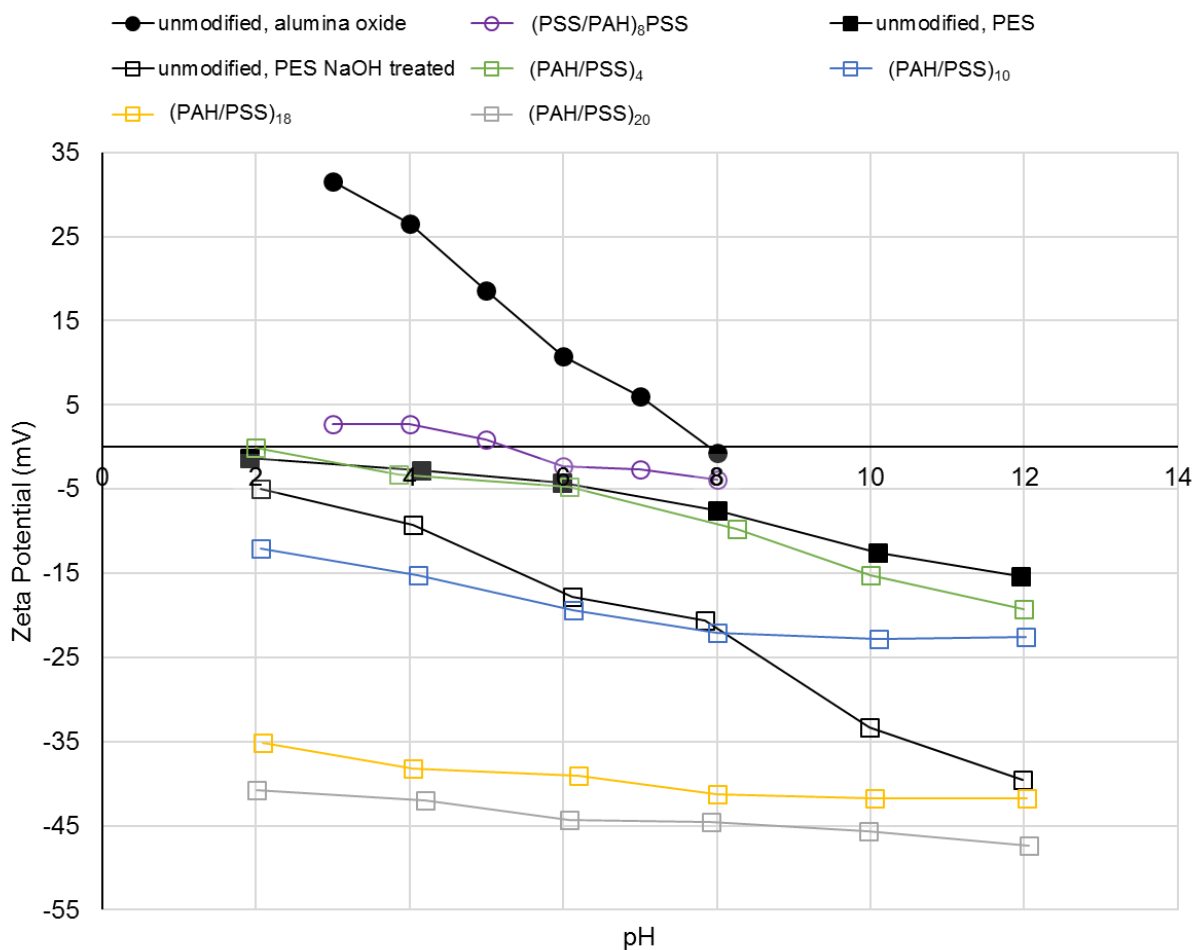


Figure 3-6: Zeta potential measurements of unmodified base membranes (black lines) and of the modified PEM membranes (colored lines). Lines connecting data markers are for guidance only. Relative error from 3 repeated measurements was $\pm 5.5\%$.

Rejection and permeance

Figure 3-7 shows the performance of modified alumina oxide base membranes with bilayers of (PSS/PAH)_nPSS that were tested for sugar and ionic liquid rejection. It is very interesting how, at lower deposited bilayers, the rejection for sugars and ILs is very similar, driven most probably to a large extent by size-exclusion. Whereas, at above 5.5 bilayers a departure from the previous trend is noticed and a selectivity becomes evident. It can be seen that, by increasing the bilayer number, the rejection for all sugar species also increases until it started to plateau around (PSS/PAH)₇PSS with almost complete (>99%) rejection of cellobiose. For the two ionic liquids, a proportional

increase in rejection with the increase in bilayer number is also observed until 7.5 bilayers were a temporary plateau is observed until the rejection increases again at 9.5 bilayers. In this manner, the deposition of polyelectrolyte layers allowed for identifying of an optimum amount of bilayers with respect to the selectivity between sugars and ionic liquids. It is believed that, at intermediate bilayers, the molecular interactions (e.g. electrostatic and hydrophilic) between feed solutes and modified surface chemistry play a more prevalent role into the rejection process in addition to just the MWCO.

While increasing the number of PE layers, the thickness of the selective layer also increases imposing a higher mass transfer resistance and an inherent decrease in membrane permeance. This translates into decreasing water permeance from about 12 to 4 L m⁻² h⁻¹ bar⁻¹ from 3.5 to 9.5 bilayers, respectively.

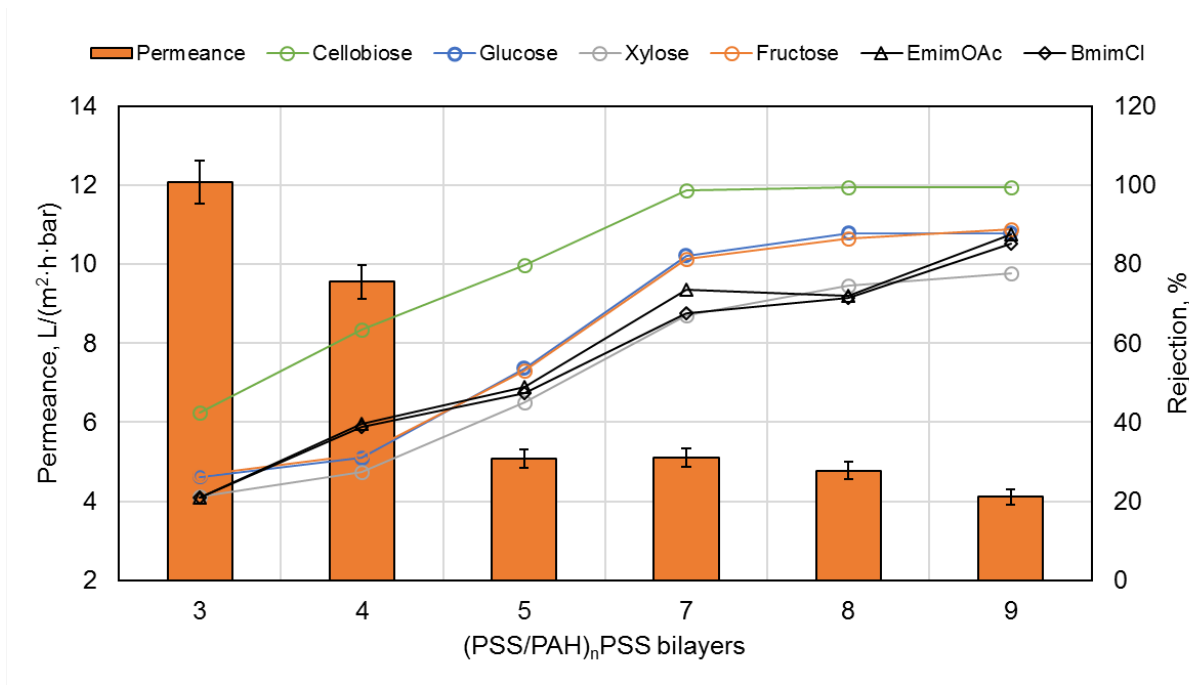


Figure 3-7: Permeance (bars) and solute rejection (lines with markers) as a function of (PSS/PAH)_nPSS bilayer number using alumina oxide disc as base membrane. Lines are there to guide the eye. Relative error for the rejection data was between ±3.2% and ±5.8% from triplicates.

PEMs have been previously shown⁶² to exhibit a response to pH changes through their amphoteric properties. E.g. permeance and rejection could change as the polyelectrolyte functional groups change their protonation state⁶³. This could have an impact on the rejection of charged species, such as the ILs discussed here. As seen in the zeta potential analysis, the only modified

nanofiltration membranes that showed a charge conversion of positive to negative were those using alumina oxide as base membrane. Therefore, the rejection of species for these membranes was tested at different pH. Data in **Table 3-3** was collected with the usual feed solutions at pH 3.0, 5.6 and 8.0 and then sampled at three different time intervals. The rejections in **Table 3-3** were stable despite the different pH values. They also showed excellent stability as a function of time pointing at a very good membrane robustness. As discussed previously in the zeta potential section, the polyelectrolyte layers deposited on alumina oxide membranes had a low positive character from pH 3 – 5 and then a low negative character from pH 6 – 8. This surface charge trait is induced by the capping layer PSS, which is a strong aromatic polyacid⁶⁴. The latter is expected to give a more stable charge dispersion, which could have made the modified membrane charge properties less susceptible to variation as a function of pH. Data shown in **Table 3-3** bolsters this assumption, as no significant change in rejection properties while changing the pH of the feed could be seen.

Table 3-3: Effect of feed pH and sampling time on compounds rejection with (PSS/PAH)₉PSS deposited on 0.2 μm alumina discs.

Time, min	Rejection, %					
	<i>Cellobiose</i>	<i>Glucose</i>	<i>Xylose</i>	<i>Fructose</i>	<i>EmimOAc</i>	<i>BmimCl</i>
pH 3.0						
25	99.5 ± 4.5	88.2 ± 4.8	78.5 ± 5.0	87.3 ± 3.9	85.2 ± 2.0	83.5 ± 1.8
50	99.6 ± 4.5	87.9 ± 4.7	77.8 ± 4.9	87.5 ± 3.9	86.0 ± 2.0	85.3 ± 1.8
75	99.5 ± 4.5	87.9 ± 4.7	79.1 ± 5.0	86.8 ± 3.9	89.9 ± 2.1	81.0 ± 1.7
unadjusted pH (~5.6)						
25	99.3 ± 4.5	90.3 ± 4.9	80.9 ± 5.1	90.3 ± 4.0	84.7 ± 2.1	87.7 ± 1.8
50	99.4 ± 4.5	89.6 ± 4.8	80.2 ± 5.1	88.7 ± 3.9	84.5 ± 2.0	85.7 ± 1.8
75	99.5 ± 4.5	88.9 ± 4.8	80.9 ± 5.1	87.9 ± 3.9	83.9 ± 2.0	83.9 ± 1.8
pH 8.0						
25	99.5 ± 4.5	90.9 ± 4.9	81.5 ± 5.2	90.8 ± 4.0	83.7 ± 2.1	86.6 ± 1.8
50	99.5 ± 4.5	90.0 ± 4.9	88.7 ± 5.6	89.5 ± 4.0	82.8 ± 2.0	84.1 ± 1.7
75	99.5 ± 4.5	89.7 ± 4.8	84.3 ± 5.3	88.9 ± 4.0	84.5 ± 2.0	84.9 ± 1.8

As seen in **Figure 3-8**, we could optimize the polyelectrolyte layer deposition on PES membranes to give almost 99% cellobiose rejection and 58% BmimCl rejection at 16 bilayers. The water permeance follows a similar decreasing trend as observed with the modified alumina oxide membranes. It starts at about $8 \text{ L m}^{-2} \text{ h}^{-1} \text{ bar}^{-1}$ for $(\text{PAH/PSS})_4$ and then levels at around $2 \text{ L m}^{-2} \text{ h}^{-1} \text{ bar}^{-1}$ from 14 through 20 bilayers.

It is interesting to see how depositing more bilayers on the PES membranes incurs a plateau in the IL rejection instead of continuously increasing as seen in **Figure 3-7** for the alumina oxide membranes. This could be explained according to the three-zone model theory in which zone I (close to substrate) and III (close to film surface) are formed after several are deposited⁶⁵. Deposition of more layers is proposed to result in the further growth of bulk zone (also core zone or zone II) only, thus decreasing membrane permeances but without considerably affecting rejection⁶⁵.

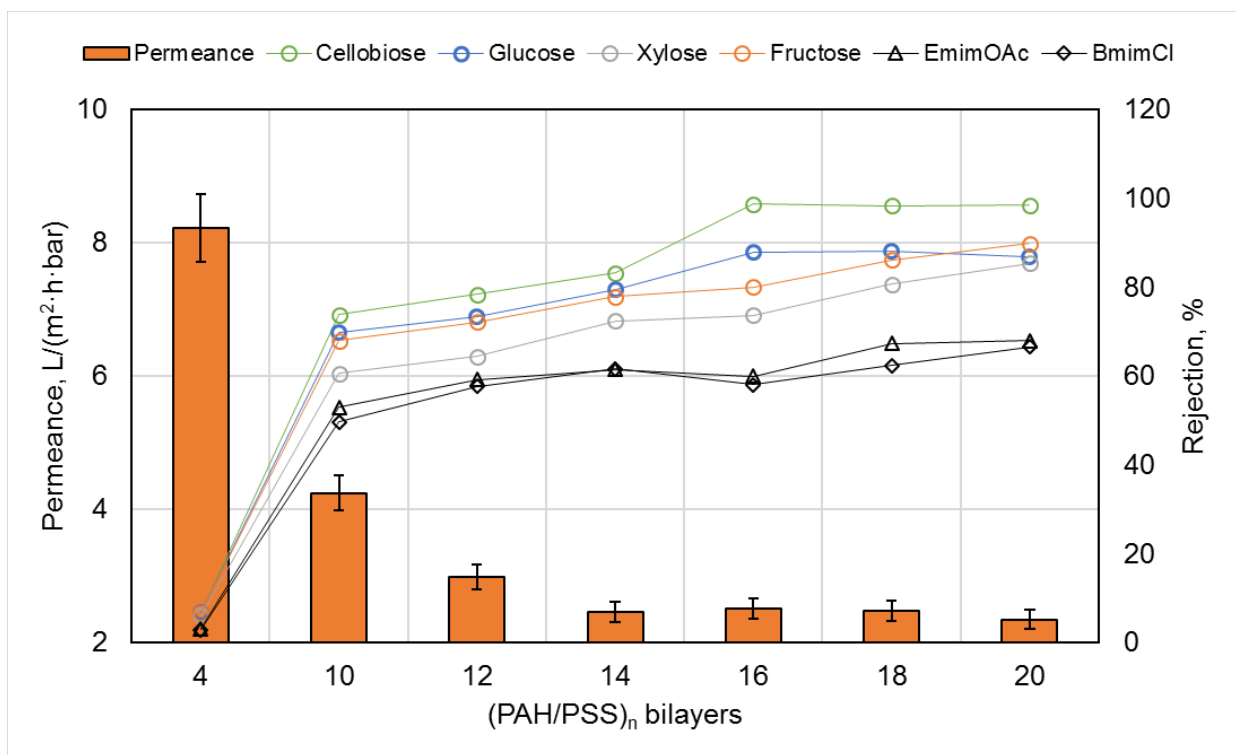


Figure 3-8: Permeance (bars) and solute rejection (lines with markers) as a function of $(\text{PAH/PSS})_n$ bilayer number using PES as base membrane. Lines are there to guide the eye. Relative error for the rejection data was between $\pm 1.7\%$ and $\pm 5.3\%$ from triplicates.

Selectivity of ionic liquid over monomeric sugar

Based on the size exclusion principle, the separation of these sugars and the ionic liquids, e.g. BmimCl and EmimOAc is challenging as seen from **Table 3-2**. The deposition-induced modified surface properties (increase in hydrophilicity, more negative value of zeta potential) were utilized here to achieve the effective separation of ionic liquid from monomeric sugars based on the latter property enhancement. There are several important observations that can be concluded from data in **Table 3-4**. At 3.5 and 4 bilayers, the modified NF membranes show very low selectivity with no significant difference between the charged ionic liquid BmimCl and the uncharged sugars cellobiose and glucose. The rejection at this regime is expected to be mostly due to size-exclusion due to the insufficient coverage of polyelectrolyte layers as suggested by literature^{44,53}. As more PE bilayers are deposited, the molecular interactions between solutes and the membrane active layer increase so that the alumina oxide (PSS/PAH)₇PSS already shows a vastly improved selectivity BmimCl/Cellobiose versus Glucose/Cellobiose. The latter two solute pairs have very similar molecular weight ratios and this finding serves as proof that rejection at this regime is governed by additional preferential molecular interactions with the PE selective layer. The charged deposited polyelectrolytes seem to interact favorably with the charged IL molecule and allow for its easier passage than e.g. for glucose. Increasing the bilayer number even further starts to decrease the selectivity towards BmimCl. However, BmimCl/Cellobiose selectivity is still considerably better than Glucose/Cellobiose, which is believed to be driven by additional favorable interactions of the BmimCl cation with the increased negative membrane surface, as shown in zeta potential analysis (**Figure 3-6**). When adding more bilayers, the selective layer thickness increases and the solutes are thus forced to pass through tighter pores of more intertwined PE networks. As a result, the selectivity decreases from 2.3 at (PSS/PAH)₈PSS bilayers to 1.2 at (PSS/PAH)₉PSS bilayers in the case of the inorganic PEMs. The same effect is seen with the organic PEMs where the selectivity also decreases from 3.5 at 16 bilayers to 2.5 at 20 bilayers. Therefore, an optimization can be achieved and its effect can be described using three rejection regimes that build up with increasing bilayer number. In all of the identified separation regimes, the primary basis for the rejection process is still size-exclusion. This can especially be seen for the PES membranes in the rejection of uncharged sugars. There the rejection followed the trend: Cellobiose > Glucose ~ Fructose > Xylose, according with the molecular weight of the molecule. However, BmimCl and

EmimOAc, although larger in molecular size than the smallest sugar (Xylose) always showed lower rejection. Therefore, it is believed that selectivity of species can be controlled via additional interactions with the deposited polyelectrolyte layers. E.g. the electrostatic interactions of the deposited polyelectrolyte layers with the ionic liquid can be utilized as an additional factor to enhance the selectivity (along with the size exclusion) in the present case.

In the first regime, rejection is governed to a larger extent by size-exclusion, whereas in the second and third regime the selectivity is to some extent controlled by superficial and stronger molecular interactions (e.g. electrostatic interactions). The optimum, as given by a BmimCl/Cellobiose selectivity of 50.5 for (PSS/PAH)₇PSS on alumina oxide and 32.3 for (PAH/PSS)₁₆ on PES was found in the second regime. PEMs fabricated on alumina oxide membranes showed better permeance due to a lower number of bilayers required to reach similar rejection. It is believed that during LBL deposition the PEs diffused and deposited inside the pores of these base membranes. This phenomena has been previously observed by Bruening *et al.*³⁷ and is reflected in our findings by a lower amount of bilayers required to reach similar rejection performance when compared to the PES base membranes, where LBL deposition has presumably occurred mainly on the membrane surface. Furthermore, SEM analysis showed protrusion of PEMs inside the alumina oxide pores (**Figure 3-5**).

Table 3-4: Summary of selected modified nanofiltration membranes with selectivity and permeance.

Base Membrane	Bilayers	Permeance, L/(m ² ·h·bar)	α , MW ratio		
			<i>BmimCl/Cellobiose</i> , 1.95	<i>BmimCl/Glucose</i> , 1.03	<i>Glucose/Cellobiose</i> , 1.90
Alumina oxide (0.2 μM)	3.5x	12.08 ± 0.75	1.4	1.1	1.3
	7.5x	5.08 ± 0.32	27.1	1.8	14.9
	8.5x	4.78 ± 0.30	50.5	2.3	21.6
	9.5x	4.11 ± 0.26	29.4	1.2	24.2
PES (50 kDa)	4x	8.22 ± 0.51	1.0	1.0	1.0
	16x	2.51 ± 0.16	32.3	3.5	9.3
	18x	2.47 ± 0.15	22.1	3.1	7.1
	20x	2.34 ± 0.15	22.3	2.5	8.8

Anti-fouling property is one of the vital properties for the nanofiltration membrane. Therefore, the reusability and resistance of the modified membranes were investigated. In **Figure S4** it can be seen that the relative water permeance after dipping the modified membrane in 200 mM BmimCl and in 1.5 M NaCl for 24 hours showed no detrimental change. Then, in **Figure S5** the rejection of sugars and of ionic liquid was carried out in three consecutive cycles and changes in the relative rejection was monitored after each cycle. These studies revealed that only insignificant changes in relative permeance and relative rejection occurred so that the modified membranes (alumina oxide and PES) are considered to be reusable and resistant for the present application.

Comparative study

The recyclability of ionic liquids via membrane technology and several other methods was previously critically studied by various groups^{18,25,66,67}. The most prominent limitation of membrane-driven processes for IL recycling is the osmotic pressure. In order to purify an ionic liquid to >90% wt. very high operational pressures would be required and these often exceed the maximum operational pressure for nanofiltration. In **Table 3-5** some previous work has been summarized, while emphasizing some advantages and disadvantages. For example, Haerens *et al.*²⁵ achieved very high rejections with a similar process as in the present work, but their main limitation was the osmotic pressure. Instead of focusing on complete recovery of IL in the retentate, like many researchers in this areas commonly do, here we have optimized membranes for purification of ILs in dilute aqueous permeates. E.g. we are taking advantage of the low molecular weight and charge property of the ILs to facilitate their permeation through fabricated nanofiltration membranes while retaining as much of the contaminants as possible. In essence, we are optimizing a pre-recycling step since the ILs will always contain water, which acts as a transporter solvent. A very promising technique with excellent selectivity for biomass compounds was developed by Binder *et al.*⁶⁶. Using ion-exchange chromatography, the researchers were able to recover up to 95% pure IL. However, chromatography suffers from several experimental

limitations that could make scale-up unfeasible, especially when considering the complicated chromatography system and its potential use with high volumes of biomass hydrolysate. With our system, dilute streams that are mostly free of other contaminants are produced and this opens the avenue for developing automated systems capable of dealing with high volumes of filtrate, possibly in continuous mode (e.g. crossflow filtration).

The main aim of Shill *et al.*¹⁷ was to study the ionic liquid pretreatment of cellulose biomass followed by enzymatic hydrolysis and the recycling of ionic liquid. As mentioned in **Table 3-5**, although ~ 95% ionic liquid can be recycled, it is expected to be contaminated with potassium salts and lignin. No further investigation on the purity of the ionic liquid was reported. While discussing the challenges for recycling ionic liquids by pressure driven membrane process, Haerens *et al.*²⁵ reported that the recycled product would be maximum 30% ionic liquid in water. The recycled ionic liquid was not subjected to any kind of purity check except water content. Based on their investigation, osmotic pressure is the limiting factor for removal of water from the ionic liquid fraction. Wu *et al.*¹⁸ in their investigation on the phase behavior of ternary systems composed of ionic liquid, saccharides and water, found out that their optimized liquid-liquid extraction technique resulted in highly pure ionic liquid with less than 1% of water content and with no sugars, which has been confirmed experimentally. The authors also quoted that the recovery of ionic liquid was not satisfactory (maximum up to 74% depending on the nature of the sugar molecules). Binder *et al.*⁶⁶ optimized an ion-exchange based separation technique for ionic liquid from sugar with a recovery of more than 95%. Although the further analysis on the purity of the sugar was not carried out, the ion-exchange chromatographic technique was assumed to produce purified ionic liquid. The present work investigated the potential of a membrane based separation to selectively allow for ionic liquid permeance while rejecting as much as possible of typical

biomass hydrolysis sugars. This separation strategy has the advantage that the ionic liquid does not accumulate and concentrate in the retentate, thus circumventing the inherent limitation by high osmotic pressure, as quoted by Haerens *et al.*²⁵. The purity of the recycled ionic liquid in this work depends on the rejection of sugar species and can be evaluated from the selectivity value in **Table 3-4**. The higher the selectivity, the less sugar impurities would permeate along with the recovered ionic liquid.

Table 3-5: Comparison of this work with other similar published work on ionic liquid recycling. Comments explain some advantages (+) and disadvantages (-).

IL recycle method	Feed solution	Results	Comments	Reference
Modified polyelectrolyte nanofiltration membranes	Model feeds comprised of 30 mM monosaccharides, 115 mM BmimCl and 115 mM EmimOAc	Clean permeate stream containing mostly IL liquid in water with less than ppm level monosaccharide impurities	(+) circumvents inherent pressure limitation due to osmotic pressure (+) one step produces a permeate stream that contains mostly IL (+) simple to perform and scale-up feasible (-) IL is very diluted and other steps are required to remove large amounts of water	this work
Nanofiltration, reverse osmosis for IL concentration followed by pervaporation for water removal	BmimBF ₄ (MW 226.0 Da), Bmim ₂ SO ₄ (MW 236.3 Da) in water with 5% v/v ethylene glycol	82% rejection with Desal DVA 032; 95% rejection with Desal DVA 00; maximum 30% v/v recovery from initial feed	(+) scale-up feasibility (-) rejection limited by osmotic pressure (-) water removal via pervaporation limited by reduced flow due to low water content on feed side	Haerens <i>et al.</i> ²⁵

Two phase liquid-liquid extraction with high concentration of sugars; IL in upper phase, sugars in lower phase	BmimBF ₄	recovery of IL is 74% for sucrose, 72% for xylose, 64% for fructose, and 61% for glucose	(+) IL is pure without any sugar and less than 1 % H ₂ O content (-) scale-up complicated (-) large amounts of solvents necessary (-) The ionic liquid recovery is not impressive	Wu <i>et al.</i> ¹⁸
Two phase liquid-liquid extraction with 40% K ₂ PO ₄ or KHPO ₄ followed by water evaporation; IL in upper phase, salt and sugars in lower phase	BmimOAc (MW 198.3 Da), EmimOAc in pretreated biomass	Recovery of 95% IL with salt impurities	(+) very good recovery of pure IL with small amounts of impurities (-) pH was very basic at 9-13 (-) large amount of solvents and salts are required (-) scale-up probably economically unfeasible	Shill <i>et al.</i> ⁶⁷
Ion-exclusion chromatography	EmimCl (MW 146.6 Da) in biomass hydrolyzate	96% recovery of pure IL	(+) selective separation of hydrolysis sugars, HCl, HMF and furfurals (+) IL can be reused as-is for new reaction (-) cannot handle large volumes continuously (-) complicated setup	Binder <i>et al.</i> ⁶⁶

3.4. Conclusion

The present investigation deals with the surface modification and characterization of alumina oxide and PES ultrafiltration membranes by polyelectrolyte deposition, and subsequent demonstration of its application on the feasibility of recycling of ionic liquid from biomass hydrolysates. An attempt was made to understand the effect of number of polyelectrolyte bilayers

on the surface properties of the membrane and its consequent membrane performance. AFM imaging, contact angle measurement and zeta potential analysis were used to analyze the surface properties and morphology of the modified membranes which were found to be directly linked with water permeance and selectivity performance. Alumina oxide membranes showed heterogeneous deposition of PEs with large smooth areas and then rougher areas around the large microfiltration pores. The former is believed to be beneficial for increased permeance, while the latter could trigger a mediated transfer of charged species and thus an increase in selectivity for ionic liquids. An optimized nanofiltration membrane was obtained at (PSS/PAH)₈PSS showing BmimCl/Cellobiose selectivity above 50. Additionally, the fabricated membranes showed excellent stability in the pH range of 3.0 through 8.0 at extended separation times. PES membranes showed a more homogenous deposition of PEs that seem to mimic the original structure of the base membranes. Coupled with increased negative charge as a function of deposited bilayers this allowed for better transfer of the charged species while retaining the non-charged species on size-exclusion basis. An optimized nanofiltration membrane was obtained at (PAH/PSS)₁₆ showing BmimCl/Cellobiose selectivity above 30.

Acknowledgements

Financial support from the National Science Foundation CBET 1264896 is gratefully acknowledged.

The authors greatly appreciate the use of the Arkansas Materials Characterization Facility for the SEM studies.

References

1. Verardi A, De Bari I, Ricca E, Calabrò V. Hydrolysis of lignocellulosic biomass: Current status of processes and technologies and future perspectives. In: Pinheiro-Lima MA, Policastro-Natalense AP, eds. *Bioethanol*. InTech; 2012:95.
2. Abels C, Carstensen F, Wessling M. Membrane processes in biorefinery applications. *J Membr Sci*. 2013;444:285-317.
3. Wang W, Turner TL, Stikeleather LF, Roberts WL. Exploration of process parameters for continuous hydrolysis of canola oil, camelina oil and algal oil. *Chemical Engineering and Processing: Process Intensification*. 2012;57–58:51-58.
4. Fairley P. Introduction: Next generation biofuels. . 2011:S2.

5. Malmali M, Stickel J, Wickramasinghe SR. Investigation of a submerged membrane reactor for continuous biomass hydrolysis. *Food Bioprod Process*. 2015;96:189-197.
6. Brennan TCR, Datta S, Blanch HW, Simmons BA, Holmes BM. Recovery of sugars from ionic liquid biomass liquor by solvent extraction. *BioEnergy Res*. 2010;3(2):123-133.
7. Lozano P, Bernal B, Jara AG, Belleville M. Enzymatic membrane reactor for full saccharification of ionic liquid-pretreated microcrystalline cellulose. *Bioresour Technol*. 2014;151:159-165.
8. Zhu S. Use of ionic liquids for the efficient utilization of lignocellulosic materials. *J Chem Technol Biotechnol*. 2008;83(6):777-779.
9. Rinaldi R, Palkovits R, Schueth F. Depolymerization of cellulose using solid catalysts in ionic liquids. *Angew Chem -Int Edit*. 2008;47(42):8047-8050.
10. Maki-Arvela P, Anugwom I, Virtanen P, Sjoholm R, Mikkola JP. Dissolution of lignocellulosic materials and its constituents using ionic liquids-A review. *Ind Crop Prod*. 2010;32(3):175-201.
11. Bokinsky G, Peralta-Yahya PP, George A, et al. Synthesis of three advanced biofuels from ionic liquid-pretreated switchgrass using engineered escherichia coli. *Proc Natl Acad Sci U S A*. 2011;108(50):19949-19954.
12. Liu C, Wang F, Stiles AR, Guo C. Ionic liquids for biofuel production: Opportunities and challenges. *Appl Energy*. 2012;92:406-414.
13. Baral NR, Shah A. Techno-economic analysis of cellulose dissolving ionic liquid pretreatment of lignocellulosic biomass for fermentable sugars production. *Biofuels Bioprod Biorefining*. 2016;10(1):70-88.
14. Feng D, Li L, Yang F, et al. Separation of ionic liquid [mmim][DMP] and glucose from enzymatic hydrolysis mixture of cellulose using alumina column chromatography. *Appl Microbiol Biotechnol*. 2011;91(2):399-405.
15. Carneiro AP, Rodríguez O, Macedo EA. Separation of carbohydrates and sugar alcohols from ionic liquids using antisolvents. *Separation and Purification Technology*. 2014;132:496-504.
16. Francisco M, Mlinar AN, Yoo B, Bell AT, Prausnitz JM. Recovery of glucose from an aqueous ionic liquid by adsorption onto a zeolite-based solid. *Chem Eng J*. 2011;172(1):184-190.
17. Shill K, Padmanabhan S, Xin Q, Prausnitz JM, Clark DS, Blanch HW. Ionic liquid pretreatment of cellulosic biomass: Enzymatic hydrolysis and ionic liquid recycle. *Biotechnol Bioeng*. 2011;108(3):511-520.

18. Wu B, Liu W, Zhang Y, Wang H. Do we understand the recyclability of ionic liquids? *Chemistry – A European Journal*. 2009;15(8):1804-1810.
19. Mai NL, Ahn K, Koo Y. Methods for recovery of ionic liquids—A review. *Process Biochemistry*. 2014;49(5):872-881.
20. Malmali M, Wickramasinghe SR, Tang J, Cong H. Sugar fractionation using surface-modified nanofiltration membranes. *Separation and Purification Technology*. 2016;166:187-195.
21. He Y, Bagley DM, Leung KT, Liss SN, Liao B. Recent advances in membrane technologies for biorefining and bioenergy production. *Biotechnol Adv*. 2012;30(4):817-858.
22. Weschenfelder SE, Fonseca MJC, Borges CP, Campos JC. Application of ceramic membranes for water management in offshore oil production platforms: Process design and economics. *Separation and Purification Technology*. 2016;171:214-220.
23. Abels C, Redepenning C, Moll A, Melin T, Wessling M. Simple purification of ionic liquid solvents by nanofiltration in biorefining of lignocellulosic substrates. *J Membr Sci*. 2012;405:1-10.
24. Hazarika S, Dutta NN, Rao PG. Dissolution of lignocellulose in ionic liquids and its recovery by nanofiltration membrane. *Separation and Purification Technology*. 2012;97:123-129.
25. Haerens K, Van Deuren S, Matthijs E, Van der Bruggen B. Challenges for recycling ionic liquids by using pressure driven membrane processes. *Green Chem*. 2010;12(12):2182-2188.
26. Trinh LTP, Lee YJ, Lee J, Bae H, Lee H. Recovery of an ionic liquid [BMIM]Cl from a hydrolysate of lignocellulosic biomass using electrodialysis. *Separation and Purification Technology*. 2013;120:86-91.
27. Wu H, Shen F, Wang J, et al. Separation and concentration of ionic liquid aqueous solution by vacuum membrane distillation. *J Membr Sci*. 2016;518:216-228.
28. Abels C, Thimm K, Wulfhorst H, Spiess AC, Wessling M. Membrane-based recovery of glucose from enzymatic hydrolysis of ionic liquid pretreated cellulose. *Bioresour Technol*. 2013;149:58-64.
29. Decher G. Fuzzy nanoassemblies: Toward layered polymeric multicomposites. *Science*. 1997;277(5330):1232-1237.
30. Decher G, Hong JD, Schmitt J. Buildup of ultrathin multilayer films by a self-assembly process .3. consecutively alternating adsorption of anionic and cationic polyelectrolytes on charged surfaces. *Thin Solid Films*. 1992;210(1-2):831-835.
31. Iler RK. Multilayers of colloidal particles. *J Colloid Interface Sci*. 1966;21(6):569-&.

32. Castleberry SA, Li W, Deng D, Mayner S, Hammond PT. Capillary flow layer-by-layer: A microfluidic platform for the high-throughput assembly and screening of nano layered film libraries. *ACS Nano*. 2014;8(7):6580-6589.
33. Ishigami T, Amano K, Fujii A, et al. Fouling reduction of reverse osmosis membrane by surface modification via layer-by-layer assembly. *Separation and Purification Technology*. 2012;99:1-7.
34. Ahmadiannamini P, Li X, Goyens W, Joseph N, Meesschaert B, Vankelecom IFJ. Multilayered polyelectrolyte complex based solvent resistant nanofiltration membranes prepared from weak polyacids. *J Membr Sci*. 2012;394:98-106.
35. Li X, Goyens W, Ahmadiannamini P, Vanderlinden W, De Feyter S, Vankelecom I. Morphology and performance of solvent-resistant nanofiltration membranes based on multilayered polyelectrolytes: Study of preparation conditions. *J Membr Sci*. 2010;358(1-2):150-157.
36. Ahmadiannamini P, Li X, Goyens W, Meesschaert B, Vankelecom IFJ. Multilayered PEC nanofiltration membranes based on SPEEK/PDDA for anion separation. *J Membr Sci*. 2010;360(1-2):250-258.
37. Harris JJ, Stair JL, Bruening ML. Layered polyelectrolyte films as selective, ultrathin barriers for anion transport. *Chemistry of Materials*. 2000;12(7):1941-1946.
38. Abdu S, Marti-Caatayud M, Wong JE, Garcia-Gabaldon M, Wessling M. Layer-by-layer modification of cation exchange membranes controls ion selectivity and water splitting. *ACS Applied Materials & Interfaces*. 2014;6(3):1843-1854.
39. Lu O, Malaisamy R, Bruening ML. Multilayer polyelectrolyte films as nanofiltration membranes for separating monovalent and divalent cations. *J Membr Sci*. 2008;310(1-2):76-84.
40. Seong Uk H, Lu O, Bruening ML. Recovery of phosphate using multilayer polyelectrolyte nanofiltration membranes. *J Membr Sci*. 2009;327(1-2):2-5.
41. Shi H, Xagorarakis I, Parent KN, Bruening ML, Tarabara VV. Elution is a critical step for recovering human adenovirus 40 from tap water and surface water by cross-flow ultrafiltration. *Appl Environ Microbiol*. 2016;82(16):4982-4993.
42. Pasco EV, Shi H, Xagorarakis I, et al. Polyelectrolyte multilayers as anti-adhesive membrane coatings for virus concentration and recovery. *J Membr Sci*. 2014;469:140-150.
43. Malmali M, Wickramasinghe SR, Tang J, Cong H. Sugar fractionation using surface-modified nanofiltration membranes. *Separation and Purification Technology*. 2016;166:187-195.

44. Malaisamy R, Bruening M. High-flux nanofiltration membranes prepared by adsorption of multilayer polyelectrolyte membranes on polymeric supports. *Langmuir*. 2005;21(23):10587-10592.
45. Stanton B, Harris J, Miller M, Bruening M. Ultrathin, multilayered polyelectrolyte films as nanofiltration membranes. *Langmuir*. 2003;19(17):7038-7042.
46. Dubas ST, Schlenoff JB. Factors controlling the growth of polyelectrolyte multilayers. *Macromolecules*. 1999;32(24):8153-8160.
47. Joseph N, Ahmadiannamini P, Hoogenboom R, Vankelecom IFJ. Layer-by-layer preparation of polyelectrolyte multilayer membranes for separation. *Polymer Chemistry*. 2014;5(6):1817-1831.
48. Miller MD, Bruening ML. Controlling the nanofiltration properties of multilayer polyelectrolyte membranes through variation of film composition. *Langmuir*. 2004;20(26):11545-11551.
49. Ang WS, Yip NY, Tiraferri A, Elimelech M. Chemical cleaning of RO membranes fouled by wastewater effluent: Achieving higher efficiency with dual-step cleaning. *J Membr Sci*. 2011;382(1-2):100-106.
50. Vaisanen P, Bird M, Nystrom M. Treatment of UF membranes with simple and formulated cleaning agents. *Food Bioprod Process*. 2002;80(C2):98-108.
51. Mohammadi T, Madaeni S, Moghadam M. Investigation of membrane fouling. *Desalination*. 2003;153(1-3):155-160.
52. Mohammadi T. Chemical cleaning of a polyamide membrane. *Desalination*. 2001;139(1-3):381-381.
53. Malmali M, Wickramasinghe SR, Tang J, Cong H. Sugar fractionation using surface-modified nanofiltration membranes. *Separation and Purification Technology*. 2016;166:187-195.
54. Li X, Goyens W, Ahmadiannamini P, Vanderlinden W, De Feyter S, Vankelecom I. Morphology and performance of solvent-resistant nanofiltration membranes based on multilayered polyelectrolytes: Study of preparation conditions. *J Membr Sci*. 2010;358(1-2):150-157.
55. SU B, Wang T, Wang Z, Gao X, Gao C. Preparation and performance of dynamic layer-by-layer PDADMAC/PSS nanofiltration membrane. *J Membr Sci*. 2012;423-424:324-331.
56. Shiratori S, Rubner M. pH-dependent thickness behavior of sequentially adsorbed layers of weak polyelectrolytes. *Macromolecules*. 2000;33(11):4213-4219.

57. Yoo D, Shiratori S, Rubner M. Controlling bilayer composition and surface wettability of sequentially adsorbed multilayers of weak polyelectrolytes. *Macromolecules*. 1998;31(13):4309-4318.
58. Ishigami T, Amano K, Fujii A, et al. Fouling reduction of reverse osmosis membrane by surface modification via layer-by-layer assembly. *Separation and Purification Technology*. 2012;99:1-7.
59. Elzbieciak M, Kolasinska M, Warszynski P. Characteristics of polyelectrolyte multilayers: The effect of polyion charge on thickness and wetting properties. *Colloid Surf A-Physicochem Eng Asp*. 2008;321(1-3):258-261.
60. Yin M, Qian J, An Q, Zhao Q, Gui Z, Li J. Polyelectrolyte layer-by-layer self-assembly at vibration condition and the pervaporation performance of assembly multilayer films in dehydration of isopropanol. *J Membr Sci*. 2010;358(1-2):43-50.
61. Teella A, Zydney AL, Zhou H, Olsen C, Robinson C. Effects of chemical sanitization using NaOH on the properties of polysulfone and polyethersulfone ultrafiltration membranes. *Biotechnol Prog*. 2015;31(1):90-96.
62. Seong Uk H, Lu O, Bruening ML. Recovery of phosphate using multilayer polyelectrolyte nanofiltration membranes. *J Membr Sci*. 2009;327(1-2):2-5.
63. Cranford SW, Ortiz C, Buehler MJ. Mechanomutable properties of a PAA/PAH polyelectrolyte complex: Rate dependence and ionization effects on tunable adhesion strength. *Soft Matter*. 2010;6(17):4175-4188.
64. Dubas ST, Schlenoff JB. Factors controlling the growth of polyelectrolyte multilayers. *Macromolecules*. 1999;32(24):8153-8160.
65. Ladam G, Schaad P, Voegel JC, Schaaf P, Decher G, Cuisinier F. In situ determination of the structural properties of initially deposited polyelectrolyte multilayers. *Langmuir*. 2000;16(3):1249-1255.
66. Binder JB, Raines RT. Fermentable sugars by chemical hydrolysis of biomass. *Proc Natl Acad Sci U S A*. 2010;107(10):4516-4521.
67. Shill K, Padmanabhan S, Xin Q, Prausnitz JM, Clark DS, Blanch HW. Ionic liquid pretreatment of cellulosic biomass: Enzymatic hydrolysis and ionic liquid recycle. *Biotechnol Bioeng*. 2011;108(3):511-520.

Supporting information

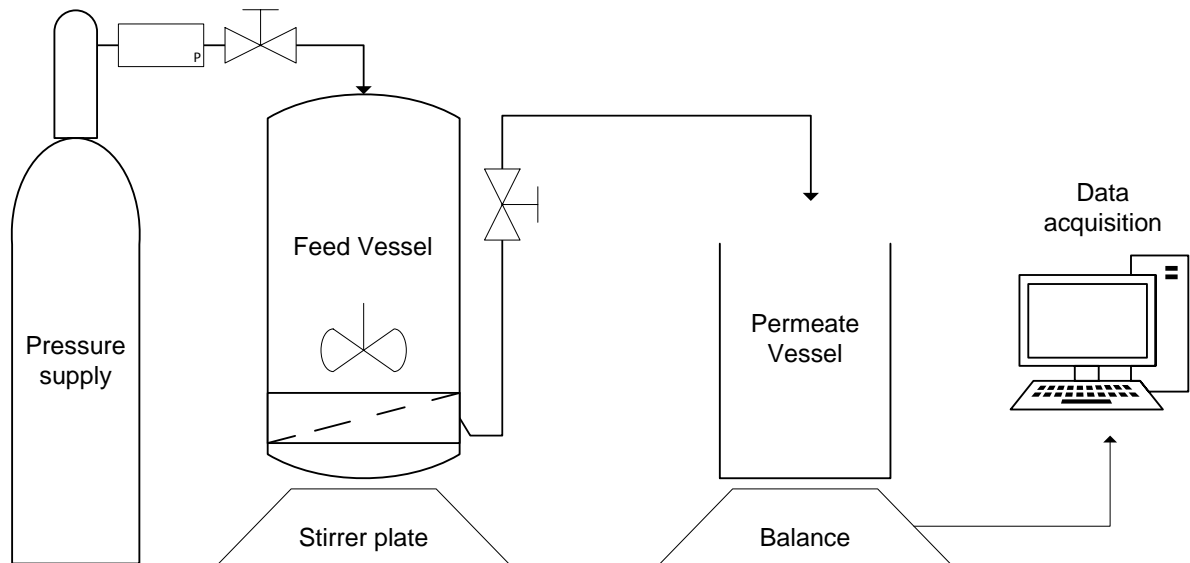


Figure S1: Dead-end filtration setup for measuring of permeance and rejection of modified membranes.

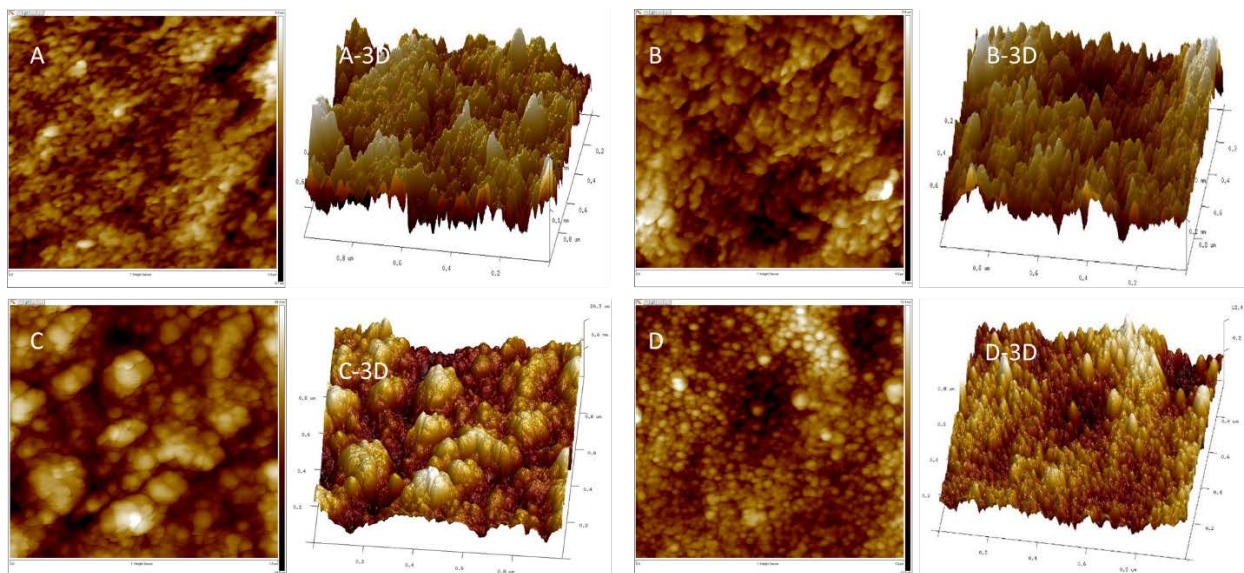


Figure S2: AFM images at 1 μm x 1 μm resolution in two dimensional and three dimensional (3D) display. (A; A-3D) unmodified PES. (B; B-3D) unmodified, NaOH treated PES. (C; C-3D) (PAH/PSS)₄. (D; D-3D) (PAH/PSS)₁₈.

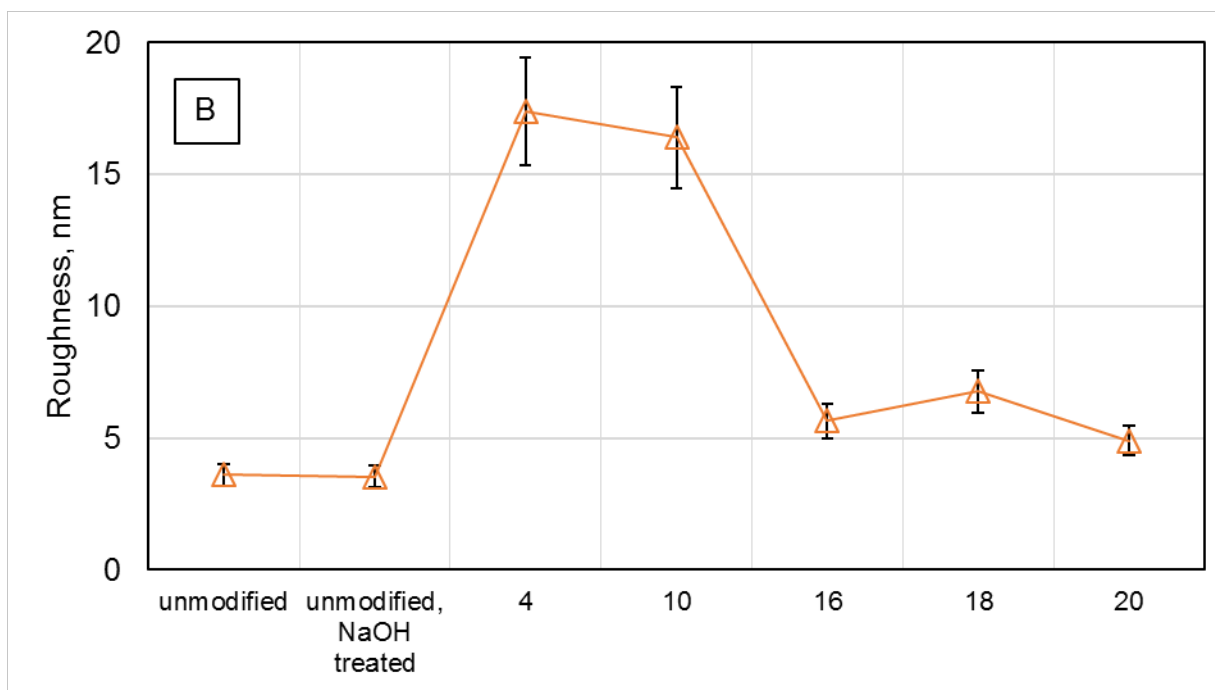
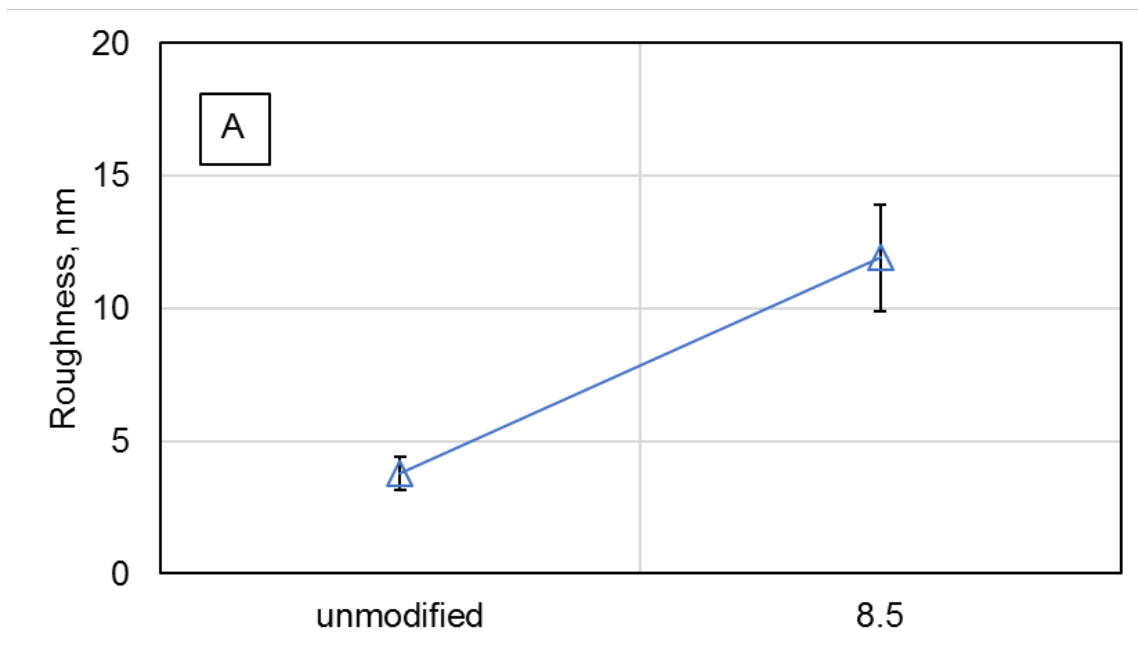
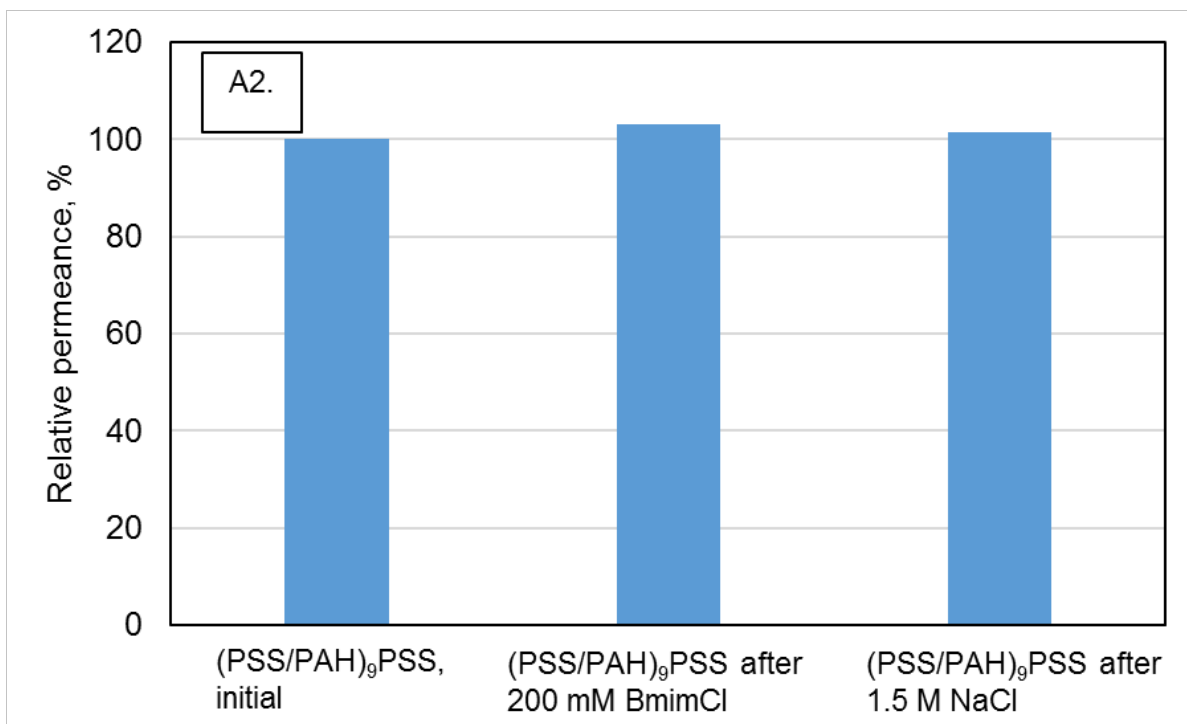
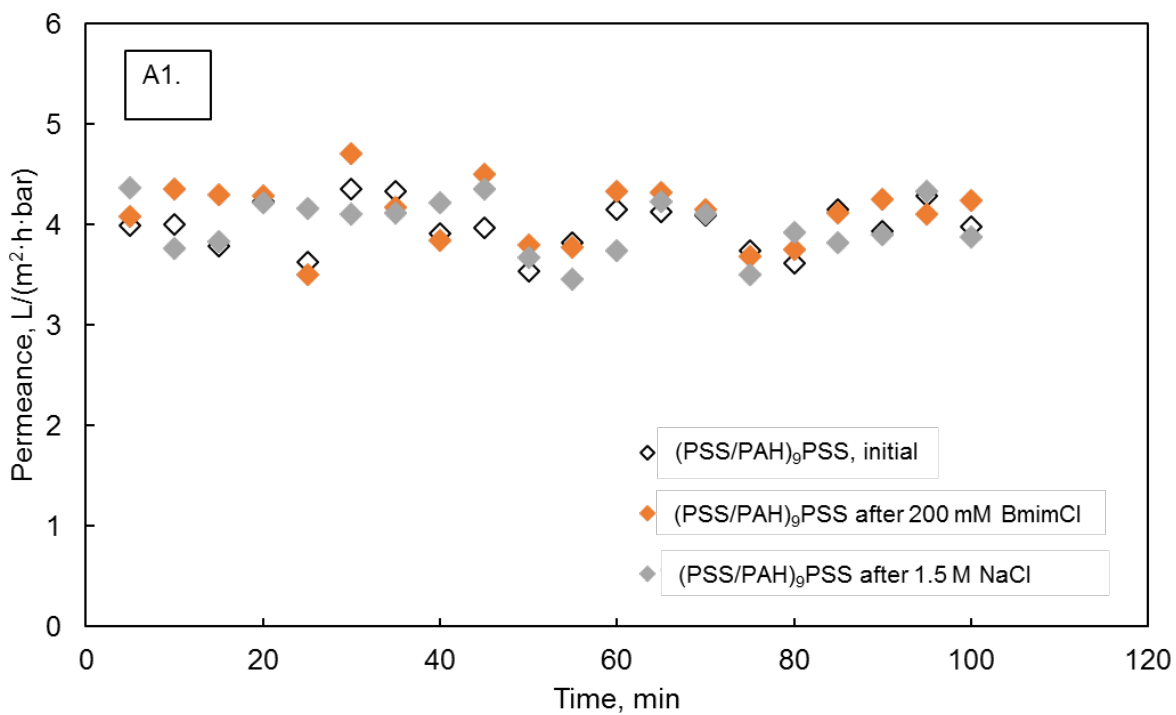


Figure S3: Roughness measured by AFM in tapping mode for PEMs using (a) alumina oxide membranes and (b) PES membranes. Values for the modified membranes represent the average of three measurements taken at three distinct locations on the membrane surface.



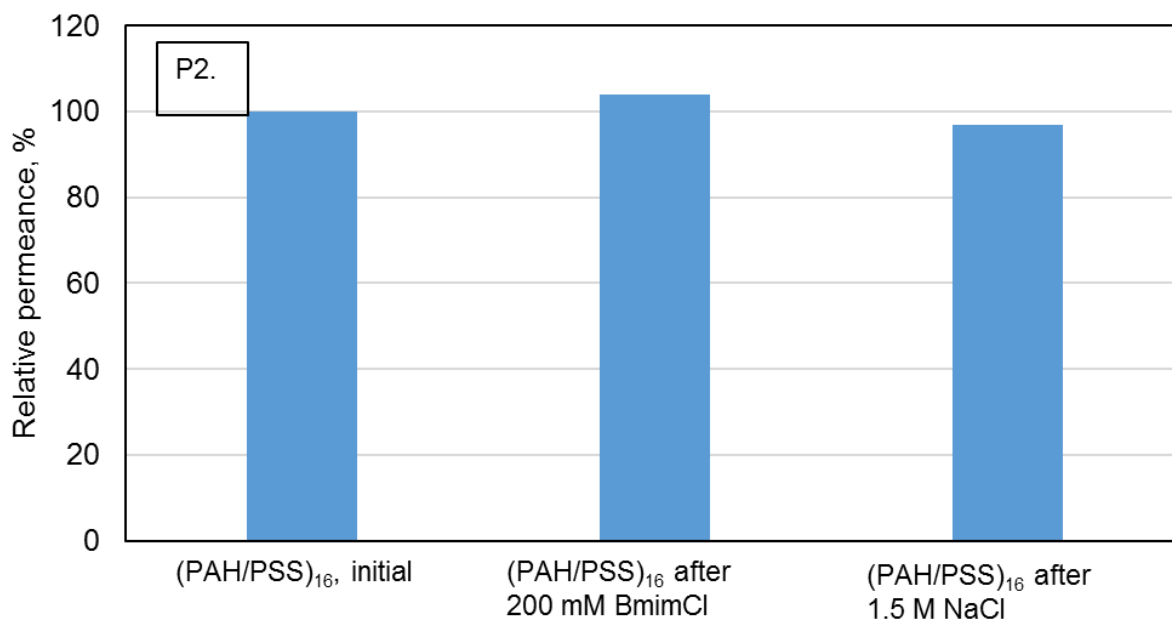
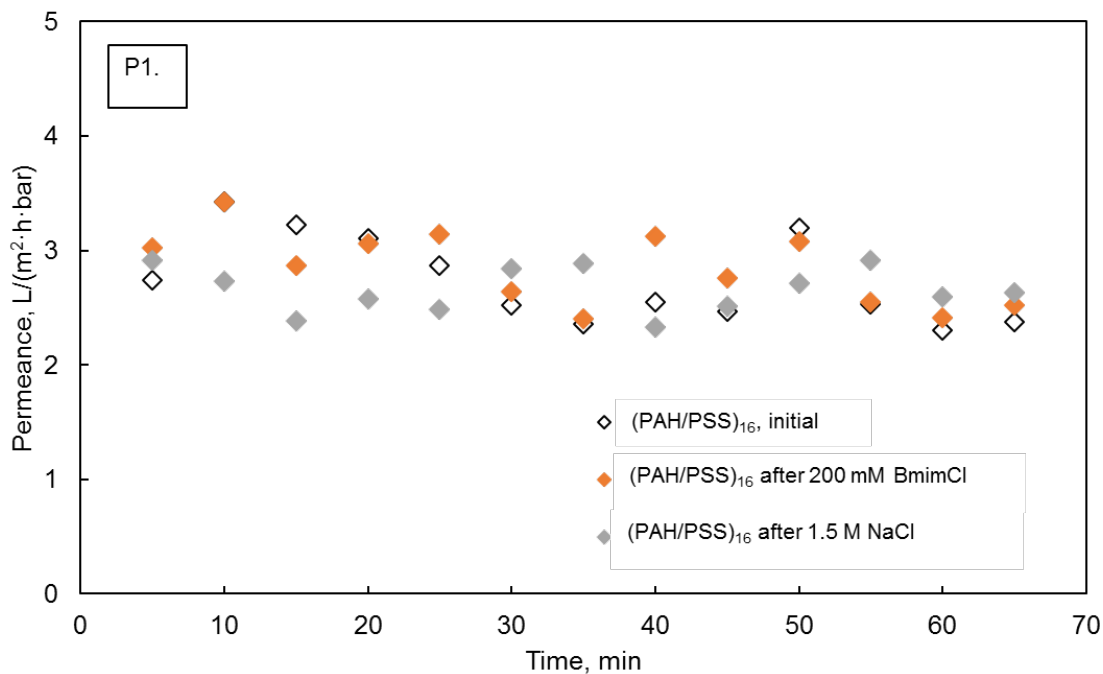


Figure S4: The changes of permeance of the modified alumina (A1-2) and PES membranes (P1-2) in presence of concentrated ionic liquid and NaCl.

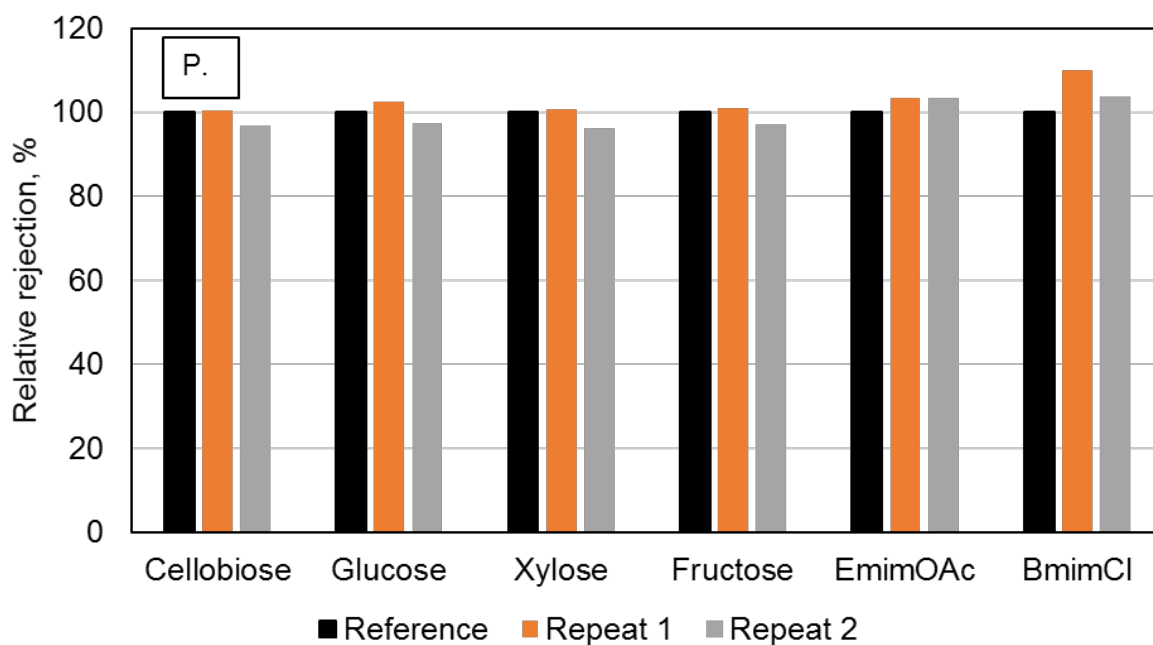
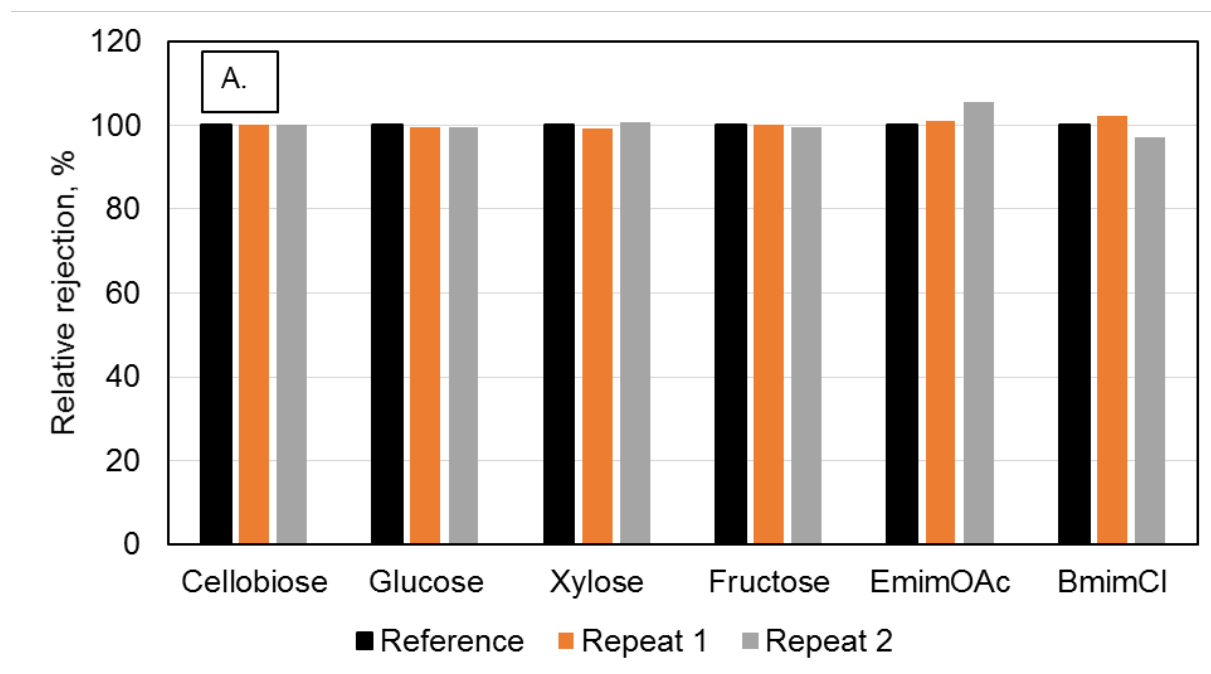


Figure S5: Reusability of the modified membranes from repeated measurements. The rejection study of the consecutive separation cycle for sugar and the ionic liquid using modified alumina (A.) and PES membrane (P.).

4. Concentration of polyphenols from blueberry pomace extract using nanofiltration*

* This chapter is based on a submitted manuscript: Alexandru M. Avram, Pauline Morin, Cindi Brownmiller, Arijit Sengupta, Luke R. Howard, S. Ranil Wickramasinghe. Food and Bioproducts Processing. Manuscript was submitted to journal on April.30.2017.

* All experiments were conducted by Mr Alexandru Avram with some assistance from Ms Pauline Morin. Ms Cindi Brownmiller helped prepare feed streams for membrane testing and conducted HPLC analysis. Profs Wickramasinghe and Howard guided the experimental work. Together with Dr Sengupta, they helped with analyzing the results and editing the manuscript.

Abstract

Polyphenols extracted from blueberry (*Vaccinium corymbosum*) pomace were concentrated using nanofiltration. Crossflow filtration was shown to be a feasible method for concentrating the polyphenols present in dilute aqueous solutions. High-performance liquid chromatography was employed for the determination of total anthocyanins, total flavonols and chlorogenic acid in the hot water extract. Both nanofiltration membranes (NF245 and NF270) showed complete rejection of phenolic compounds at good permeances, whereas crossflow mode of filtration was found to reduce membrane fouling considerably. Furthermore, a suitable protocol was developed for clean-in-place of the used membranes. After repeated filtrations followed by the cleaning protocol, the rejection performance was preserved unaltered and the relative permeance was recovered up to 73% for NF245 membrane and more than 99% for NF270 membrane.

4.1. Introduction

Blueberries (*Vaccinium corymbosum* L.) contain large amounts of polyphenols¹. It has been suggested that consumption of blueberries can help suppress inflammation^{2,3}, display anti-cancer properties⁴, improve human gut microbiome⁵, reduce the risk of coronary heart disease^{6,7} and

scavenge oxidative radicals ⁸. Most of these benefits are attributed to the high content of monomeric and polymeric anthocyanins, a class of polyphenols. These belong to a wide variety of arabinosides, galactosides and glucosides of cyanidin, delphinidin, malvidin, peonidin and petunidin ⁹ possessing orange-red, purple and blue plant pigments that have significant importance in the food industry as they determine color, taste and health benefits of marketed products.

For commercial purposes, an ample amount of the blueberries is processed either into juice or juice concentrate and then the remaining solid residue (pomace) is generally treated as a waste product. The skins of blueberry fruits contain most of anthocyanins by weight ¹⁰ so that, depending on the complexity of the juice extraction method, the pomace is left with a substantial amount of valuable polyphenolics. Therefore, there is an incentive to further process the blueberry pomace and extract those remaining polyphenolics for applications as natural colorants, encapsulated supplements or added nutraceuticals ^{11,12}.

Most of the pomace extraction methods lead to dilute aqueous juice fractions and processing them into concentrates facilitates storage and transportation. Particularly, volume reduction and separation techniques are highly employed to produce juice concentrates and fractionate the dilute extracts. Multiple techniques have been developed aiming at the production of stable, nutrient-rich concentrated streams ¹³. Freeze concentration (cryoconcentration) ¹⁴, osmotic distillation ¹⁵, membrane filtration ¹⁶⁻¹⁸ and other multi-stage evaporation techniques are commonly reported in the literature ^{15,19,20}. Anthocyanins are labile compounds that have been shown to easily degrade and lose biological activity under severe processing parameters such as high temperatures, UV radiation and cross reaction with other processing chemicals ²¹. Therefore, a careful consideration has to be given to the choice of processing techniques which should not only be economically feasible but also limit the deactivation and loss of the bioactive compounds.

Membrane technology could be a promising technology for recovery of these fragile biologically active compounds. Here, we focus on nanofiltration, a pressure-driven membrane process. There has been a growing interest in pressure-driven membrane unit operations for concentration of polyphenols from dilute aqueous fractions and several membrane systems have been reviewed by Jiao et al.¹⁸. For example Diaz-Reinoso et al.¹⁶ have coupled ultrafiltration and nanofiltration membranes to concentrate and subsequently fractionate the sugars out of grape pomace extracts. Ferrarini et al.¹⁷ tested the performance of nanofiltration and reverse osmosis membranes to concentrate grape juice as an alternative to pervaporation and cryoconcentration. More recently, Popovic et al.²² used nanofiltration to concentrate aromatic compounds, phenolic acids and flavonols from chokeberry juice. Cassano et al.²³ tested five nanofiltration membranes with MWCO between 200-1000 Da for the fractionation of artichoke brines and the recovery of bioactive compounds. With the advent of recent progress on the separation, purification and fractionation of dilute juice extracts, membrane separations are gaining interest. Among these, multi-step crossflow pressure-driven membrane steps show promising results with increased process efficiency by reducing membrane fouling and cake formation¹⁹. Moreover, recent advances in nanofiltration suggest that it may be ideally suited for recovery of food-grade small organic species in aqueous solutions²⁴⁻²⁷. In this work, the performance of two commercially available nanofiltration membranes with MWCO 100-300 Da were evaluated for concentration of anthocyanins, flavonols and chlorogenic acid. Furthermore, we have developed a cleaning procedure with clean-in-place potential to investigate the reconditioning of used membrane as a step forward to develop a simple, economically feasible method of concentrating the blueberry extracts.

4.2. Materials and Methods

Blueberry (*Vaccinium corymbosum L.*) pomace was obtained by processing of non-clarified juice, which was carried out in accordance with the protocol described by ²⁸. NF245 and NF270 polyamide thin-film composite nanofiltration membranes with nominal molecular weight cut-off of 200-400 Da were obtained in form of flat sheets from Filmtec™ (*Dow, Minneapolis, MN*). Prior to insertion in the dead-end filtration vessel, the membranes were cut by hand and then soaked in deionized water for at least 24 hours. The active separation areas were 14.6 cm² for dead-end setup and 42.0 cm² for crossflow setup. Disposable filters (0.22 μm and 0.45 μm) were purchased from GE Healthcare Life Sciences (Whatman®, Pittsburgh, PA) and used to prefilter large particles. Sodium hydroxide (analytical grade) was purchased from Macron Fine Chemicals (Avantor Performance Materials, Center Valley, PA). Hydrochloric acid (37% v/v) was purchased from EMD Millipore (Billerica, MA). Deionized water was produced with Thermo Scientific, model Smart2Pure 12 UV/UF (Waltham, MA), 18.0 MΩ·cm.

Pressurized hot water extraction

Frozen blueberry pomace was allowed to thaw to 21°C prior to extraction. A Dionex model 200 accelerated solvent extractor (ASE) system interfaced with a solvent controller (Dionex Corp., Sunnyvale, CA) was used to extract anthocyanins from blueberry pomace (**Figure 4-1**). Samples (0.5 g) were loaded into 22 mL stainless steel extraction cells with a cellulose paper filter inserted at the bottom of the cells. The ASE extraction was carried out using water as solvent; 68 bar pressure, 120°C temperature, five extraction cycles, 70% flush volume, 90 sec nitrogen purge time (no static time and no preheat time). For each extraction cycle it took approximately 5-6 min for the water to heat to 120°C for a total run time of 25-30 min.

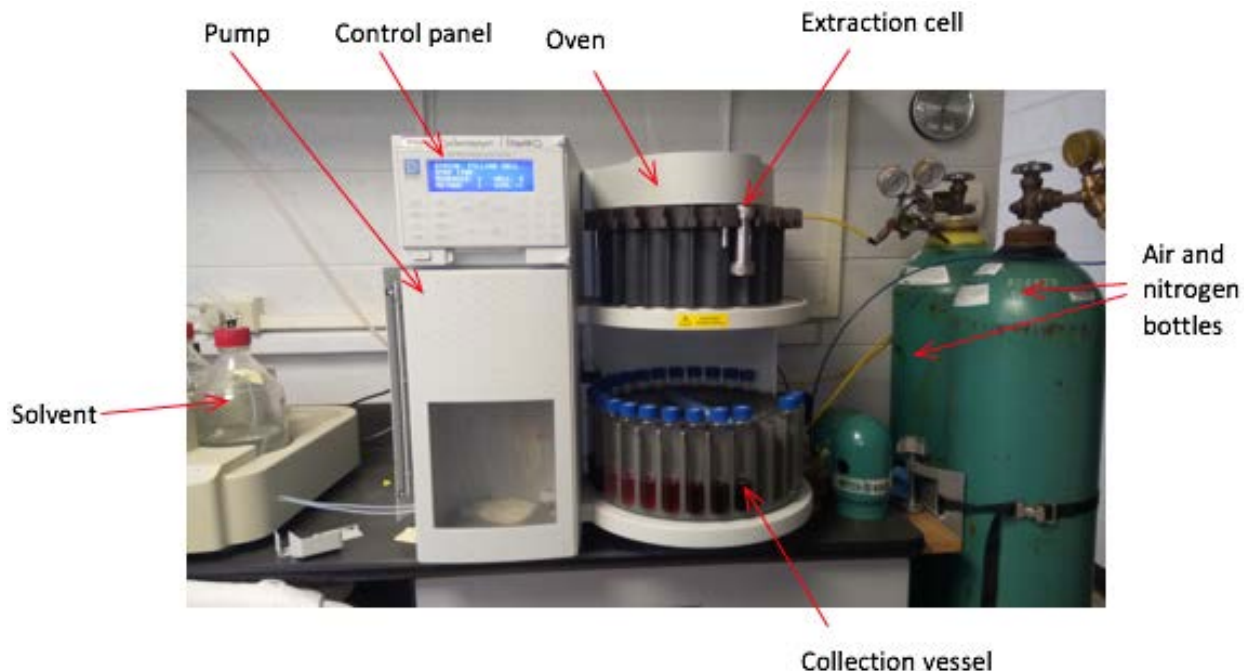


Figure 4-1: Accelerated Solvent Extraction system. The pomace is loaded in the extraction cell, water is pumped through the system, and polyphenols are recovered as aqueous solution in the collection vessels.

Approximately 22 mL of extract from each extraction cycle was pooled after passing through a large microporous sieve. Pressurized hot water extracts were stored at -20°C prior to total anthocyanin analysis and nanofiltration testing.

Non-filtered or prefiltered ($0.22\ \mu\text{m}$ and $0.45\ \mu\text{m}$) blueberry pomace hot water extracts are collectively described here as feed solution. The extract concentration was found to naturally vary in the range 85-125 mg/L.

Dead-end filtration

A starting volume of 200 mL feed was loaded in a stainless steel pressure vessel (Sterlitech, Kent, WA), which was continuously stirred on a magnetic stirrer plate (OptiChem, Vineland, NJ). The feed side was pressurized with nitrogen at pressures between 10-17 bar. The flow through the membrane was quantified by collecting the solution on an electronic balance (Mettler Toledo

PL602-S, Columbus, OH) connected to a computer. The setup can be seen in **Figure S1**. The temperature of feed, permeate and concentrate was measured before and after filtration it was found to not change by more than $\pm 1.3^{\circ}\text{C}$ for any of the filtration experiments.

Permeance was calculated from:

$$P = \frac{V}{A \cdot \Delta t \cdot p} \quad (1)$$

where V is the volume of permeate, Δt is the time of permeation, A is membrane area, and p is applied pressure.

Crossflow filtration

A crossflow system was custom built as shown in **Figure 4-2**. An initial volume of 600 mL was loaded into the stainless steel vessel and then placed on a magnetic stirrer plate (Corning PC-210, Corning, NY) at 200 rpm. The feed was pumped through the pressurized system with a twin piston pump (Milton Roy Company, Houston, TX) at a constant crossflow rate of 57 mL/min. The transmembrane pressure was kept constant at 3 bar. The flow through the membrane was quantified in a similar manner as explained for dead-end mode. The temperature of feed, permeate and concentrate was measured before and after filtration and it was found not to change by more than $\pm 1.6^{\circ}\text{C}$.

Permeance was calculated from:

$$P = \frac{V}{A \cdot \Delta t \cdot TMP} \quad (2)$$

$$TMP = \frac{p_{inlet} + p_{outlet}}{2} - p_{permeate} \quad (3)$$

where V is the volume of permeate, Δt is the time of permeation, A is membrane area, and TMP is the transmembrane pressure calculated from the pressures read at inlet, outlet and permeate (0 bar).

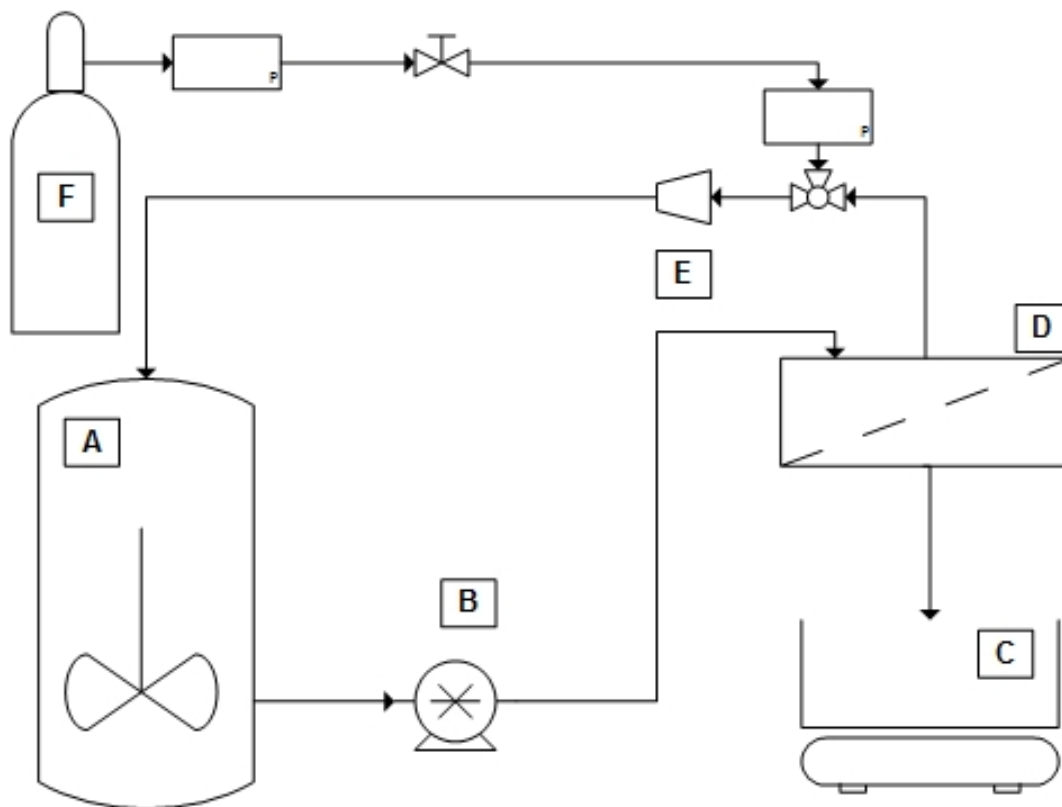


Figure 4-2: Process flow of experimental setup for nanofiltration in crossflow mode. A: Feed stirred vessel; B: Piston pump; C: Permeate collection and balance; D: Crossflow cell; E: Pressure regulator and F: gas supply.

Total polyphenol analysis

Blueberry ASE extracts were screened for the determination of total anthocyanins and total flavonols content using a method adapted from Cho *et al.*²⁹ on HPLC (Waters Corp, Milford, MA) equipped with a 4.6 mm x 250 mm Symmetry® C18 (Waters Corp, Milford, MA). Mobile phase (linear gradient) was comprised of (A) 5% formic acid and (B) 2% - 60% methanol at 1 mL/min. Flavonols were detected at 360 nm and anthocyanins were detected at 510 nm. Total anthocyanins (ACY) were determined as the sum of delphinidin, cyaniding, petunidin, penidin and malvidin

glycoside equivalents. Total flavonols (FLA) were detected as the sum of myricetin and quercetin equivalents. Total chlorogenic acid (CLA) were quantified using an authentic method ²⁹. Total polyphenols, flavonols and chlorogenic acid are referred here cumulatively as total polyphenols. For rejection analysis, samples from feed, retentate and permeate were evaluated for total monomeric anthocyanin content by the pH differential assay using a Hewlett Packard Model 8452A Diode Array Spectrophotometer (Palo Alto, CA) ³⁰. For each sample, two dilutions were prepared: one with 0.5 mL of sample and 4.5 mL of pH 1.0 buffer; the other one with 0.5 mL of sample and 4.5 mL of pH 4.5 buffer. Then, after 1 hour in the dark, the optical density (OD) was measured at 510 and 700 nm wavelength against a deionized water blank. The absorbance was calculated using:

$$A = [OD_{510} - OD_{700}]_{pH1.0} - [OD_{510} - OD_{700}]_{pH4.5} \quad (4)$$

where A = absorbance, OD = optical density at specified λ wavelength (nm).

Total monomeric anthocyanin pigment concentration (c in mg/L), expressed as malvidin-3-glucoside equivalents was calculated using:

$$c = \frac{A \cdot MW \cdot DF \cdot 1000}{\epsilon \cdot d} \quad (5)$$

where MW = molecular weight for malvidin-3-glucoside (493.2 g/mol), DF = dilution factor (1:10), ϵ = molar extinction coefficient for malvidin-3-glucoside (28,000), d = optical path length (1 cm).

Sugars concentrations were analyzed using a previously developed assay on HPLC (1200 series (Agilent Technologies, Palo Alto, CA) equipped with a Hi-Plex Ca (Duo) column (Agilent, 300 x 6.5 mm length x internal diameter, 8 μm pore size), injection volume: 5 μL, mobile phase: deionized water, flow rate: 0.6 mL/minutes, column temperature: 80°C, refractive index detector detector temperature: 45°C, run time: 30 minutes.

Rejection of total polyphenols and sugars was calculated from:

$$R_i = \left(1 - \frac{c_{ip}}{c_{if}}\right) \cdot 100\% \quad (6)$$

where c_{ip} and c_{if} are solute concentration in permeate and feed, respectively.

Membrane cleaning and fouling index

Used membranes were cleaned with the following protocol: (1) soak in deionized and stirred gently for 24 hrs; (2) soak in 0.2% wt HCl for 30 min and then clean-in-place for 1 hr with deionized water; (3) soak in 0.1% wt NaOH for 30 min and then clean-in-place for 1 hr with deionized water.

The performance of the reconditioned membranes was then tested for analyzing the recovery of initial permeance and rejection. Additionally, the following relationship was used to quantify the dynamic fouling index:

$$FI = \left(1 - \frac{P_{(V/A)}}{P_{initial}}\right) \cdot 100 \quad (7)$$

where $P_{(V/A)}$ is permeance at a constant permeate volume over membrane active area ratio and $P_{initial}$ is the initial permeance.

4.3. Results and Discussion

Total polyphenols and sugar retention

The HPLC data for total anthocyanins, flavonols and chlorogenic acid in the ASE extract, retentate and permeate were summarized in **Table 4-1**. The study revealed that the highest amount of polyphenols was due to total anthocyanins (with over 82% wt.), while the highest amount of sugars was due to fructose (with over 70% wt.) in the feed (ASE extract). The HPLC chromatograms of total polyphenols 16 anthocyanins and 7 flavonols were identified. can be seen in **Figure S2**. The most prevalent ACYs were malvidin-3-galactoside (15% wt, 493 M⁺), delphinidin-3-galactoside (14% wt, 465 M⁺) and malvidin-3-glucoside (13% wt, 493 M⁺). The most prevalent FLA were quercetin-3-galactoside (37% wt, 463 M⁺), quercetin-3-glucoside (16% wt, 463 M⁺) and quercetin-3-acetylramnoside (11% wt, 489 M⁺). Chlorogenic acid represented only 6% of total polyphenols and has a relative molecular ion weight of 353 M⁻. Both NF270 and NF245 exhibited complete retention of total polyphenols, total chlorogenic acid and sucrose. Only small amounts of glucose and fructose were found in the permeate fractions so that the rejections were higher than 97%. The rejection of sugars is in good agreement with the work of Malmali *et al.*, 2014 who used NF270 for rejection of sugars from biomass hydrolysates ³¹.

Table 4-1: HPLC analysis results for ASE extract and for retentate and permeate fractions after rejection in dead-end mode.

Sample	Total ACY ^{b)}	Total FLA ^{b)}	CLA ^{b)}	Sucrose ^{c)}	Glucose ^{c)}	Fructose ^{c)}
ASE extract (feed)	61.0	7.9	4.7	0.05	0.60	1.54
NF270 retentate ^{a)}	73.9	9.9	6.1	0.07	0.72	2.12
NF270 permeate	n.d. ^{d)}	n.d.	n.d.	n.d.	0.01	0.02
NF245 retentate ^{a)}	84.7	10.7	6.6	0.09	1.14	2.39
NF245 permeate	n.d.	n.d.	n.d.	n.d.	0.01	0.02

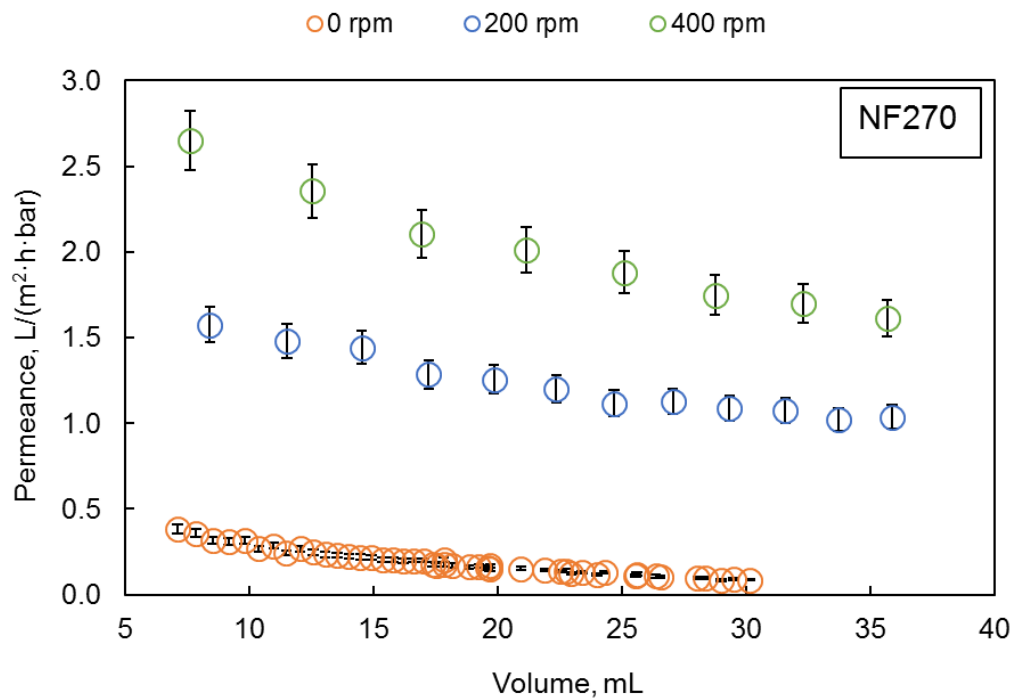
^{a)} dead-end filtration; ^{b)} mg / 100 mL; ^{c)} mg / mL; ^{d)} n.d. – not detected.

Dead-end filtration

The concentration of polyphenols from blueberry pomace extract was tested using two commercially available nanofiltration membranes and then optimized experimentally based on (1) mixing speed, (2) prefiltration and (3) filtration time. Due to their low molecular weight cut-off, both membranes showed complete rejection of polyphenols regardless of the experimental parameter (**Table S1**). Membrane performance based on permeance using pomace extract was tested at 0 rpm, 200 rpm and 400 rpm while holding the filtration volume constant. As seen in **Figure 4-3** the permeance changes drastically as a function of mixing speed; especially when no stirring is applied the permeance reaches unfeasible slow values. This parameter was investigated as part of finding optimum experimental parameters that would decrease fouling and disrupt cake formation – effects inherent to batch separation processes in the juice industry ³². Because the pomace extract is passed through a sieving filter (1 micron) after the ASE extraction there should be no solids present in the feed. Thus, it is expected that the main phenomena leading to an

exacerbated decrease in permeance are typical concentration polarization and pore blocking (membrane properties) as factors of polyphenols agglomeration, adsorption and precipitation (feed composition properties). For example Heinonen *et al.* have identified polyphenols agglomeration and precipitation during the concentration process of polyphenols from purple potatoes³³.

At 400 rpm, mechanical mixing has been found to increase the starting permeance 6.8 times (NF270) and 2.1 times (NF245) over as compared to no stirring condition, while at 200 rpm it was 4.0 times (NF270) and 2.0 times (NF245) higher. The appearance of the used membranes showed a dark purple coloration for the non-stirred experiments, while the other membranes remained just slightly tainted when stirring was applied. This leads to hypothesize that fouling due to polyphenol agglomeration or adsorption can be efficiently disrupted if mechanical stirring is applied. The rejection of total polyphenols was complete and independent of stirring speed.



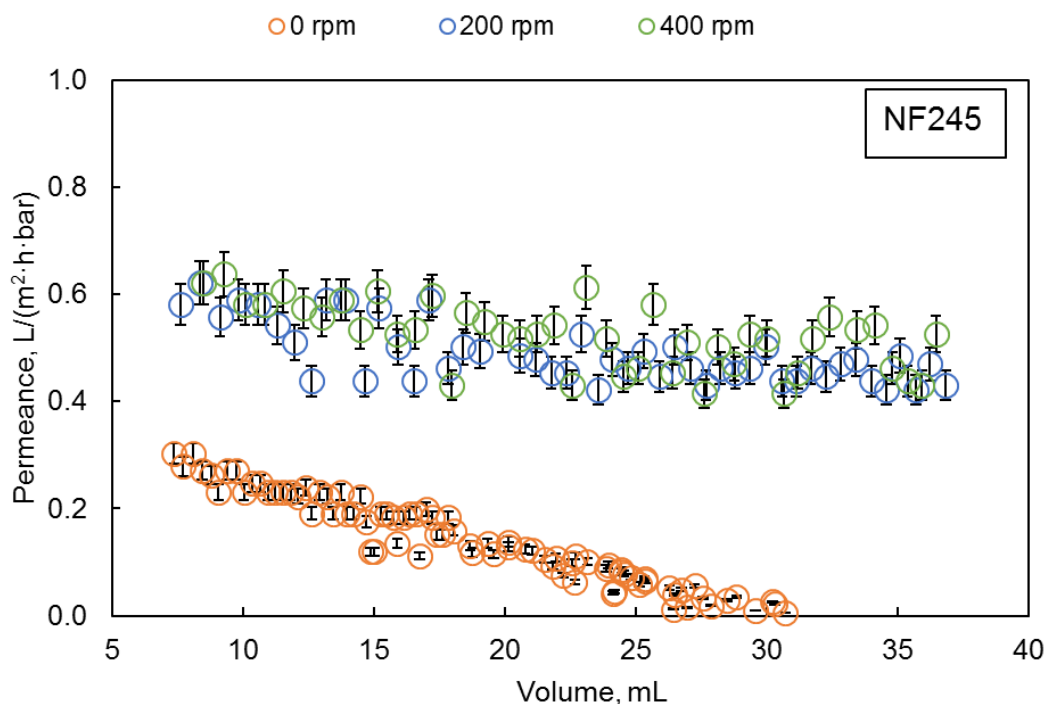


Figure 4-3: Effect of stirring speed on permeance. Data reflects the feed permeance after a constant volume for both membranes was collected in permeate.

Prefiltration with 0.45 μm and 0.22 μm filters was used as a simple pre-treatment method to assess the effect on membrane permeance (**Figure 4-4**). Measuring the polyphenol concentration before and after each prefiltration step, we observed a 15% wt. decrease after the feed was passed through 0.45 μm and then an additional 10% wt. decrease after passing through 0.22 μm . The majority of the polyphenols have molecular weights significantly smaller than the pore size of the prefilters so that it is believed that the retained polyphenols were agglomerated large particles ⁹. This was an important observation for designing the experimental setup in crossflow mode and will be discussed in the next section. No polyphenols could be detected in the permeate of any of the prefiltered series so that the rejection was complete.

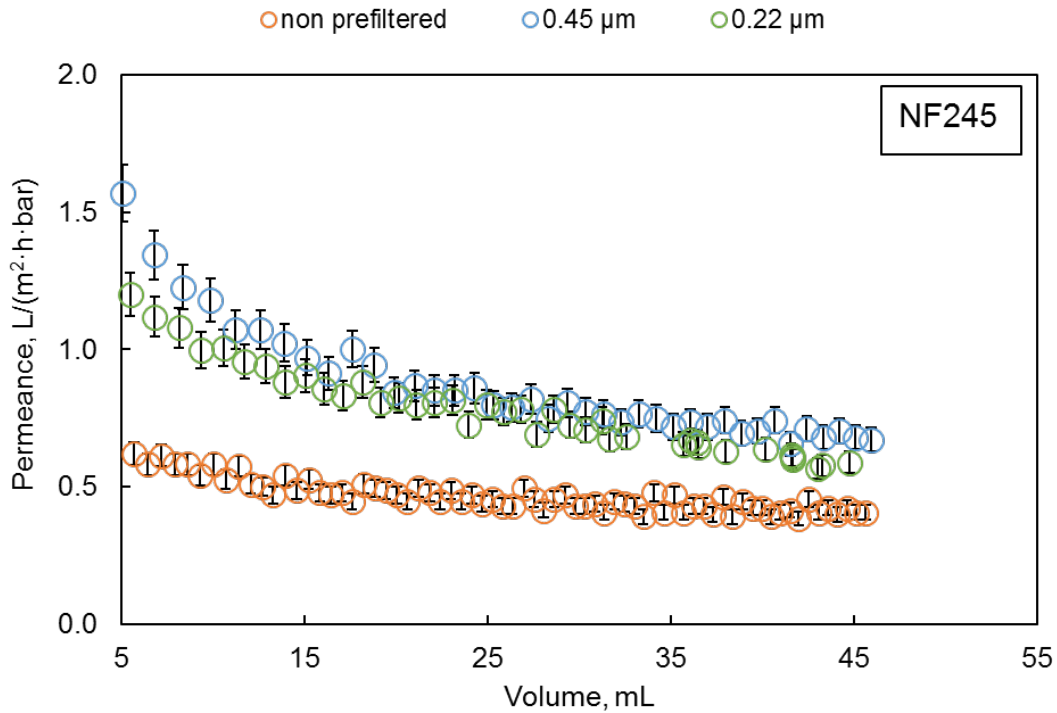
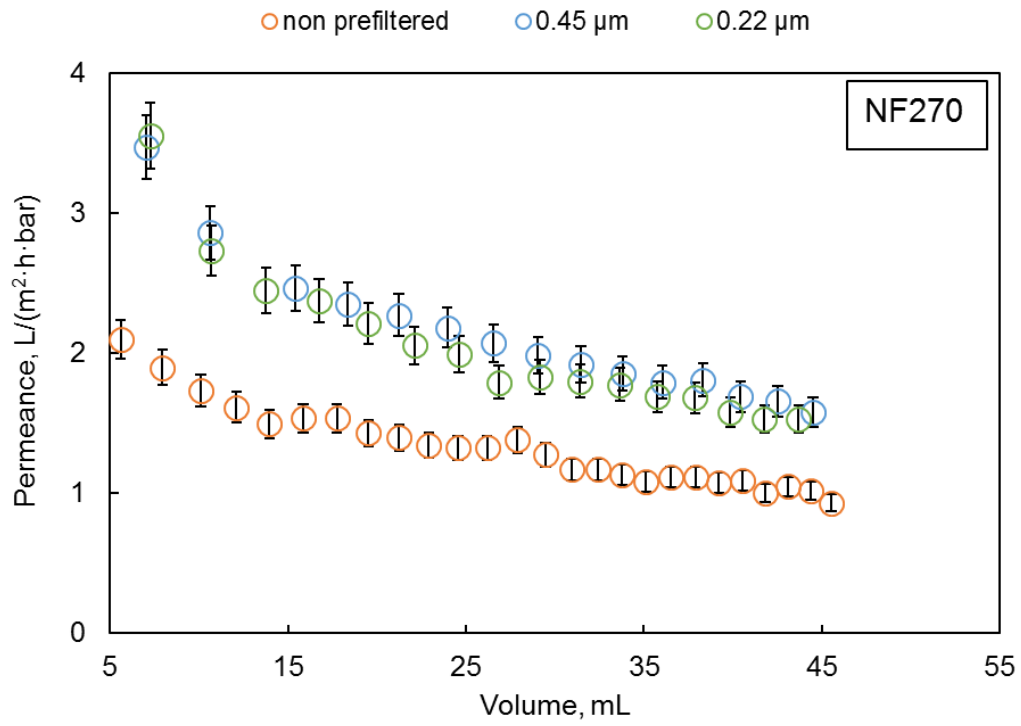


Figure 4-4: Permeance with non-prefiltered and filtered blueberry pomace extract, 200 rpm.

The nanofiltration membranes were next tested at extended filtration times until the maximum amount of feed volume could be removed. As permitted by the dead-end setup, a minimum of 20% v/v of initial feed should remain in the pressure vessel to not disrupt mixing. This analysis allowed to compare the performance of the two membranes in terms permeance, rejection, anti-fouling properties, and also to investigate degradation of polyphenols at longer reactor residence time. In **Table 4-2** it can be recognized that NF270 showed better performance than NF245. NF270 required approximately 19 hours to remove 80% of the initial volume and the polyphenols content was concentrated by a factor of 4.6. In the same amount of time NF245 reduced the volume by 60% and concentrated the polyphenols by a factor of 2.2. It required almost 30 hours to reduce the feed volume to the same performance as with NF270 but the flux started to decrease considerably after 21 hours, due to increased fouling (**Figure 4-5**). The temperature of the feed and retentate was monitored at the start and at the end of each filtration and it was found to not change by more than $\pm 1.0^{\circ}\text{C}$. Both membranes showed complete rejection of polyphenols and during analysis no polyphenol degradation was detected. However, both NF270 and NF245 showed adsorbed polyphenols on their surfaces, as observed from the dark purple color of the used membranes. This could be an effect of particle agglomeration and polyphenol adsorption as seen previously in unstirred systems.

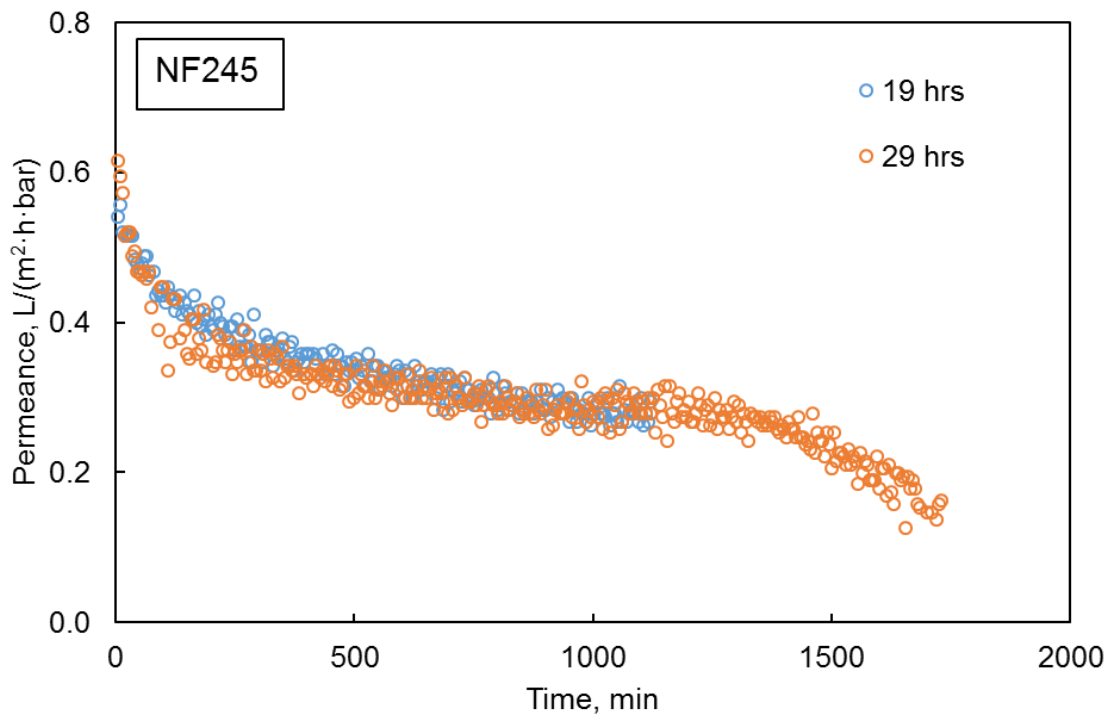
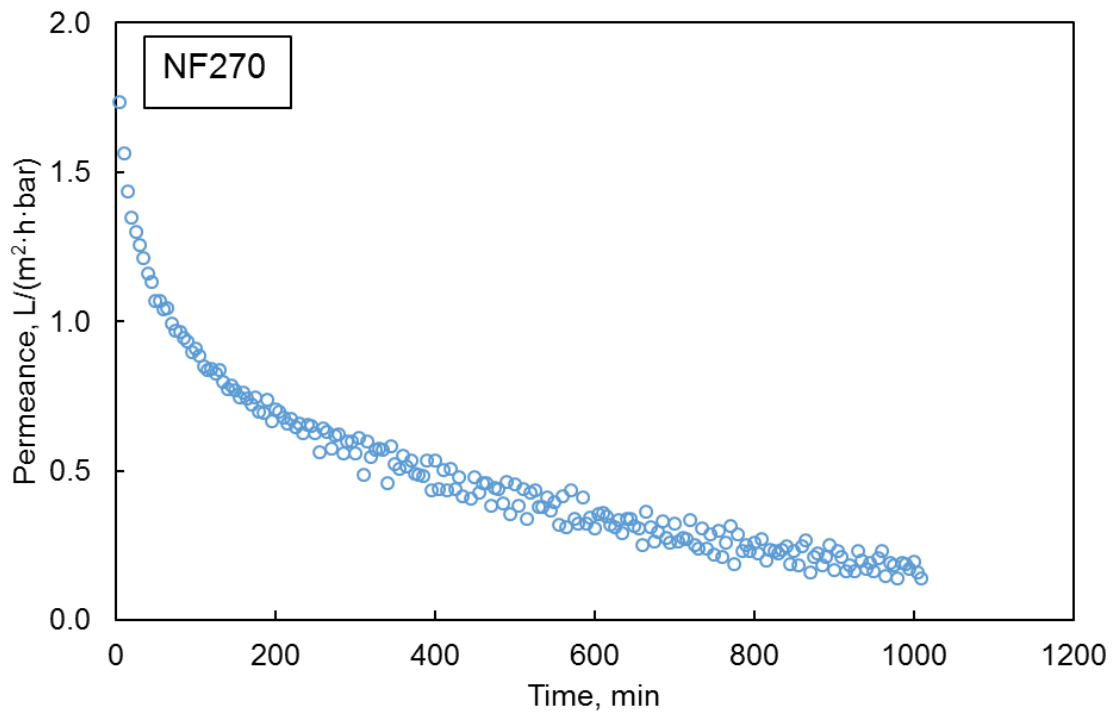


Figure 4-5: Filtration at extended times. Stirring speed 200 rpm.

Table 4-2: Volume reduction and concentration factor for dead-end filtration at extended times.

Membrane, filtration time	Feed volume, mL	Volume reduction, % v/v	Concentration factor
NF270, 19 hrs	250	80	4.59
NF245, 19 hrs	250	60	2.19
NF245, 29 hrs	250	78	3.14

Crossflow filtration

Previously, the filtration performance in dead-end mode was tested under different experimental parameters and those findings were determinant in the design of the crossflow setup shown in **Figure 4-2**. The setup was constructed to keep the feed continuously stirred and the crossflow rate was set at a maximum flowrate of 57 mL/min. Then, the feed was passed through a 0.22 μm prefilter to remove larger aggregated particles. Total polyphenols were rejected completely (**Table S2**) and no polyphenol degradation was observed during analysis. The permeance was considerably higher with NF270, which started at $3.5 \text{ L m}^{-2} \text{ h}^{-1} \text{ bar}^{-1}$ and then reached approximately $2.0 \text{ L m}^{-2} \text{ h}^{-1} \text{ bar}^{-1}$ after 3 hours of filtration. For NF245 the permeance started at $1.5 \text{ L m}^{-2} \text{ h}^{-1} \text{ bar}^{-1}$ and then decreased to $0.6 \text{ L m}^{-2} \text{ h}^{-1} \text{ bar}^{-1}$ after the same filtration time.

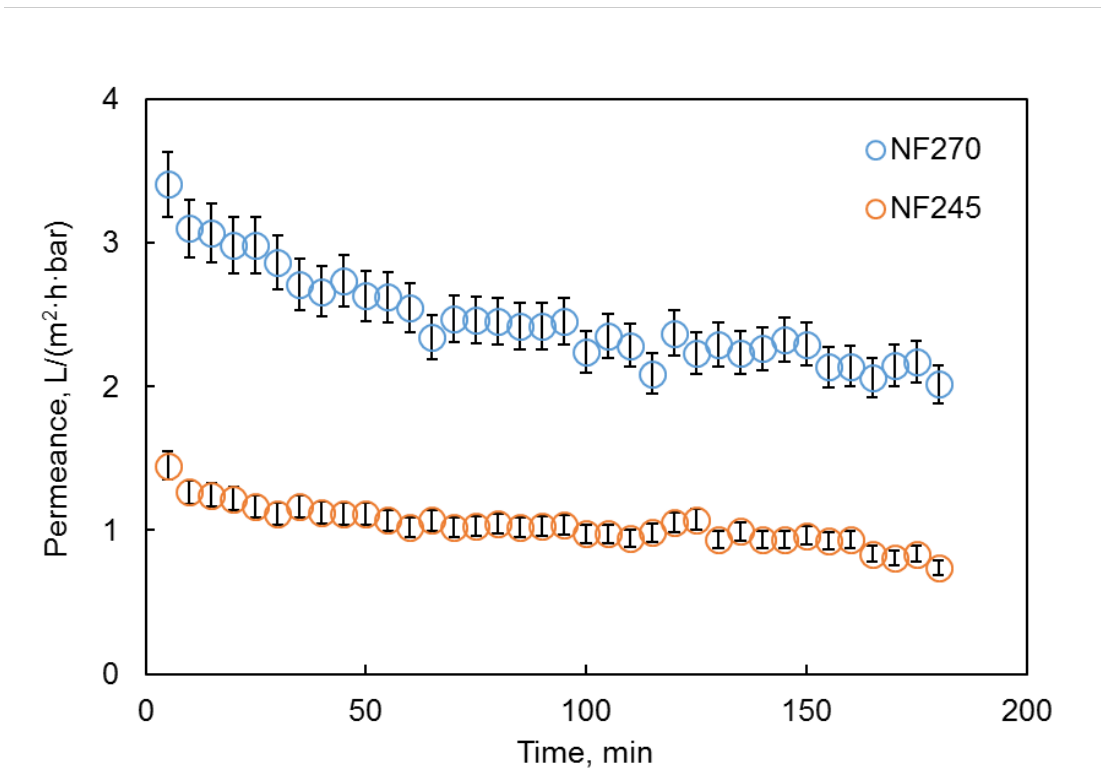


Figure 4-6: Crossflow filtration with 0.22 μm prefiltered feed, 200 rpm, performed at a crossflow rate of 57 mL/min and 3 bar transmembrane pressure.

After 3 hours of filtration time with NF270, 15% v/v of total volume were removed and the polyphenol concentration factor was 1.24. With NF245 approximately 7% v/v were removed and the polyphenol concentration factor was 1.11.

Table 4-3: Volume reduction and concentration factor for crossflow filtration.

Membrane, filtration time	Feed volume, mL	Volume reduction, % v/v	Concentration factor
NF270, 3 hrs	600	15.1	1.24
NF245, 3 hrs	600	7.3	1.11

Membrane reconditioning

Membrane fouling is a serious drawback for membrane separations as it leads to reduced flow through the membrane³⁴. Fouling happens as the concentration polarization film in the vicinity of the membrane selective layer becomes more pronounced due to effects such as adsorption, compound agglomeration and precipitation as well as pore blockage³⁵. Here, several experimental strategies have been employed to attempt to disrupt or minimize the effects leading to concentration polarization. Membrane selective area of NF270 and NF245 are constructed with polyamide networks containing aromatic moieties and these structures have non-beneficial surface affinity towards the rejected polyphenols, possibly leading to enhanced adsorption of polyphenols³³. Regardless of the mode of operation or nanofiltration membrane, fouling was observed on all membranes used in this work to some extent. This was visible from staining coloration and it is quantified using the dynamic fouling index (**Equation 7**). In **Table 4-4** the dynamic fouling index is used to quantify the extent of membrane fouling for NF270 and NF245. Comparing the dynamic fouling index at a constant ratio of permeate volume versus membrane active area, it can be seen that NF270 showed better anti-fouling behavior than NF245 in dead-end and in crossflow mode. Furthermore, crossflow filtration was more successful at reducing fouling for the NF270. In the case of NF245, the MWCO of the membrane is smaller so that soluble compounds with small molecular weight, such as monomeric sugars could get stuck easier in the aromatic polyamide network of the membrane selective layer leading to pore blockage.

Table 4-4: Dynamic fouling index at constant permeate volume over active membrane area ratio (V/A).

Filtration mode (V/A, mL/cm ²)	FI and membrane	
	NF270	NF245
Dead-end (0.50)	19	31
Dead-end (0.70)	23	38
Dead-end (0.95)	33	46
Crossflow (0.50)	16	29
Crossflow (0.70)	20	35
Crossflow (0.95)	28	45

For the purpose of membrane reconditioning, the used membranes were cleaned with the following protocol: (1) washed in deionized water for 24 hrs; (2) washed in 0.2% w/v HCl and (3) washed with 0.1% w/v NaOH. After steps (2) and (3) the membrane was cleaned-in-place with deionized water until the pH was constant. While establishing the wash protocol it was observed that step (2) leaves the previously purple stained membrane slightly pink in color, step (3) changes the staining to light brown and, for the membranes used in crossflow, the latter staining was eventually removed completely. The membranes used in dead-end maintained the light brown color and, as it can be seen from **Figure 4-7**, the fouling was irreversible. Only 37% of the initial water permeance could be recovered for NF270 and less than 20% for NF245.

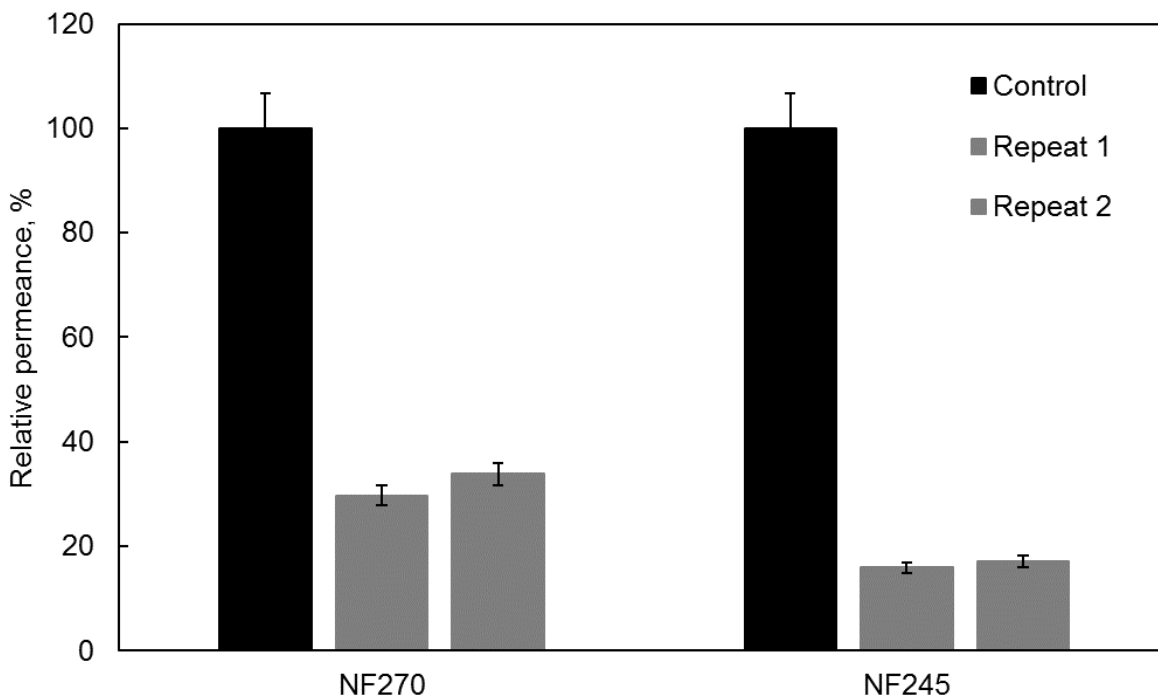


Figure 4-7: Recovery of permeance for membranes used in dead-end mode using 0.22 μm prefiltered feed at 200 rpm. Data is shown in duplicates for each membrane and water was used as testing feed. 100% relative permeance was 14.1 and 5.4 $\text{L m}^{-2} \text{h}^{-1} \text{bar}^{-1}$ for NF270 and NF245, respectively.

Using the same cleaning protocol, the used membranes from crossflow showed excellent water permeance recovery. For NF270 the recovery was almost complete, while for NF245 up to 73% of the initial permeance was recovered. Comparing dead-end and crossflow, the angle of the feed passing over the membrane surface seems to play a crucial role in the recovery of the permeance. In dead-end mode, the feed is mixed perpendicular to the membrane area, while in crossflow mode the feed flows tangentially over the membrane area. A tangential flow direction has therefore been shown beneficial in disrupting irreversible fouling. Additionally, while designing the wash protocol it has been observed that reversing step (3) with (2) will considerably decrease the cleaning efficiency. This is probably due to acid/base effect on the polyphenols. Polyphenols are better soluble in acid solution while they degrade and precipitate in more basic solutions^{36,37}.

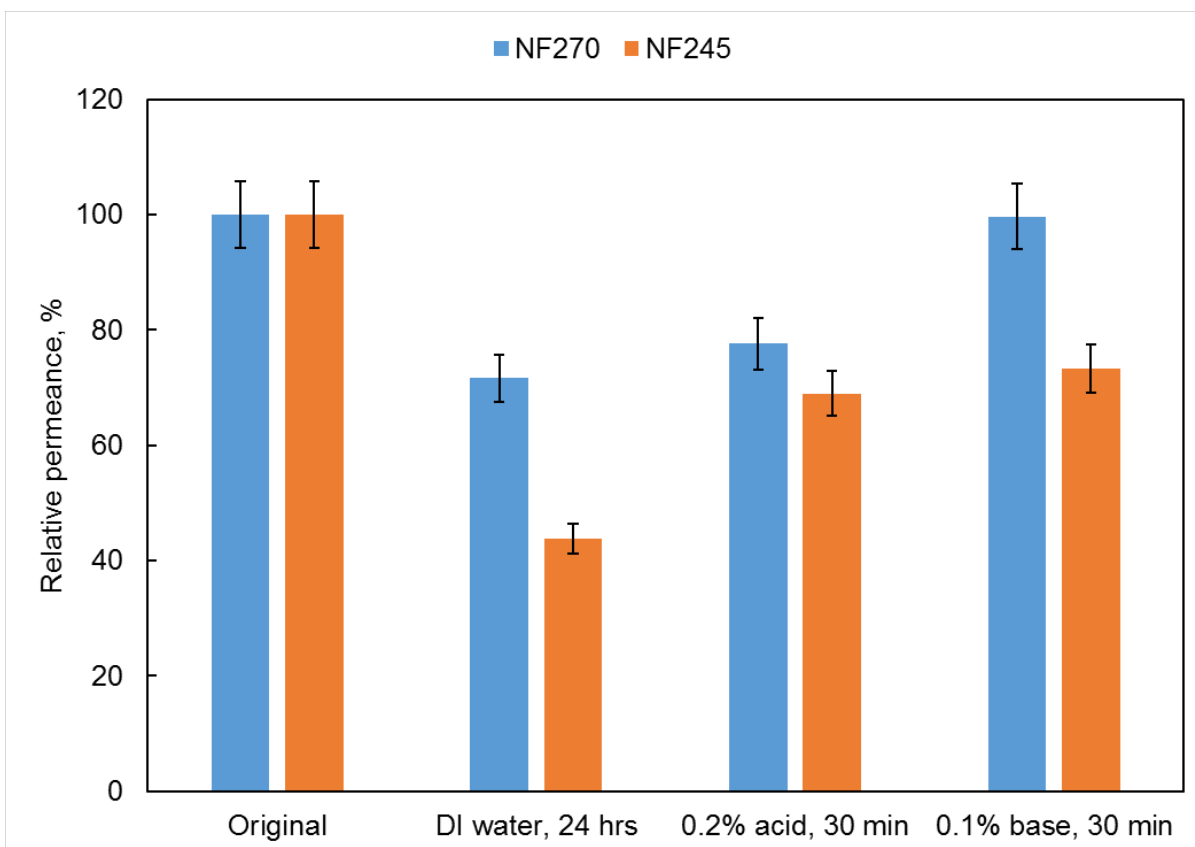


Figure 4-8: Recovery of permeance for membranes used in crossflow mode using 0.22 μm prefiltered feed at 200 rpm. Water was used as feed and all other parameters were constant. Washing steps are shown in chronological order. For NF270 100% relative permeance corresponds to $13.2 \text{ L m}^{-2} \text{ h}^{-1} \text{ bar}^{-1}$ and for NF245 100% relative permeance corresponds to $4.6 \text{ L m}^{-2} \text{ h}^{-1} \text{ bar}^{-1}$.

4.4. Conclusion

Nanofiltration technology was used in dead-end and in crossflow mode to concentrate polyphenol content from blueberry pomace. The most prevalent polyphenols were identified as total anthocyanins, total flavonols and chlorogenic acid. The sugar content analyzed using HPLC revealed that fructose was the predominant monosugar. Both nanofiltration membranes showed complete rejection of total anthocyanins, total flavonols, chlorogenic acid, sucrose and more than 95% rejection for glucose and fructose. The rejection performance was unaffected by the experimental parameter of the filtration mode. In dead-end mode 80% of water volume was

removed in 19 hours using NF270, while only 60% of water volume was removed with NF245. Stirring was found crucial for obtaining good permeances and crossflow mode was found to improve membrane fouling considerably. The membrane reconditioning protocol delivered almost complete recovery of water permeance for NF270 used in crossflow mode and up to 73% recovery for NF245.

Based on our experimental work, we recommend the following best operation procedures for polyphenol concentration using nanofiltration membranes:

Table 4-5: Unit operations and the recommended best procedure to assist with observed issues.

Unit operation	Recommended best procedure
blueberry extract is preserved best frozen but polyphenols tend to precipitate at low temperatures	warm up to room temperature under continuous stirring before separation
prefiltration	if prefiltration is used as pretreatment method, use a stirred device if possible to help break particle aggregation
membrane fouling	membranes used in dead-end seem to foul irreversibly compared to those used in crossflow crossflow, although a more complicated setup is a better option for reducing fouling
clean-in-place	membranes used in crossflow can be reconditioned to almost complete permeance if acid wash is used first followed by base wash

Acknowledgements

The help of Jerry W. King from Food Sciences Department at University of Arkansas, Fayetteville, AR is greatly acknowledged.

References

1. Kraujalytė V, Venskutonis PR, Pukalskas A, Česonienė L, Daubaras R. Antioxidant properties, phenolic composition and potentiometric sensor array evaluation of commercial and new blueberry (*vaccinium corymbosum*) and bog blueberry (*vaccinium uliginosum*) genotypes. *Food Chem.* 2015;188:583-590.
2. Torri E, Lemos M, Caliaro V, Kassuya CAL, Bastos JK, Andrade SF. Anti-inflammatory and antinociceptive properties of blueberry extract (*vaccinium corymbosum*). *J Pharm Pharmacol.* 2007;59(4):591-596.
3. Youdim K, McDonald J, Kalt W, Joseph J. Potential role of dietary flavonoids in reducing microvascular endothelium vulnerability to oxidative and inflammatory insults. *J Nutr Biochem.* 2002;13(5):282-288.
4. Katsube N, Iwashita K, Tsushida T, Yamaki K, Kobori M. Induction of apoptosis in cancer cells by bilberry (*vaccinium myrtillus*) and the anthocyanins. *J Agric Food Chem.* 2003;51(1):68-75.
5. Vendrame S, Guglielmetti S, Riso P, Arioli S, Klimis-Zacas D, Porrini M. Six-week consumption of a wild blueberry powder drink increases bifidobacteria in the human gut. *J Agric Food Chem.* 2011;59(24):12815-12820.
6. de Lange DW, Verhoef S, Gorter G, Kraaijenhagen RJ, van de Wiel A, Akkerman JN. Polyphenolic grape extract inhibits platelet activation through PECAM-1: An explanation for the french paradox. *Alcoholism-Clinical and Experimental Research.* 2007;31(8):1308-1314.
7. Opie LH, Lecour S. The red wine hypothesis: From concepts to protective signalling molecules. *Eur Heart J.* 2007;28(14):1683-1693.
8. Giovanelli G, Buratti S. Comparison of polyphenolic composition and antioxidant activity of wild italian blueberries and some cultivated varieties. *Food Chem.* 2009;112(4):903-908.
9. Ancillotti C, Ciofi L, Rossini D, et al. Liquid chromatographic/electrospray ionization quadrupole/time of flight tandem mass spectrometric study of polyphenolic composition of different *vaccinium* berry species and their comparative evaluation. *Analytical and Bioanalytical Chemistry.* 2017;409(5):1347-1368.
10. Lee J, Durst R, Wrolstad R. Impact of juice processing on blueberry anthocyanins and polyphenolics: Comparison of two pretreatments. *J Food Sci.* 2002;67(5):1660-1667.
11. Lee J, Wrolstad R. Extraction of anthocyanins and polyphenolics from blueberry-processing waste. *J Food Sci.* 2004;69(7):C564-C573.

12. Galanakis CM. Emerging technologies for the production of nutraceuticals from agricultural by-products: A viewpoint of opportunities and challenges. *Food Bioprod Process.* 2013;91(4):575-579.
13. Kalt W. Effects of production and processing factors on major fruit and vegetable antioxidants. *J Food Sci.* 2005;70(1):R11-R19.
14. Versari A, Ferrarini R, Parpinello G, Galassi S. Concentration of grape must by nanofiltration membranes. *Food Bioprod Process.* 2003;81(C3):275-278.
15. Cassano A, Drioli E, Galaverna G, Marchelli R, Di Silvestro G, Cagnasso P. Clarification and concentration of citrus and carrot juices by integrated membrane processes. *J Food Eng.* 2003;57(2):153-163.
16. Diaz-Reinoso B, Moure A, Dominguez H, Carlos Parajo J. Ultra- and nanofiltration of aqueous extracts from distilled fermented grape pomace. *J Food Eng.* 2009;91(4):587-593.
17. Ferrarini R, Versari A, Galassi S. A preliminary comparison between nanofiltration and reverse osmosis membranes for grape juice treatment. *J Food Eng.* 2001;50(2):113-116.
18. Jiao B, Cassano A, Drioli E. Recent advances on membrane processes for the concentration of fruit juices: A review. *J Food Eng.* 2004;63(3):303-324.
19. Vladisavljevic GT, Vukosavljevic P, Veljovic MS. Clarification of red raspberry juice using microfiltration with gas backwashing: A viable strategy to maximize permeate flux and minimize a loss of anthocyanins. *Food Bioprod Process.* 2013;91(C4):473-480.
20. Fazaeli M, Emam-Djomeh Z, Kalbasi Ashtari A, Omid M. Effect of spray drying conditions and feed composition on the physical properties of black mulberry juice powder. *Food Bioprod Process.* 2012;90(4):667-675.
21. Zhao Y, Wu X, Yu L, Chen P. Retention of polyphenols in blueberries (*vaccinium corymbosum*) after different cooking methods, using UHPLC–DAD–MS based metabolomics. *Journal of Food Composition and Analysis.* 2017;56:55-66.
22. Popovic K, Pozderovic A, Jakobek L, Rukavina J, Pichler A. Concentration of chokeberry (*aronia melanocarpa*) juice by nanofiltration. *Journal of Food and Nutrition Research.* 2016;55(2):159-170.
23. Cassano A, Cabri W, Mombelli G, Peterlongo F, Giorno L. Recovery of bioactive compounds from artichoke brines by nanofiltration. *Food Bioprod Process.* 2016;98:257-265.
24. Yadav JSS, Yan S, Ajila CM, Bezawada J, Tyagi RD, Surampalli RY. Food-grade single-cell protein production, characterization and ultrafiltration recovery of residual fermented whey proteins from whey. *Food Bioprod Process.* 2016;99:156-165.

25. Balyan U, Sarkar B. Integrated membrane process for purification and concentration of aqueous syzygium cumini (L.) seed extract. *Food Bioprod Process.* 2016;98:29-43.
26. Cordova A, Astudillo C, Giorno L, et al. Nanofiltration potential for the purification of highly concentrated enzymatically produced oligosaccharides. *Food Bioprod Process.* 2016;98:50-61.
27. Conidi C, Cassano A. Recovery of phenolic compounds from bergamot juice by nanofiltration membranes. *Desalination and Water Treatment.* 2015;56(13):3510-3518.
28. Brownmiller C, Howard LR, Prior RL. Processing and storage effects on monomeric anthocyanins, percent polymeric color, and antioxidant capacity of processed blueberry products. *J Food Sci.* 2008;73(5):H72-H79.
29. Cho M, Howard L, Prior R, Clark J. Flavonoid glycosides and antioxidant capacity of various blackberry, blueberry and red grape genotypes determined by high-performance liquid chromatography/mass spectrometry. *J Sci Food Agric.* 2004;84(13):1771-1782.
30. Giusti M, Rodriguez-Saona L, Wrolstad R. Molar absorptivity and color characteristics of acylated and non-acylated pelargonidin-based anthocyanins. *J Agric Food Chem.* 1999;47(11):4631-4637.
31. Malmali M, Stickel JJ, Wickramasinghe SR. Sugar concentration and detoxification of clarified biomass hydrolysate by nanofiltration. *Separation and Purification Technology.* 2014;132:655-665.
32. Mondor M, Girard B, Moresoli C. Modeling flux behavior for membrane filtration of apple juice. *Food Res Int.* 2000;33(7):539-548.
33. Heinonen J, Farahmandazad H, Vuorinen A, Kallio H, Yang B, Sainio T. Extraction and purification of anthocyanins from purple-fleshed potato. *Food Bioprod Process.* 2016;99:136-146.
34. Mattaraj S, Jarusutthirak C, Charoensuk C, Jiraratananon R. A combined pore blockage, osmotic pressure, and cake filtration model for crossflow nanofiltration of natural organic matter and inorganic salts. *Desalination.* 2011;274(1-3):182-191.
35. Shirazi S, Lin C, Chen D. Inorganic fouling of pressure-driven membrane processes - A critical review. *Desalination.* 2010;250(1):236-248.
36. Castañeda-Ovando A, Pacheco-Hernández MdL, Páez-Hernández ME, Rodríguez JA, Galán-Vidal CA. Chemical studies of anthocyanins: A review. *Food Chem.* 2009;113(4):859-871.
37. Reque PM, Steffens RS, Jablonski A, Flores SH, Rios AdO, de Jong EV. Cold storage of blueberry (*vaccinium* spp.) fruits and juice: Anthocyanin stability and antioxidant activity. *Journal of Food Composition and Analysis.* 2014;33(1):111-116.

Supplemental Information

Dead-end filtration

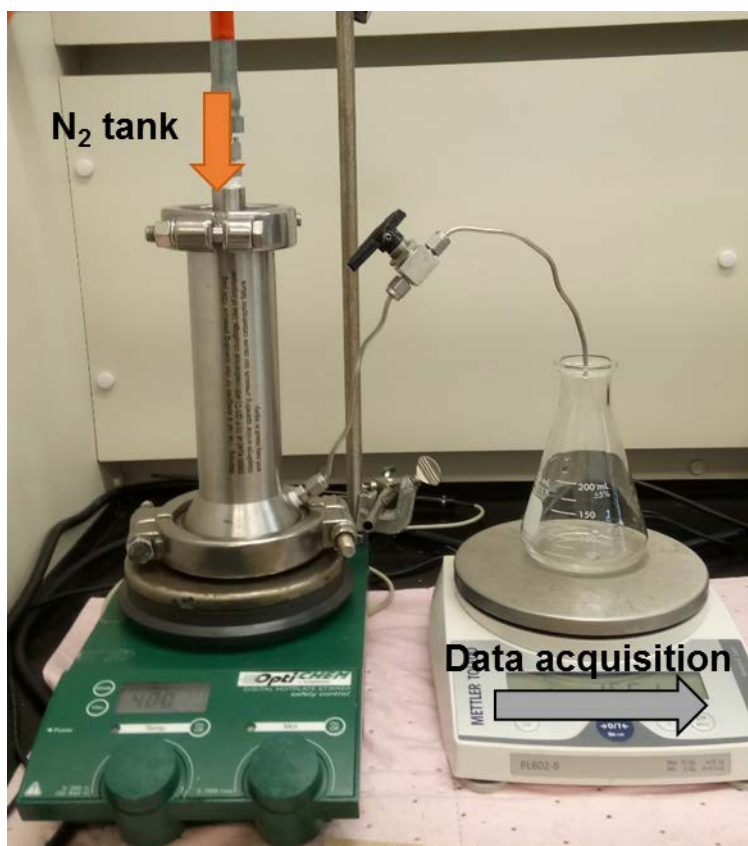


Figure S1: Process experimental setup for nanofiltration in dead-end mode.

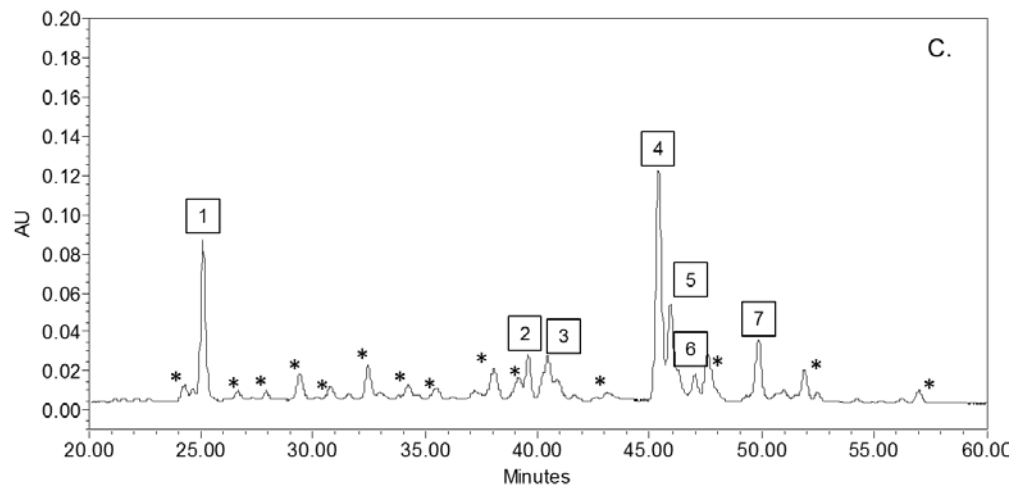
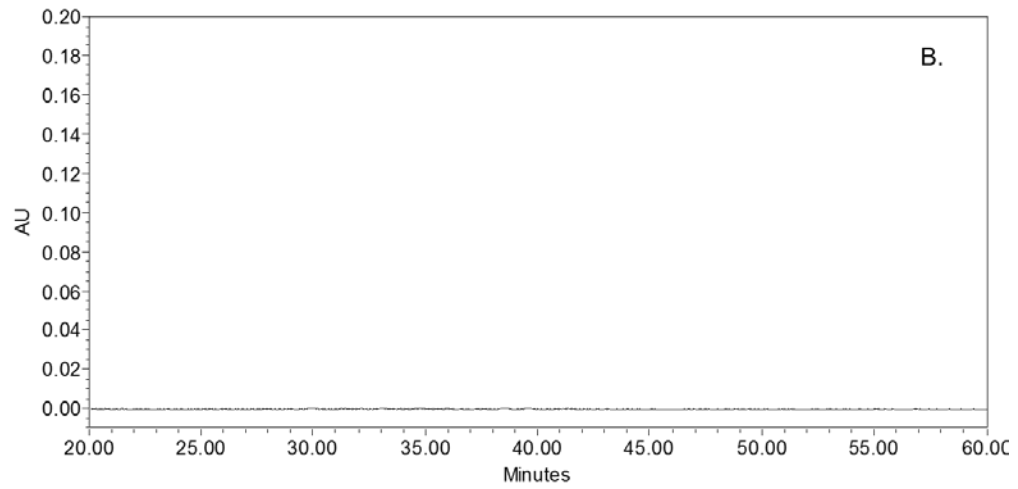
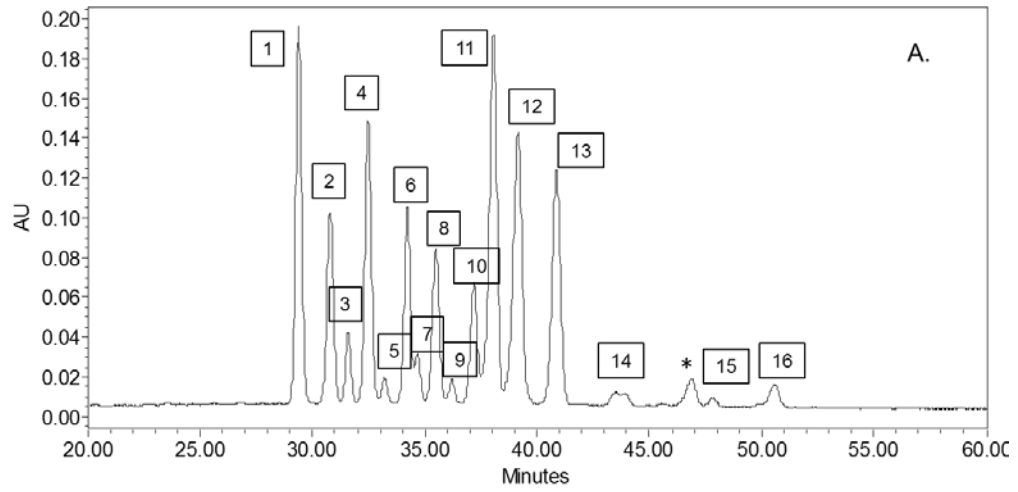
Dead-end - Rejection

Table S1: Rejection of polyphenols and anthocyanins at different experimental parameters in dead-end filtration mode.

Filtration parameter	Total polyphenol rejection^{a)}	
	NF270	NF245
Stirring speed, rpm		
0	100%	100%
200	100%	100%
400	100%	100%
Pre-filtration		
none	100%	100%
0.22 μm	100%	100%
0.45 μm	100%	100%
Filtration time		
1 hr	100%	100%
19 hrs	100%	100%
29 hrs	n.a.	100%

^{a)} as sum of total anthocyanins, total flavonols and chlorogenic acid.

HPLC analysis of ASE extract



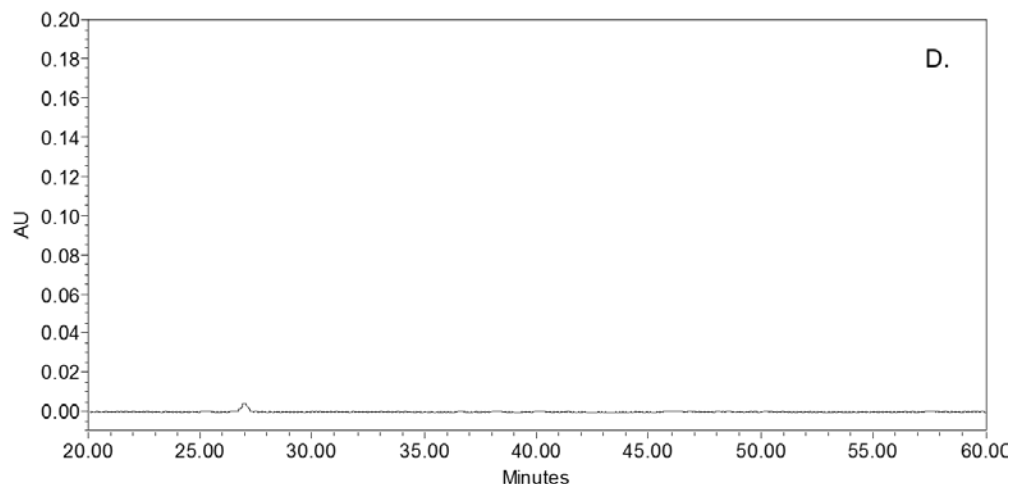


Figure S2: HPLC analysis of anthocyanins. A. 510 nm, ASE extract; B. 510 nm, permeate after nanofiltration in dead-end mode with NF270; C. 360 nm, ASE extract and D. 360 nm, permeate after nanofiltration in dead-end mode with NF270. Numbered peaks are identified below. * - not identified peak.

Peak identification using standards as follows:

Figure S2, A. (510 nm):

1. delphinidin-3-galactoside
2. delphinidin-3-glucoside
3. cyanidin-3-galactoside
4. delphinidin-3-arabinoside
5. cyanidin-3-glucoside
6. petunidin-3-galactoside
7. cyanidin-3-arabinoside
8. petunidin-3-glucoside
9. peonidin-3-galactoside
10. petunidin-3-arabinoside
11. malvidin-3-galactoside
12. malvidin-3-glucoside

13. peonidin-3-arabinoside
14. malvidin-3-arabinoside
15. delphinidin-3-acetylglucoside
16. cyanidin-3-acetylglucoside

Figure S2, C. (360 nm):

1. chlorogenic acid
2. myricetin-3-galactoside/glucoside
3. myricetin-3-rhamnoside
4. quercetin-3-galactoside
5. quercetin-3-glucoside
6. quercetin-3-rutinoside
7. quercetin-3-acetylramnoside

Crossflow filtration

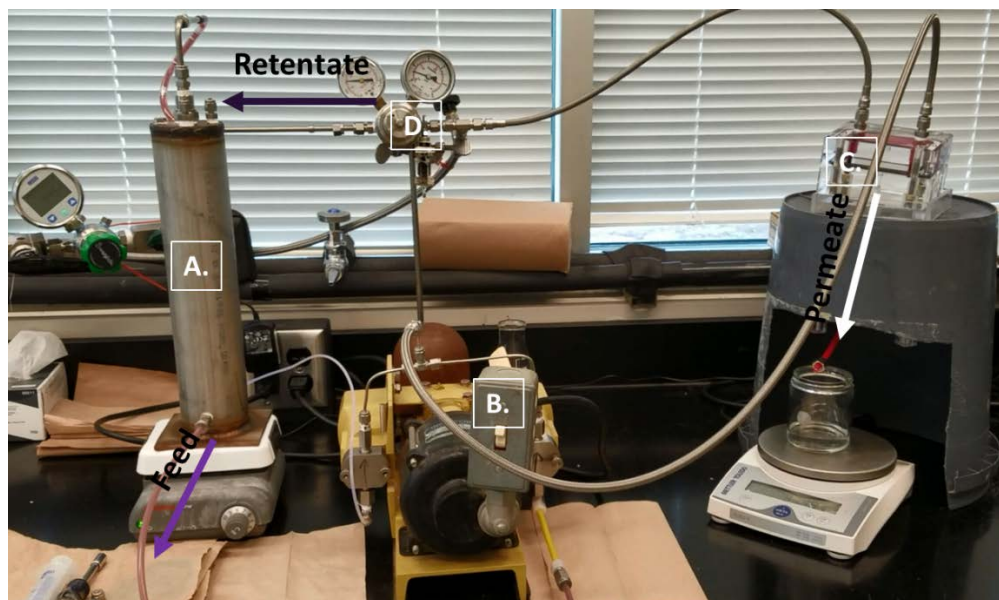


Figure S3: Process experimental setup for nanofiltration in crossflow mode. Arrows show the direction of fluid. A: Feed stirred vessel; B: Piston pump; C: Crossflow cell; D: Pressure regulator.

Crossflow filtration - Rejection

Table S2: Rejection of polyphenols at constant experimental parameters in crossflow filtration mode. Stirring speed 200 rpm, 0.22 μm prefiltered feed, crossflow flowrate 57 mL/min, TMP 3 bar, feed volume 600 mL.

Sampling time, min	Polyphenols rejection ^{a)}	
	NF270	NF245
50	100%	100%
100	100%	100%
180	100%	100%

^{a)} as sum of total anthocyanins, total flavonols and chlorogenic acid.

5. Conclusion and future outlook

Nanofiltration is a very promising separation technology that has the potential to deliver completely new technologies or advance already existing ones. In this work have developed novel chemistry to modify poly(ethersulfone) membrane via interfacial polymerization for use in the recycling of expensive ionic liquids. This is especially relevant, since ionic liquids and low molecular weight sugars, such as glucose, are cumbersome to separate by size-exclusion only. Our results indicate that careful control of the thickness and structure of the interfacial polymerization layer will be essential to maximize rejection of sugars, recovery of ionic liquids in the permeate and the permeability of the membrane. In addition to development of appropriate membranes, integration of a nanofiltration step in the entire process must be considered as it will determine the viability of nanofiltration for ionic liquid recovery.

The second membrane modification dealt with deposition of charged polyelectrolytes on the surface of alumina oxide and poly(ethersulfone) ultrafiltration membranes. We demonstrated their application on the feasibility of recycling of ionic liquid from biomass hydrolysates. An attempt was made to understand the effect of number of polyelectrolyte bilayers on the surface properties of the membrane and its consequent membrane performance. Atomic force microscopy imaging, contact angle measurement and zeta potential analysis were used to analyze the surface properties and morphology of the modified membranes, which were found to be directly linked with water permeance and selectivity performance. Alumina oxide membranes showed heterogeneous deposition of polyelectrolyte layers with large smooth areas and then rougher areas around the large microfiltration pores. The former is believed to be beneficial for increased permeance, while the latter could trigger a mediated transfer of charged species and thus an increase in selectivity for ionic liquids. Poly(ethersulfone) membranes showed a more homogenous deposition of

polyelectrolytes, which seem to mimic the original structure of the base membranes. Coupled with increased negative charge as a function of deposited bilayers this allowed for better transfer of the charged species while retaining the non-charged species on size-exclusion basis.

For the third part of this work, nanofiltration technology was tested in dead-end and crossflow mode to investigate the feasibility of reducing water volume and thus concentrating health beneficial polyphenolic compounds from blueberry (*Vaccinium corymbosum*) pomace extracts. The pomace represents an underused raw material that is usually discarded in the food manufacturing industry after the juice was extracted. However, the skins of the blueberry fruit contain the most polyphenols by mass and their extraction and concentration could deliver an interesting market product as e.g. anti-oxidant enhanced drinks and foods. The separation techniques were optimized based on stirrer speed, prefiltration step and feed temperature. Both NF245 and NF270 showed complete rejection of phenolic compounds at good permeances. A clean-in-place protocol was developed for cleaning the used membranes after filtration and an excellent relative permeance was obtained for the NF270 membrane.

As future work, it would be interesting to investigate if interfacial polymerization and polyelectrolyte deposition could be combined and optimized to fabricate membranes with even better selectivity for the recycling of ionic liquids and with even better permeabilities. Since interfacial polymerization allows for easy addition of reactive monomers, it would be interesting to test other boronic acids that could be used to tune the selective layer towards complete rejection of sugars (and thus increased selectivity and recycling of ionic liquids).

For the recovery and concentration of polyphenols from blueberry pomace, it would be worthwhile developing a larger scale system and investigate the economic feasibility as well as bioactivity of

concentrated polyphenols. Since the polyphenols have shown to adhere to membrane surface, fouling studies and optimization based on reducing membrane fouling could be of interest.